CHARACTERIZATION AND APPLICATION OF AMADUMBE STARCH NANOCRYSTALS IN BIOCOMPOSITE FILMS

By

Agnes R Mukurumbira

N.Dip: Food Technology, B.Tech: Food Technology

Submitted in fulfilment of the academic requirement for the degree Masters of Applied Sciences in Food Science and Technology

Department of Biotechnology and Food Technology

Faculty of Applied Sciences

Durban University of Technology, Durban, South Africa

Supervisor: Prof Eric Oscar Amonsou

Co-supervisor: Dr John Mellem

2017

DECLARATION

I hereby declare that the work reported in this thesis and submitted at the Department of Biotechnology and Food Technology at the Durban University of Technology for a Masters Degree is my original work. I confirm that it has not been previously submitted for a degree at any Higher Education Learning Institution.

16 August 2017

Agnes Mukurumbira
Student

Date

As the candidate's supervisors we agree to the submission of this thesis

16 August 2017

Prof Eric Amonsou
Supervisor

Date

16 August 2017

Dr John Mellem
Co-Supervisor

Date

DEDICATION

This thesis is dedicated to the love of my life, my king, my Lord Jesus Christ. It is also dedicated to my parents Hilda and Alois Mukurumbira**.**

ACKNOWLEDGEMENTS

Almighty God, my human vocabulary is inhibited to fully express my gratitude to you. I am deeply grateful for your hand that was over my life throughout this program. This work is a testimony of your tender mercies, lovingkindness and faithfulness, there is truly no one like you my Father. The financial support rendered to me by the National Research Foundation throughout this program is well appreciated. I am very grateful to my supervisor Prof Eric Amonsou for igniting my passion for science, for challenging my perspectives and opening my eyes to new ideologies and ways of thinking. Thank you for going beyond your supervisor duties and being a father and advisor. To my co-supervisor Dr John Mellem, I greatly appreciate your support and guidance throughout the program. Your attention to detail has been instrumental in my writing. I would like to appreciate the entire Department of Biotechnology and Food Technology for their holistic contribution to my well-being and the success of my work. To the HOD, I greatly appreciate you, thank you for giving a listening ear to our issues, advising and ultimately creating a conducive environment for our learning. I would like to sincerely thank Prof Alain Dufresne for hosting me as a visiting at the Grenoble Institute of Technology. I am very grateful to the staff and students at the Grenoble Institute of Technology especially Mariano Marcos who assisted me with all my laboratory work. My sincere gratitude also goes to my parents Hilda and Alois Mukurumbira for believing in me and constantly praying for me. I am truly grateful to my siblings Nyasha, Joy, Nyasha, Vongai, Kupa and James Mukurumbira for being my number one cheerleaders and providing support. To my in-laws Mudadisi, Janet, Allen and Chipo thank you for adding sunshine to my life and for being listening ears. I would like to appreciate my colleagues and friends, Tafadzwa Ndadziyira, Nyasha Busu, Thobela Nconco, Faith Chibvura, Gillian Mandizvidza, Thelma Zindoga, Shame Mugova, Siyaduduzwa Dlamini, Sinethemba Sokhela, Luvo Gugwana, Adebola Oladunjoye, Brinah Senzere, Faith Semwayo, Abimbola Arise, Sylvia Thondlana, Patience Mutsvairigwa, Chido Madhanga, Van Kakwere, Johnson Zininga, Faith Seke, Sithembile Shongwe, Zikhona Nyawose, Bruce Mawoyo, Paballo Ntokabi, Cynthia Moyo, Bruce Chakara, Betty Ajibade and Ajibola Oyedji. Thank you for your assistance, support and motivation, your fingerprints will truly never fade from my life. A special thank you goes to Samson Oyeyinka for being always available to assist and offer guidance. I would like to thank Enactus DUT especially Lana-Ann Brady for inspiring, motivating and being a shoulder to lean on throughout the program. I would also like to thank my church

family at Harvest House International Church Durban for their support and prayers. Finally, I wish to extend my gratitude to anyone who contributed in any way to the success of this program whom I have not mentioned by name.

ABSTRACT

Amadumbe (*Colocasia Esculenta)* commonly known as Taro is an underutilized tuber crop that produces underground corms. It is a promising tropical tuber grown in various parts of the world including South Africa, where it is regarded as a traditional food. It is a significant subsistence crop, mostly cultivated in rural areas and by small scale farmers. Amadumbe is adapted to growing in warm and moist conditions. The tubers are characterised by a high moisture content and consequently high post-harvest losses. The losses can be minimized through the utilization of various preservation techniques such as flour and starch production. Amadumbe corms may contain up to 70-80% starch. The starch granules are characterised by a small size and relatively low amylose content. The combination of high starch content, low amylose and small starch granules thus make amadumbe a potentially good candidate for nanocrystal production.

In this study two amadumbe varieties were utilized to extract starch. Amadumbe starch nanocrystals (SNC) were produced using an optimized hydrolysis method. The physicochemical properties (morphology, crystallinity, thermal properties) of the resulting SNC were investigated. The SNC were then applied as fillers in three different matrices namely, amadumbe starch, potato starch and soy protein. The influence of the SNC at varying concentrations (2.5, 5 and 10%) on the physicochemical properties of bio-composite films was examined.

Amadumbe starch produced a substantially high yield (25%) of SNCs. The nanocrystals appeared as aggregated as well as individual particles. The individual nanocrystals exhibited a square-like platelet morphology with sizes ranging from 50-100 nm. FTIR revealed high peak intensities corresponding to O-H stretch, C-H stretch and H_2O bending vibrations for SNCs compared to their native starch counterparts. Both the native starch and SNC exhibited the A–type crystalline pattern. However, amadumbe SNCs showed a higher degree of crystallinity possibly due to the removal of the armorphous material during acid hydrolysis to produce SNCs. Amadumbe SNC showed slightly reduced melting temperatures compared to their native starches. The SNC presented similar thermal decomposition properties as compared to their native starches.

In general, the inclusion of SNCs significantly decreased water vapour permeability (WVP) of composite films whilst thermal stability and tensile strength were increased. The degree of improvement in the physicochemical properties of the films varied with the type of matrix as well as the concentration of the nanocrystals. It generally seemed that the enhancement of the physicochemical properties of starch matrices occurred at a lower SNC concentration in comparison to that of soy protein films. Amadumbe SNC can indeed potentially be used as a filler to improve the properties of biodegradable starch and protein films

PREFACE

This thesis is organized into six chapters and presented in the format submitted for publication. Chapter One is a general introduction to the thesis. Chapter Two presents a critical review of relevant literature. Some areas covered in the literature review include starch structure, various properties of starch, methods of starch nanocrystal production, morphological properties of SNCs and applications of SNCs. Chapter Three focuses on the characterization of amadumbe SNCs. Chapter Four and Five presents the effect of amadumbe SNCs on the physicochemical properties of amadumbe starch, potato starch and soy protein films. Chapter Six covers the general discussion of the work and highlights the conclusion derived from the research and providing recommendations for future work.

Table of Contents

ABBREVIATIONS

SNC: Starch nanocrystals

SEM: Scanning Electron Microscopy

FEGSEM: Field Electron Gun Scanning Electron Microscopy

AFM: Atomic Force Microscopy

DSC: Dynamic Scanning Calorimetry

TGA: Thermogravimetric Analysis

WVP: Water Vapour Permeability

TS: Tensile strength

XRD: X-ray Diffraction

T_g: Glass transition

T_p: Peak melting temperatures

PUBLICATIONS AND CONFERENCES ATTENDED

Publications

Agnes R. Mukurumbira, John J. Mellem and Eric O. Amonsou (2017) Physicochemical properties of amadumbe starch nanocrystal-soy protein composite films. *Food Hydrocolloids* (Under review - FOODHYD-D-17-00011)

Agnes R. Mukurumbira, John J. Mellem and Eric O. Amonsou (2017). Effects of amadumbe starch nanocrystals on the physicochemical properties of starch bio-composite films. *Carbohydrate Polymers*, 165: 142-148

Agnes R. Mukurumbira, Marcos Mariano, Alain Dufresne, John M. Mellem, Eric O. Amonsou (2017). Microstructure, thermal properties and crystallinity of amadumbe starch nanocrystals. *International Journal of Biological Macromolecules,* 107: 241-247

Agnes R. Mukurumbira (2015). Nanotechnology takes industry forward: industry talk. *Food Manufacturing Africa*, *3*: 25.

Conferences attended

Mukurumbira, A.R., Mellem, J. & Amonsou, E.O. Physicochemical properties of soy protein films reinforced with amadumbe starch nanocrystals. 30th European Federation of Food Science and Technology (EFFoST) Conference, Vienna, Austria, 28-30th November 2016.

Mukurumbira, A.R., Mellem, J., & Amonsou, E.O. Preparation and characterisation of amadumbe starch nanocrystals for potential application in bio-composite films. 18th World Congress of Food Science and Technology (IUFoST) Conference, Dublin, Ireland, 21st-25th August 2016.

Mukurumbira, A.R., Mellem, J., & Amonsou, E.O. Application of amadumbe starch nanocrystals as nano reinforcements in polysaccharides and protein films. 21st South African Association for Food Science and Technology (SAAFoST) Biennial International Congress and Exhibition, Durban South Africa 69th September 2015.

Agnes R. Mukurumbira, John J. Mellem and Eric O. Amonsou. Amadumbe an underutilised African crop for starch nanocrystal production. International Research Day, Durban University of Technology, Durban, South Africa. 26th November 2015

CHAPTER ONE

1.0 Introduction

Nanotechnology is defined as the characterization, fabrication and/or manipulation of structures, devices or materials that have at least one dimension in the nanoscale range (Duncan, 2011). The reduction of particle size from macro molecular to nanoscale range results in materials that exhibit novel optical, catalytic and reactive properties (Azeredo, 2009, Duncan, 2011, Cushen et al., 2012,). These nanomaterials can be in the form of nanoparticles, nanowhiskers, nanotubes, and nanocrystals (Cushen et al., 2012). Nanocrystals in particular, have attracted interest from both academia and industry due to their functionality and versatility.

Nanocrystals can be derived from synthetic or natural sources like starch and cellulose. Starch nanocrystals have received considerable attention due to their biodegradability, ease of production, low cost and cyclic availability of starch. They are produced through the hydrolysis of starch granules (Angellier et al., 2004, Le Corre et al., 2010). The starch granule essentially consists of alternating crystalline and amorphous lamellae (Eliasson, 2004, Qiang, 2005, BeMiller, 2009, Le Corre et al., 2011). The amorphous regions are relatively soft and are selectively hydrolysed when the starch granule is exposed to acid resulting in nanocrystals, a crystalline residue with platelet morphology (Le Corre et al., 2010, Lin et al., 2011, Kim et al., 2015).

The morphology of starch nanocrystals varies based on the crystalline pattern of the starch source as well as the relative proportion of amylopectin to amylose (Lin et al., 2011, LeCorre et al., 2011b). A-type starches generally produce square-like nanocrystals whilst B-type starches produce round shaped nanocrystals (Dufresne, 2008, Le Corre et al., 2010). One promising area of application of starch nanocrystals is in bio-composite films.

Biodegradable films have attracted a lot of attention as potential alternatives to petro-chemical based plastics. This is due to the imminent fossil energy depletion, environmental problems posed by synthetic plastics and growing concerns for their long term sustainability (Sorrentino et al., 2007, Azeredo, 2009). In comparison to synthetic plastics, biodegradable plastics are limited due to their poor barrier, mechanical and thermal properties (Sorrentino et al., 2007, González and Igarzabal, 2015). The application of starch nanocrystals to protein and polysaccharide films to form nanocomposites open new possibilities of addressing some of the limitations of these films. The resulting nanocomposites exhibit improved mechanical,

thermal and permeability properties due to the synergistic effect produced by the combination of the matrix (film) and the reinforcement (nanocrystals) at the reinforcement matrix interface (Bradley et al., 2011, Duncan, 2011). Furthermore gas and water vapour permeability is reduced as the dispersed nanoparticles create a tortuous pathway that hinders diffusion of molecules (Duncan, 2011, Lin et al., 2012, Condés et al., 2015). Previous studies have indeed reported an improvement in mechanical, thermal and permeability properties of biodegradable films with the addition of starch nanocrystals (García et al., 2009, Zheng et al., 2009, Piyada et al., 2013, Condés et al., 2015, González and Igarzabal, 2015). Starch nanocrystals for application in biodegradable films can be derived from various sources of starch including cereals, legumes and tubers. Currently cereals are the predominant source of starch for production of nanocrystals.

Amadumbe *(Colocassia esculenta*) also known as taro is a tropical tuber that produces underground corms (Aboubakar et al., 2009). Amadumbe corms are starch rich and may contain 70-80% starch (Aboubakar et al., 2008). Furthermore amadumbe starch granules have been reported to be characterized by a relatively low amylose content (12-20%) and small granular size (Naidoo et al., 2015). The main limitation in starch nanocrystal production is the low yield of nanocrystals. The yield of starch nanocrystals could be influenced by the hydrolysis conditions, starch granule size, amylose content and granule surface porosity. Small granule size and low amylose content of starch have been shown to ease the hydrolysis process (Vasanthan and Bhatty, 1996, Jayakody and Hoover, 2002, LeCorre et al., 2010), which consequently improves the yield of starch nanocrystals. In consideration of these findings, the high starch content, low amylose and small starch granules thus make amadumbe a potentially good candidate for nanocrystal production. Conventional sources of starch have been utilised for starch nanocrystal production. However, to the best of our knowledge amadumbe has never been employed in starch nanocrystals production yet it is equally competitive. The use of amadumbe in nanocrystals production will add value to, and thereby promote commercial usage of this underutilised crop.

CHAPTER TWO

2.0. Literature review

2.1. Tubers

Tuber crops are the second most cultivated species after cereals (Lebot, 2009). The most common tubers worldwide are potato (*Solanum tuberosum*), sweet potato (*Ipomea batatas*), yams (*Dioscorea spp*) and cocoyams (*Colocasia spp* and *Xanthosoma spp*) (Onwueme and Charles, 1994). Tubers are categorized into root tubers like cassava and sweet potato and stem tubers like potato and cocoyams (Onwueme and Charles, 1994). Cassava, yams and cocoyams thrive in warm weather and are considered tropical tubers (Onwueme and Charles, 1994). Most tropical tubers are grown for human consumption and contribute greatly towards food security (Onwueme and Charles, 1994, Lebot, 2009). Their nutritional composition is comparable to most cereals (Table 2.1). The commercial exploitation of tropical tubers in the future may come from their potential use as alternative starch sources (Lebot, 2009).

Amadumbe is a promising tropical tuber that is grown in various parts of the world including South Africa (Aboubakar et al., 2008). It is commonly known as taro in many parts of the world including the Pacific Islands and cocoyam in West Africa (McEwan et al., 2010). The scientific name for amadumbe is *Colocasia esculenta.* Amadumbe belongs to the monocotyledonous family *Araceae* and is among the most important genera of this family (Falade and Okafor, 2013). It is amongst the few edible species within the genus *Colocasia* and generally cultivated for food (Falade and Okafor, 2013). *Colocasia* species are often classified as *C. esculenta* (L) Schott var *esculenta,* which is characterised by large corms with very few cormels and *C. esculenta* (L) Schott var *antiquorum* that generally comprises of a central corm surrounded by many cormels (Fig 2.1) (Hoover, 2001).

Amadumbe (Fig 2.2) has long been introduced in South Africa and it is regarded as a traditional food. It is an significant subsistence crop, mostly cultivated in the rural areas and by small scale farms (Mare, 2009, McEwan et al., 2010). The Kwazulu Natal Province is one of the major areas of cultivation of amadumbe in South Africa (Mare, 2009, McEwan et al., 2010). Similar to other tropical tubers, amadumbe is adapted to growing in warm and moist conditions (Mare, 2009). Amadumbe is characterised by a high moisture content and consequently high post-harvest losses (Dai et al., 2015). It is estimated that an average 30% of produce loss occurs during storage of amadumbe corms (Dai et al., 2015). Amadumbe tuber losses can be minimized by their conversion from perishable to non-perishable commodities through various food processing

operations (Dai et al., 2015). Promising processing techniques to preserve and add commercial value to amadumbe include flour and starch production (Pérez et al., 2005).

Table 2.1 Proximate composition of tuber crops

	Cassava ***Manihot esculenta***	**Sweet Potato** ***Ipomoea batatas***	**Yams** ***Dioscorea spp***	**Aroids** ***Colocassia Esculenta &Xanthosoma sagittifolium***
Total sugars (% FW)	0.5-2.5	1.5-5.0	0.5-2.0	2.0- 3.0
Protein (% FW)	0.5-2.0	1.0-3.0	2.0-4.0	1.5-3.0
Fibres(% FW)	1.0	1.0	0.6	0.5-3.0
Vitamin A (mg/ 100g/ FW)	17	900	117	0-42
Vitamin C (mg/ 100g/ FW)	50	35	25	10
Minerals (% FW)	0.5-1.5	1.0	0.5-1.0	0.5-1.5
Energy (kj/100g/FW)	600	500	440	400

Adapted from Lebot (2009) (FW-Fresh Weight)

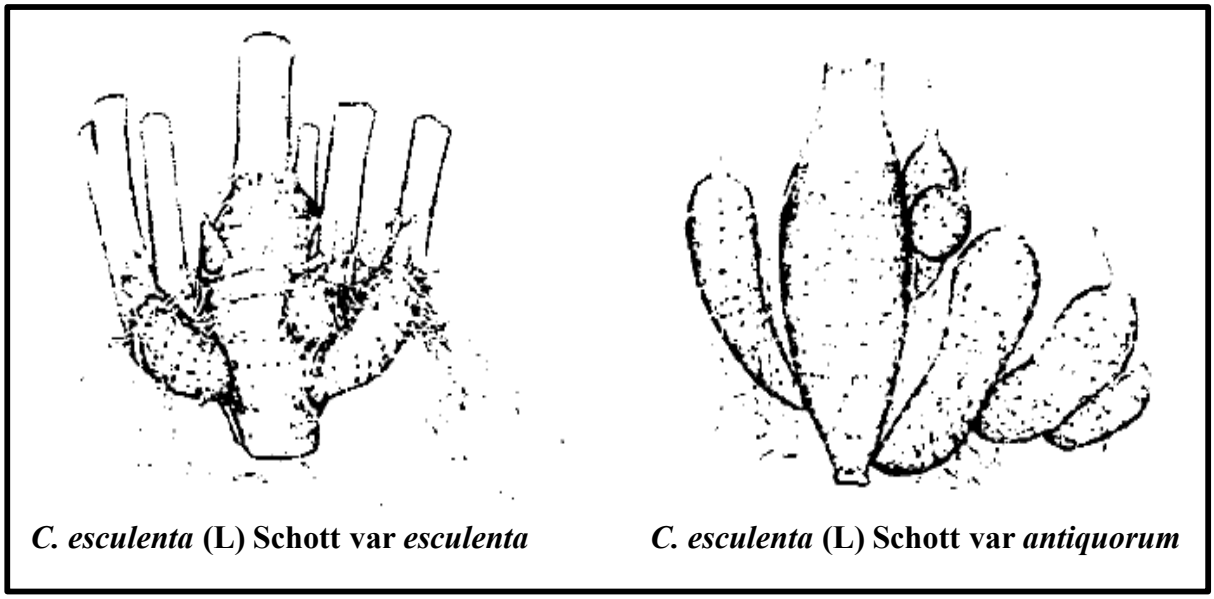

Figure 2.1: Two common edible amadumbe species. Adapted from Mare (2009)

Fig 2.2: South African amadumbe corms

2.2. Tuber starches

Tropical tuber crops represent an important source of starch (Onwueme and Charles, 1994, Lebot, 2009). Despite being good sources of starch, most tuber crops have not been explored for commercial production of starch. In general, tubers and roots have been found to contain between 16 and 37% starch on a dry weight basis (Hoover, 2001, Lebot, 2009). However, some amadumbe tuber varieties have been reported to contain starch as high as 66 to 87% on a dry weight basis (Aboubakar et al., 2008).

2.2.1. Starch morphology

The morphology and composition of tuber starch granules vary depending on the botanical origin (Hoover, 2001, Copeland et al., 2009). Tuber starch granule size commonly ranges from 1 to 110 µm (Table 2.2) (Hoover, 2001). Starch granule shapes that have been reported in literature include oval, polygonal, lenticular, round and irregularly shaped (Fig 2.3) (Hoover, 2001, Copeland et al., 2009). Aboubakar et al. (2008) observed polygonal and irregular shaped starch granules (Fig 2.3) of a diameter lower than 5 µm for six amadumbe varieties. Similar polygonal and irregularly shaped granules were also reported by Naidoo et al. (2015) who worked on South African wild and cultivated varieties of amadumbe.

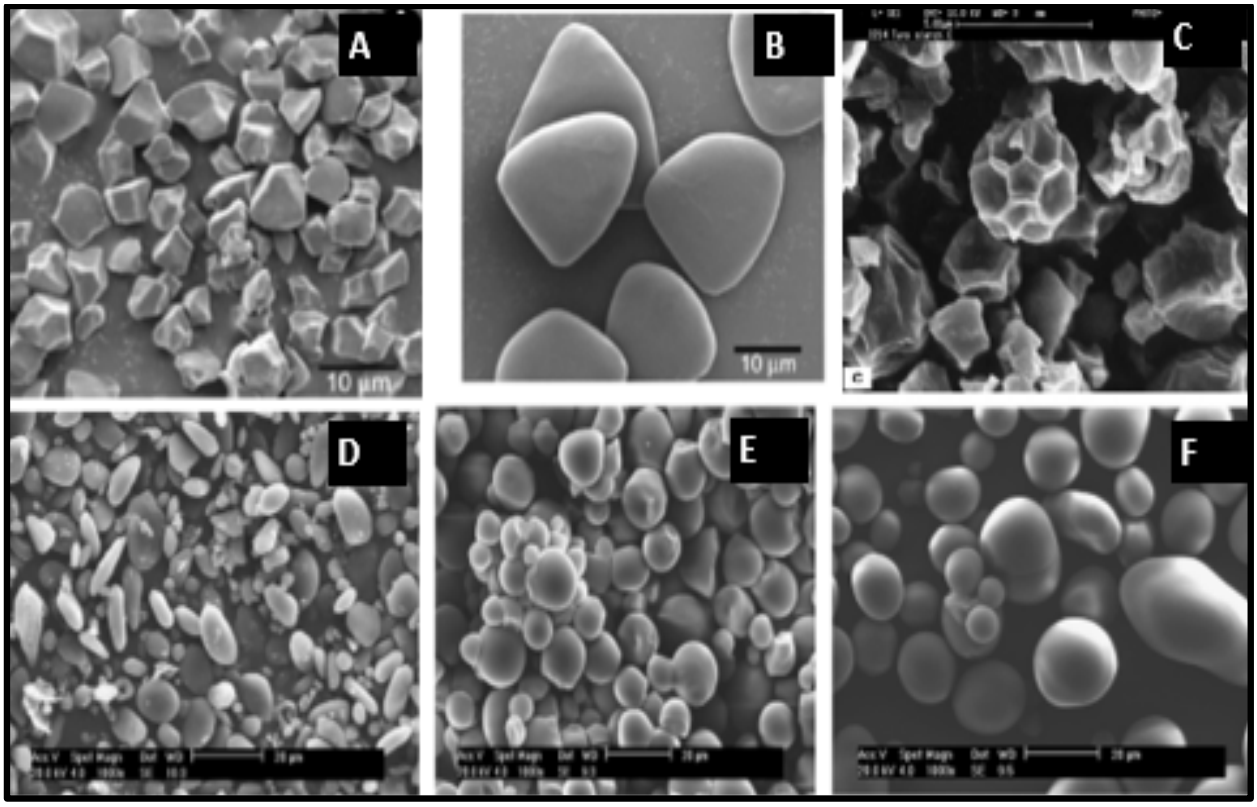

Figure 2.3: Scanning electron micrograph of tuber crops [a]*Dioscorea esculenta*(A), [a]*Dioscorea alata* (B), [b]amadumbe (C), [c]*Dioscorea nipponica* (D), [c]tapioca starch (E), [c] potato starch (F). .Adapted from [a]Jayakody (2007), [c]Yuan (2007) and [b]Aboubakar et al. (2008)

Table 2.2 : Size and shape of some root and tuber starches

Starch source	Size µm	Shape
Potato (*Solanun tuberosum*)	15-110	Oval, spherical
Sweet potato (*Ipomea babatas*)	2-42	Round, oval and polygonal
True yam (*Dioscorea abysssinia*)	29.2	Round
Amadumbe (*Colocassia Esculenta*)	3.0-3.5	Round-polygonal
Cassava (*Manihot Esculenta*)	5.40	Round

Adapted from Hoover (2001)

2.2.2. Starch composition

Starch is a polymeric carbohydrate comprising primarily of two polymers, amylose and amylopectin which represent 98-99% of the total dry weight (Buléon et al., 1998, Copeland et al., 2009). The remaining 1-2% consists of small quantities of non-carbohydrate elements such as lipids, proteins and phosphates (Qiang, 2005). Amylose and amylopectin are anhydroglucose polymers consisting of α-D-glucopyranose units (Williams, 2009).

Amylose is fundamentally a linear molecule of starch consisting of α-D-glucopyranose residues interconnected by α-(1- 4) glycosidic bonds (Fig 2.4) (McWilliams 2001,Cui, 2005, BeMiller, 2009). Each amylose molecule possess one reducing and one non-reducing end (Qiang, 2005). The degree of polymerization (DP) of amylose is between one hundred and ten thousand (Qiang, 2005). Its molecular weight ranges from a few thousand to a hundred and fifty thousand. Amylose is predominantly found in the low density layers of the growth rings. However, some amylose molecules have been reported to be interspersed between amylopectin in the crystalline layers (BeMiller, 2009). Amylose readily adopts a helical conformation which could be a single or double helix (Williams, 2009). The double helices can further associate, particularly in high amylose starches, which contributes to the crystallinity of starch granules (Tester et al., 2004, Copeland et al., 2009).

The amylose content of starch is influenced by the botanical source, species variety, climatic environments and cultivation soil type (Singh et al., 2003, Tester et al., 2004). In general, waxy starches comprise of less than 15% amylose, normal maize (20-35%) whilst high amylose starches contain amounts greater than 40% (Tester et al., 2004). The amylose content of tuber crops has generally been reported to range between 3-45 % (Lebot, 2009). Aboubakar et al. (2008) reported amylose contents ranging from approximately 16 to 31% for six amadumbe varieties.

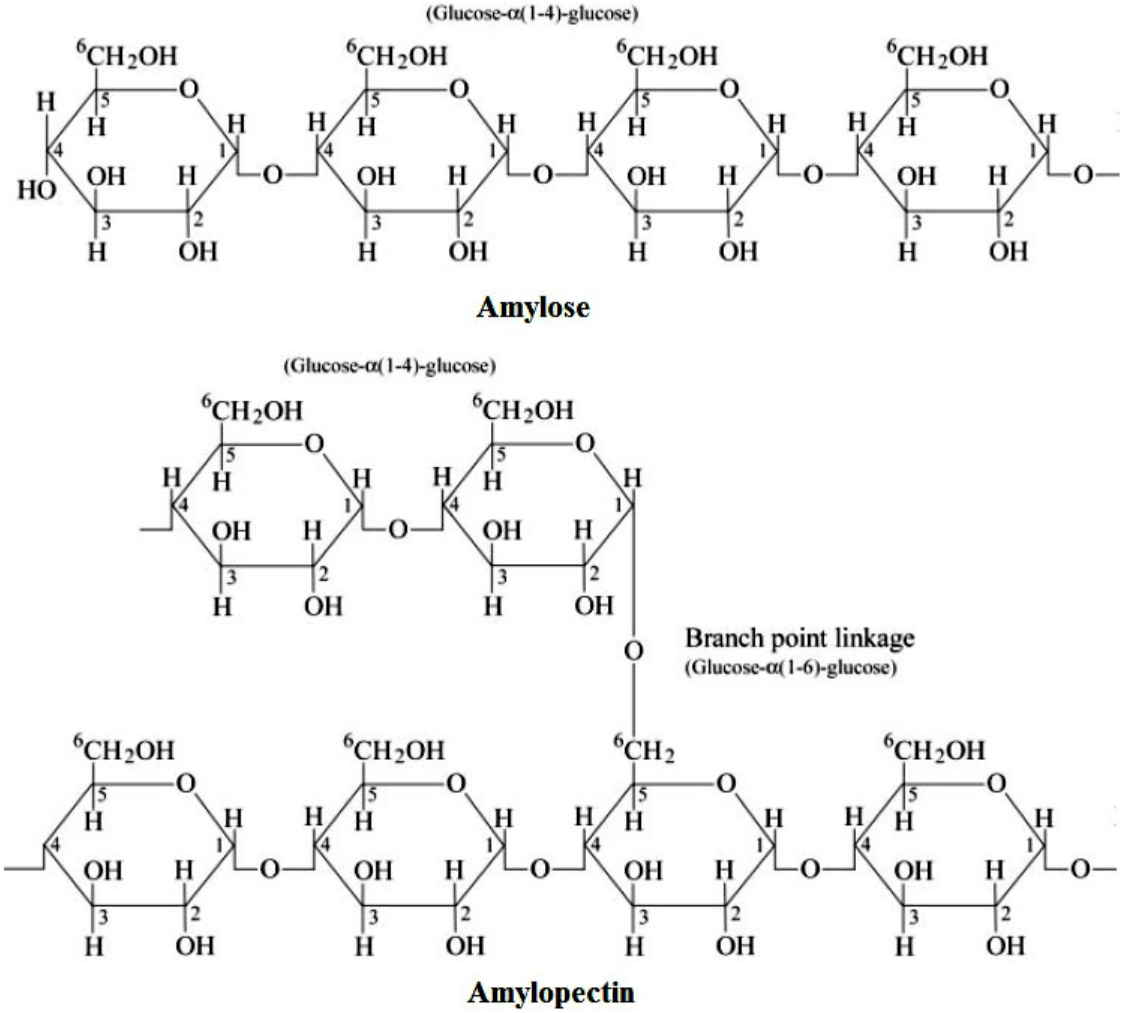

Figure 2.4: Amylose and amylopectin chains Adapted from BeMiller (2009)

Amylopectin is the highly branched portion of the starch molecule and is formed through chains of α -D–glucopyranose residues joined together primarily by α(1-4) glycosidic bonds but with a proportion of non-random α(1-6) linkages at branch points (Fig 2.4) (Eliasson, 2004, Qiang, 2005, BeMiller, 2009, Le Corre et al., 2011). When amylopectin chains have more than ten glucose units they conform into double helices, which are organized into either A or B-crystalline forms that are identified by distinctive X-ray diffraction (XRD) spectrum patterns (Fig 2.5). The double helices of A-and B-type crystalline forms are in essence the same (Buléon et al., 1998) but differ in the degree of hydration and packing arrangements of the helices (Tester et al., 2004). The packing within the A-type polymorph is fairly compact with minimal water content whilst the B type is characterized by a more open structure containing a hydrated helical core (Fig 2.6) (Tester et al., 2004, Copeland et al., 2009).

Cereal starches usually exhibit the A-type pattern, whereas tuber starches and amylose-rich starches exhibit the B-type pattern. Legumes, roots, some fruits and stem starches tend to exhibit the C-type pattern which is a combination of A and B-types (Tester et al., 2004).

In addition to classification based on the crystalline type, the individual amylopectin chains are further classified into A, B and C chains based on their length and branching points (Eliasson, 2004, Williams, 2009). The A chains are the shortest and are α (1-6) bonded to B chains or the backbone of the amylopectin only at one position (Eliasson, 2004, Tester et al., 2004, Williams, 2009). B chains are linked to at least one A chain and other B chains. B chains can be further classified into B1, B2, B3, B4 based on their respective length and the number clusters they span (Eliasson, 2004). B1 span one cluster, B2 span two clusters and so on. There is only a single C chain that carries B chains and contain the only reducing terminal residue (Eliasson, 2004, Tester et al., 2004). Fig 2.7 is a diagrammatic representation of the A, B and C chains of amylopectin.

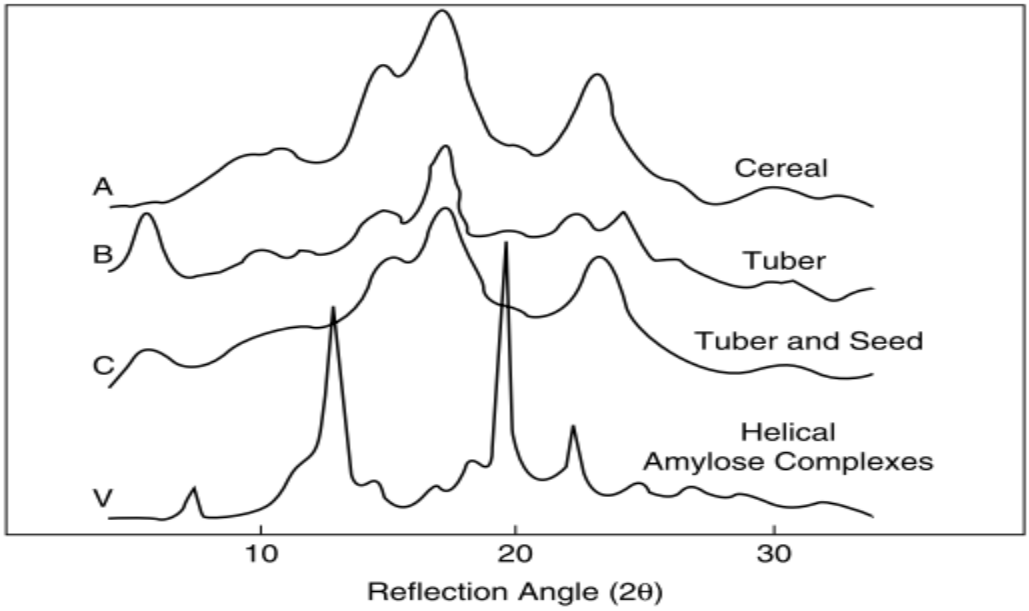

Figure 2.5: XRD patterns for A, B, C and V amylose. Adapted from Cui (2005)

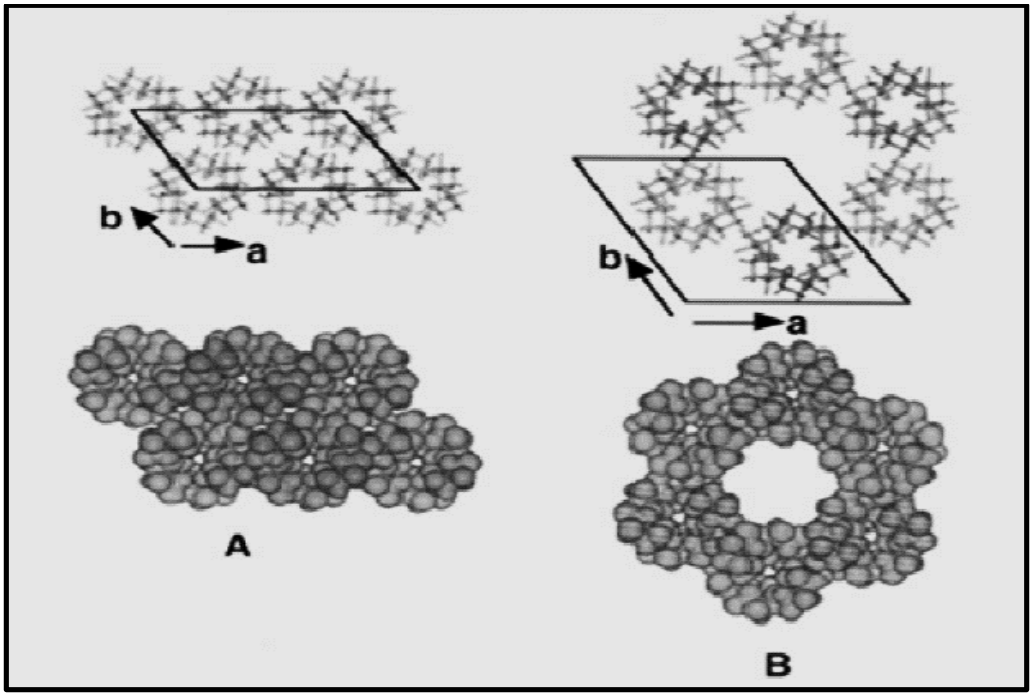

Figure 2.6: Double helixes packing configuration according to crystalline type. Adapted from Le Corre et al. (2011)

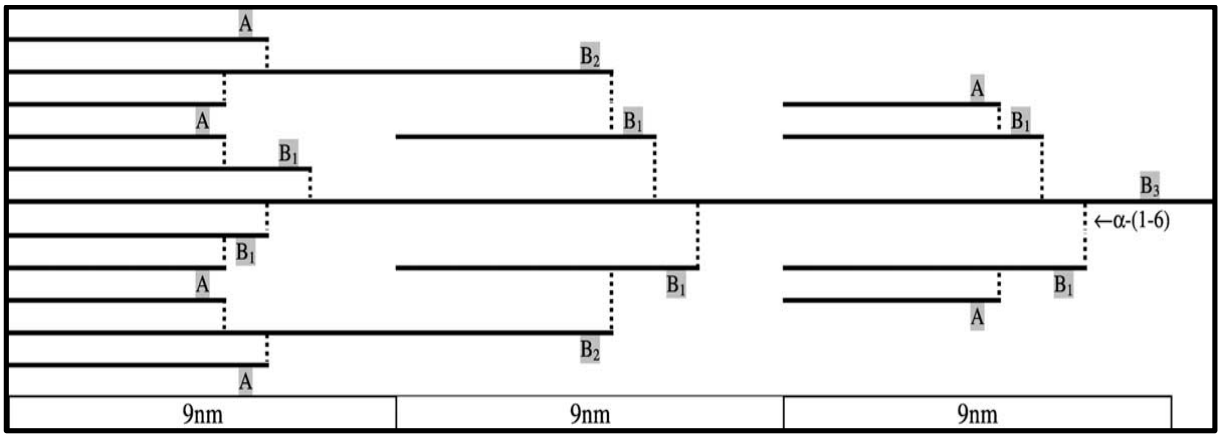

Figure 2.7: Diagrammatic representation of a part of amylopectin showing the branching patterns of unit chains A, B and C. Tester et al. (2004)

2.2.4. Starch granule organisation

The molecular organisation of starch is still not clearly understood but evidence from Scanning Electron Microscopy (SEM) and Atomic Force Microscopy (AMF) has given insight on the organisation of the starch granule. The starch granule is a multiscale structure that possess a hierarchical structural organisation (Fig 2.8) (Copeland et al., 2009). The starch granule (2-100 μm) has growth rings (120-500 nm) which are concentric layers of increasing

diameter extending from the centre of the growth which is the hilum towards the surface of the granules (Copeland et al., 2009). The growth rings are composed of blocklets (20-50 nm) made of alternating amorphous and crystalline lamellae (9 nm) comprising of amylose and amylopectin chains (0.1-1 nm) (Fig 2.8) (Le Corre et al., 2011). The amorphous regions of starch primarily contain amylose whilst amylopectin is located in the crystalline regions. The amorphous regions are more susceptible to hydrolysis (Williams, 2009).

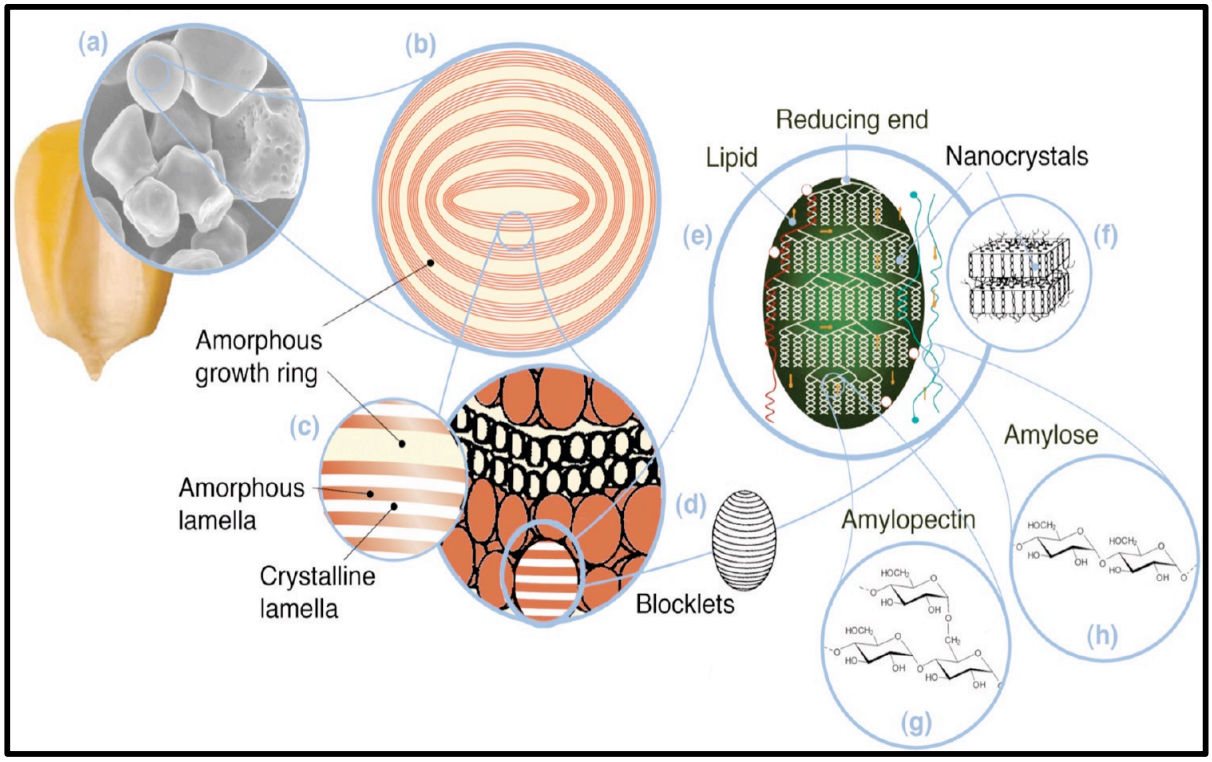

Figure 2.8: Overview of starch granule multi-scale structure Adapted form Le Corre et al. (2011)

2.3. Starch nanocrystals

Exposure of starch granules to acid and/enzymatic treatment, causes the selective hydrolysis of the amorphous regions resulting in crystalline residue in nanoscale size, with platelet morphology known as nanocrystals (Cushen et al., 2012, Jivan et al., 2013, Kim et al., 2015). The size of these nanocrystals is normally 100 nm or less. They have often been referred to as starch crystallite, microcrystalline starch and hydrolysed starch (Le Corre et al., 2011). The terms nanoparticle and nanocrystals have often been used interchangeably, but Le Corre et al. (2011) distinguished nanocrystals from nanoparticles as the latter may contain amorphous matrices (Fig 2.9).

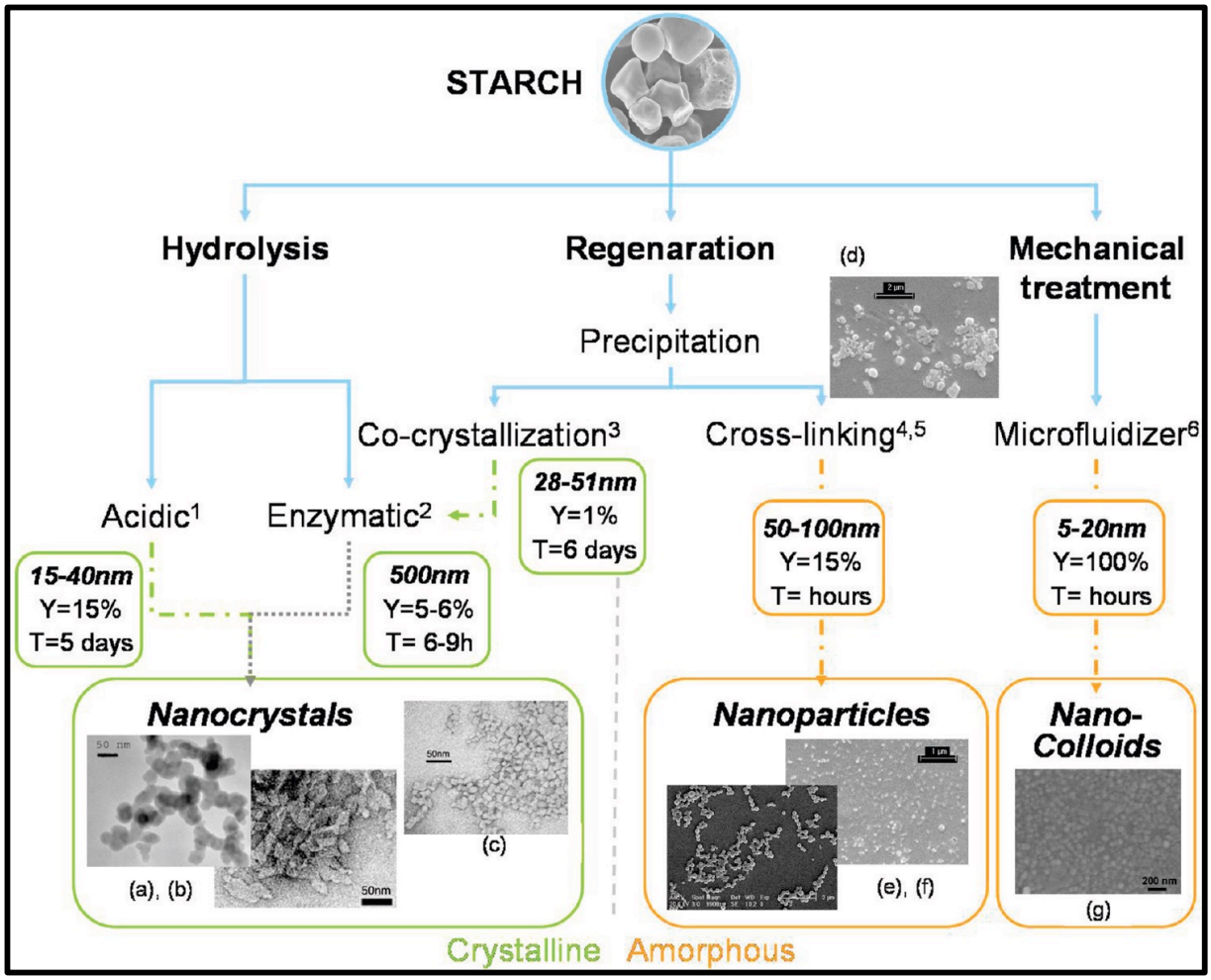

Figure 2.9: Different methods of producing nanocrystals and nanoparticles. Adapted from Le Corre et al. (2011)

Two building strategies that can be utilised in the production of nanomaterials are the "top-down" approach and the "bottom-up" approach (Kim et al., 2015). The bottom-up approach, permits nano-structures to be fabricated from discrete atoms or molecules that have the ability to self-assemble (Azeredo, 2009, Kim et al., 2015). The top-down approach is commonly used and involves the production of nanometric structures by size reduction of bulk materials, using various techniques (Azeredo, 2009, Kim et al., 2015). Some of the top-down approaches of starch nanocrystal production include acid hydrolysis, enzymatic treatment and physical treatments.

2.4. Methods of starch nanocrystals production

2.4.1. Acid Hydrolysis

Acid hydrolysis is generally the most frequently used method for nanocrystal production (Kim et al., 2015). Different acids have been employed in nanocrystal production and these include hydrochloric acid, nitric acid and sulphuric acid. When exposed to these acids, all starches exhibit a two-stage hydrolysis profile (Kim et al., 2015). The initial fast hydrolysis stage has been ascribed to hydrolysis of the amorphous regions which are highly susceptible to acid (Le Corre et al., 2011, Kim et al., 2015). The second slow hydrolysis step is assumed to be hydrolysis of the crystalline regions (Le Corre et al., 2011, Kim et al., 2015). Two hypothesis have been put forward to explain the slow rate of hydrolysis of the crystalline regions. The first hypothesis states that the compact packing of starch in the crystalline region hinders penetration of H_3O^+ (Le Corre et al., 2011, Kim et al., 2015). The second hypothesis states that there is a need for conformational change from chair to half chair to allow hydrolysis of the glycosidic bonds in the crystalline regions (Le Corre et al., 2011, Kim et al., 2015).

Starch characteristics (granule size, amylose content, granule surface porosity) and hydrolysis conditions (time, acid type and concentration and temperature) influence hydrolysis of starch. Jayakody and Hoover (2002) working with normal maize, waxy maize, amylomaize V & VII, rice and oat starch showed that hydrolysis of the amorphous zones is influenced by the amount of lipid complexed amylose chains, amylose content, granular size, and granule surface porosity. The authors reported that granule surface pores, small granule size and low amylose content effect hydrolysis positively. Hydrolysis conditions that influence the hydrolysis kinetics of starch include time, acid type, acid concentration and temperature.

The most commonly used acids for nanocrystal production are hydrochloric acid (HCl) and sulphuric acid (H_2SO_4). HCl hydrolysis requires a minimum of 15 days while H_2SO_4 hydrolysis require 5-7 days (Lin et al., 2011). HCl hydrolysis has been found to produce individual starch nano-platelets, but has a disadvantage of the long treatment time and low yield (Lin et al., 2011). H_2SO_4 hydrolysis results in the formation of sulphate-ester bonds on the surface of nanocrystals that reduce the flocculation of nanocrystals and thus results in a nano-suspension with increased stability and dispersion (Angellier et al., 2004, Lin et al., 2011). The sulphate-ester linkages, however reduce the thermal stability of the nanocrystals, which could adversely affect their usage in nanocomposites (Kim et al., 2015).

However, the addition of small amounts of ammonia has been reported to increase the thermal stability of the SNPs suspensions (Lin et al., 2011). Angellier et al. (2004) worked with waxy maize and optimised the method for starch nanocrystal production using sulphuric acid, which yielded 15% wt of nanocrystals after 5 days of hydrolysis and had a similar shape as those prepared by the classical HCl hydrolysis method for 40 days yielding 0.5% wt of starch nanocrystals.

During nanocrystal production by acid hydrolysis, the temperature and acid concentration should be moderate (Le Corre et al., 2011). Acid hydrolysis is usually carried out at sub gelatinisation temperatures between 35-45°C. Low temperatures are employed to prevent starch gelatinisation and destruction of starch crystalline structure (Lin et al., 2011). Angellier et al. (2004) studied the influence of acid concentration and temperature on nanocrystal production using a surface response methodology and concluded that the optimum conditions for starch nanocrystal production were 3.16 M acid concentration and a temperature of 40°C.

2.4.2. Enzymatic treatment

Nanocrystals have rarely been prepared by enzymatic treatment alone but a combination of enzyme pre-treatment and acid or physical treatments have been used. Various enzymes have been employed for nanocrystal production and these include α-amylase, β-amylase and glucoamylase. These enzymes create a pathway by breaking glycosidic bonds for easier diffusion of acid into the granules. This in turn makes the amorphous zones more readily hydrolysable thus reducing acid hydrolysis time (LeCorre et al., 2011c, Kim et al., 2015). In addition, the pre-treatment has been found to increase the yield of the nanocrystals. It is important to note that low nanocrystal yield has limited the wide scale commercial production of starch nanocrystals. LeCorre et al. (2011c) working with corn starch observed that at the same extent of hydrolysis (∼70%), the pre-treated starch produced a higher yield of nanocrystals but were however larger (∼145 nm). The authors also noted that further hydrolysis for 24 h allowed a reduction of size to more conventional sizes (50-100 nm) as seen on the micrograph (Fig 2.10) of suspension obtained after 24 h of hydrolysis. Of the enzymes utilised for pre-treatment (α-, β-, amylase and glucoamylase), the latter was found to be the most effective for producing micro-porous starch while preserving the semi-crystalline structure of starch (LeCorre et al., 2011c). This could be attributed to the enzyme's ability to cleave both α-1, 4 and α-1, 6 glycosidic bonds.

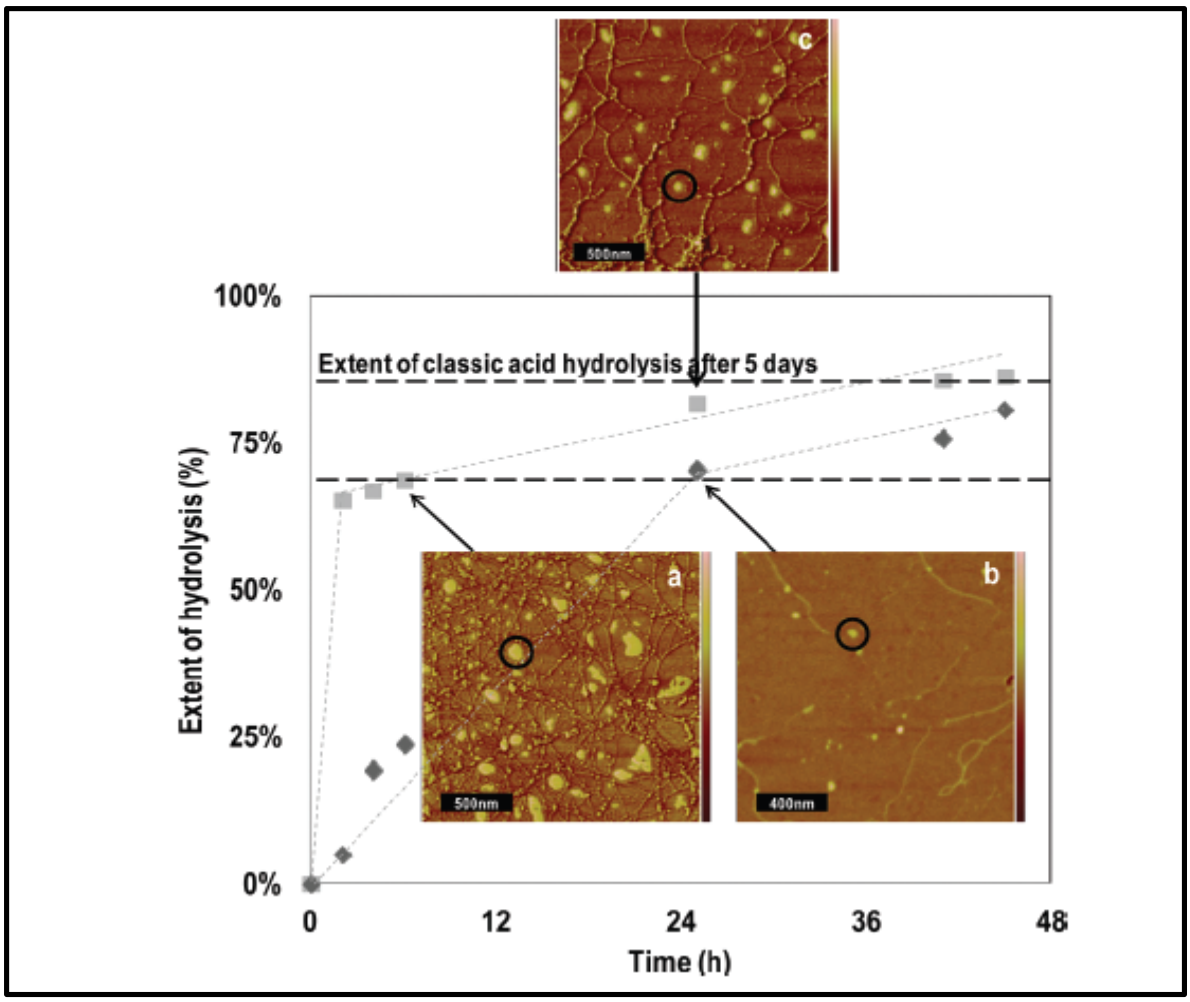

Figure 2.10: Atomic Force Microscopy measurements of (a) pre-treated waxy maize starch after 6 hrs of hydrolysis, (b) non-pre-treated waxy maize starch after 25 hrs, and (c) pre-treated starch after 25 hrs. Adapted from LeCorre et al. (2011c)

2.3.3. Physical treatments

Physical treatments have often been utilized to produce starch nanocrystals but their major drawback is that they often result in partial or complete disintegration of the starch crystalline structure (Kim et al., 2015). Physical treatments used in the production of nanocrystals include high pressure homogenization, ultrasonication, reactive extrusion and gamma irradiation. A combination of acid hydrolysis and physical treatment has often been employed to produce nanocrystals (Kim et al., 2015). Combination treatments of acid and physical treatments have been reported to be efficient in improving the yield of starch nanocrystals whilst also reducing nanocrystal production time (Namazi and Dadkhah, 2010, Kim et al., 2015). Namazi and Dadkhah (2010) used a combination of ultrasound and acid hydrolysis to produce starch nanocrystals from corn starch.

The authors reported an increase in yield from the previously reported 15% to 21.6% and produced the nanocrystals within 45 minutes in comparison to the traditional 5 day hydrolysis with acid alone (Namazi and Dadkhah, 2010).

Acid hydrolysis is the most acceptable method of starch nanocrystal production amongst the various methods that can be utilised. Sulphuric acid is regarded as the most ideal acid. The optimized method for acid hydrolysis using sulphuric acid has been widely accepted by researchers. However, the optimization was done using corn starch and the optimal conditions could possibly vary once the starch source is changed. Therefore, it is important for researchers to determine the optimal acid hydrolysis conditions for the specific starch being utilized. Using the optimized method, the hydrolysis time is 5 days. This is a major limitation for large scale production of starch nanocrystals using acid hydrolysis. Physical and enzymatic pre-treatment could possibly play a role in reducing the hydrolysis time. Therefore, there is need to explore these treatments.

2.5. Physicochemical properties of starch nanocrystals

2.5.1. Morphology

Starch nanocrystals have generally been observed as either square-like platelets or round shaped platelets (LeCorre et al., 2011b). Various sizes of starch nanocrystals ranging from 15 to 100 nm have been reported (Table 2.3). The heterogeneity in nanocrystal sizes could be ascribed to the differences in starch types and difficulty in obtaining individual non-aggregated nanocrystals during imaging.

The shape and size of starch nanocrystals were initially regarded to be primarily dependent on the botanical origin and the preparation method utilized (Kim et al., 2015). However, several scholars have shown that the botanical source has a limited effect on the morphology of starch nanocrystals but rather is influenced by the amylose content and crystalline pattern (Dufresne et al., 2013). In general, the nanocrystals produced from A-type starches (e.g., waxy maize, normal , wheat) are square-like platelets, whereas those derived from B-type starches (e.g., high amylose maize, potato) produce round-shaped platelets (Fig 2.11) (Kim et al., 2015).

Lecorre et al. (2012b) working with waxy maize, normal maize, high amylose maize, potato and wheat starches observed platelets with pronounced differences in shape of the nanocrystals (Fig 2.12).

Nanocrystals obtained from high amylose maize (B-type) exhibited a fairly round shape whilst potato starch nanocrystals (B-type) appeared as both round and rounded-corner-square particles (LeCorre et al., 2011b). The nanocrystals derived from waxy maize and wheat were parallelepipedic, and square-like nanocrystals and those from normal maize starch did not exhibit any precise shapes (LeCorre et al., 2011b). The differences were attributed to the difference in packing arrangements of amylopectin chains within A and B-type starches. The A-type tightly packed configuration displays a parallelepipedic pattern, whereas the B-type, exhibits an open and cavity like circular configuration thereby rendering, square-like and disk-like nanoparticles respectively. However, Xu et al. (2014) working with corn, barley, potato, chickpea and mung bean starch observed round shaped nanocrystals for all starch sources regardless of their crystalline type (Fig 2.13). Although most researchers generally accept that the shape of starch nanocrystals is influenced by the crystalline pattern the results obtained by Xu et al. (2014) indicate that the hypothesis maybe untrue or other factors may play a role in influencing the shape.

Despite their distinct shapes, individual starch nanocrystals have a tendency to form aggregates due to the large number of hydroxyl groups on their surfaces (Kim et al., 2015, Visakh and Yu, 2015). The aggregation behaviour is amongst some of the factors that limit their wide scale industrial application (Kim et al., 2015). Modification of starch nanocrystals can be utilized to minimize aggregation.

LeCorre et al. (2011c) confirmed the effect of amylose on the size of starch nanocrystals. The authors observed an increase in particle size with an increase in amylose content for the same botanical source (waxy maize, normal maize and high amylose maize). The results were attributed to amylose blocking pathways of hydrolysis hence, making it slower and harder and resulting in bigger particles when amylose content is high. However, other studies have attributed size differences to the botanical source of the starch (Dufresne et al., 2013). Depending on the botanical source, amylose can be found in the amorphous regions e.g. wheat or interspersed among amylopectin clusters in both the amorphous and crystalline regions (e.g. normal maize starch), or in bundles between amylopectin clusters or co-crystallized with amylopectin (e.g. potato starch) (LeCorre et al., 2011c). These arrangements could possibly influence the hydrolysis kinetics of starches and thus, the nanocrystal particle size. LeCorre et al. (2011b) observed that despite having the same amylose content, wheat starch nanocrystals (W28) are nearly two times larger than normal maize starch nanocrystals (M27) (Fig 2.14).

Table 2.3: Sizes of starch nanocrystals from different sources

Source	Size (nm)
High amylose starch	118 ± 53[a]
Normal maize starch	58 ± 56[a]
Waxy maize starch	47 ± 42[a]
Wheat starch	100 ± 50[a]
Potato starch	52 ± 4[a]
Pea starch	60-150[b]
Potato starch	3.0[c]
Corn starch	47.0 ± 10.5[d]
Barley starch	54.6 ± 10.8[d]
Tapioca starch	25.5 ± 2.0[d]
Mungbean starch	81.4 ± 7.1[d]
Chickpea starch	61.7 ± 11.7[d]

Adapted from, [b]Zheng et al. (2009), [a]LeCorre et al. (2011b), [c]Rajisha et al. (2014) and [d]Xu et al. (2014)

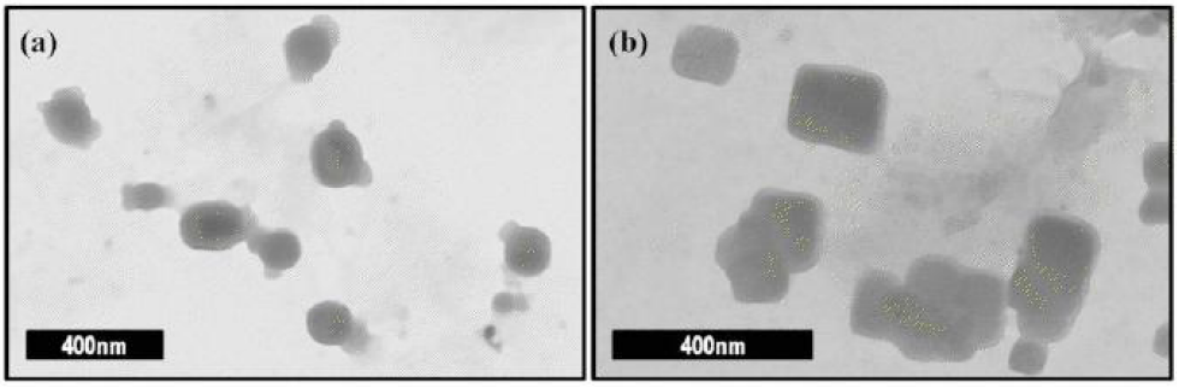

Figure 2.11: Starch nanocrystals derived from a) high amylose (B- crystalline type) b) wheat (A-crystalline type). Adapted from Dufresne et al. (2013)

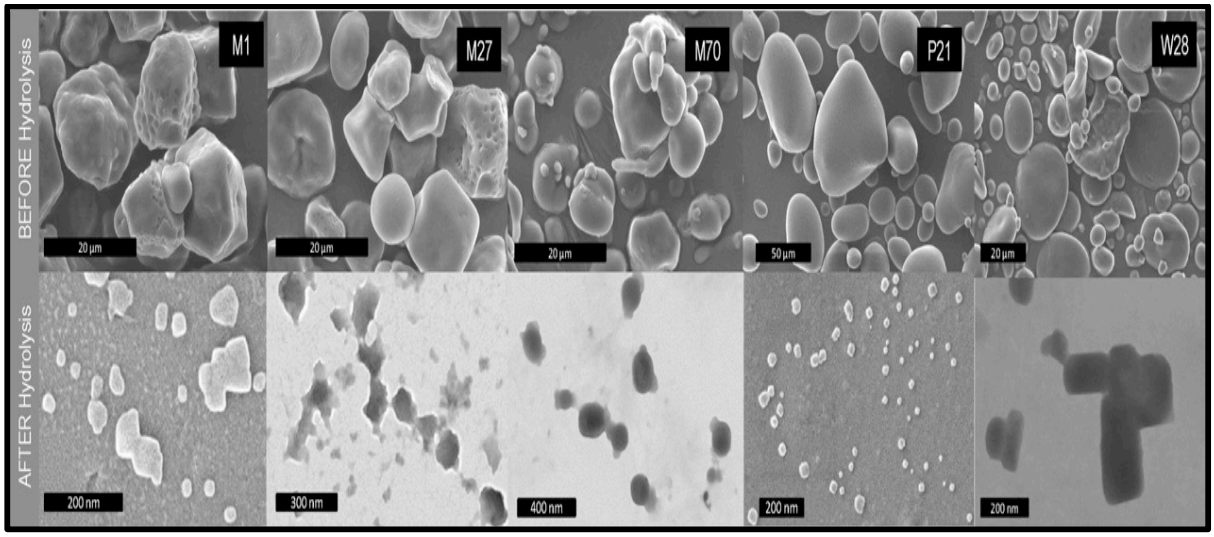

Figure 2.12: Micrograph of native starches and corresponding SNC of normal maize (M 27), high amylose maize (M70), waxy maize (M1), potato (P21) and wheat (W28) respectively. Adapted from Lecorre et al. (2012b)

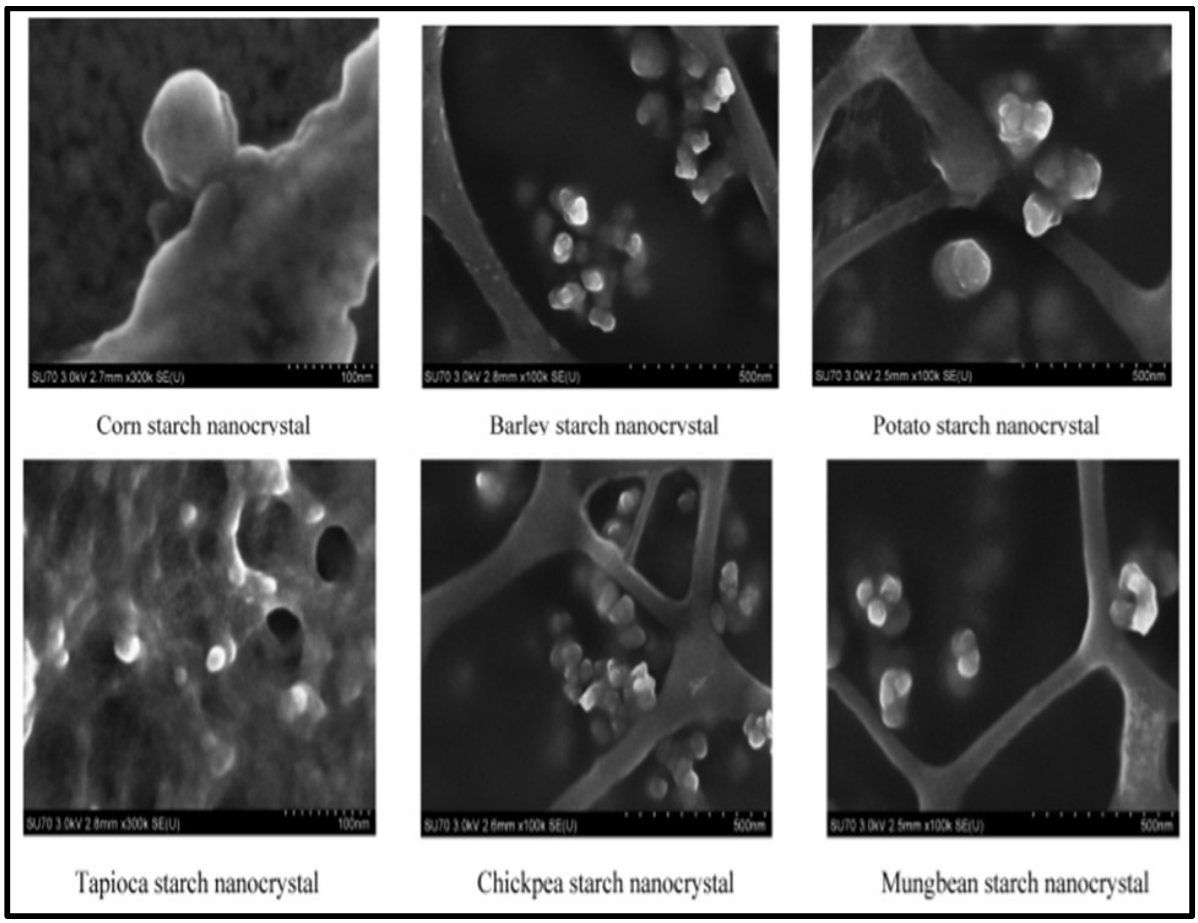

Figure 2.13: Round shaped starch nanocrystals obtained for different starch sources. Adapted from Xu et al. (2014)

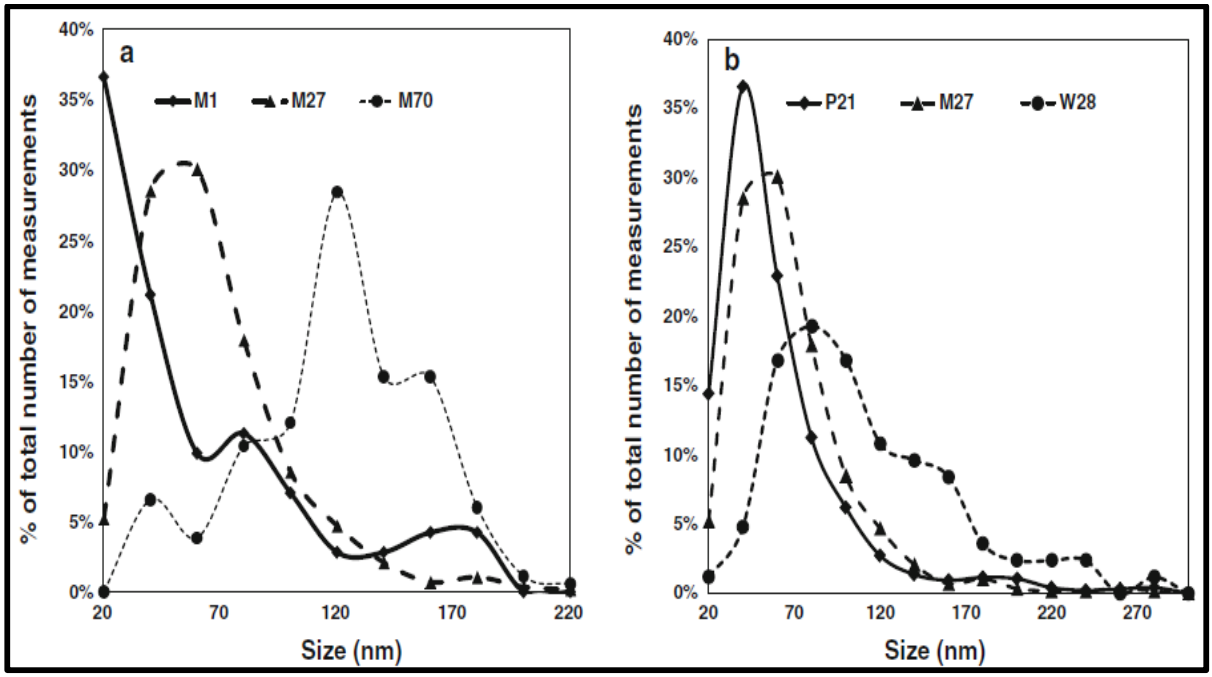

Figure 2.14: Size distribution for a) the same botanic origin and b) the same amylose content. Adapted from LeCorre et al. (2011b)

2.5.2. Crystallinity

Generally, the crystalline type as shown by X-ray Diffraction (XRD) of starch does not change but rather remains the same after acid hydrolysis to produce starch nanocrystals (Kim et al., 2015). However, in comparison to the native starches, the relative crystallinity of starch nanocrystals is higher (Kim et al., 2015). This is due to the selective hydrolysis of the amorphous layer, making the crystalline more distinct (Kim et al., 2015). Kristo and Biliaderis (2007) working with waxy maize starch observed that the A-type crystalline pattern shown by the native starch was preserved after hydrolysis to produce starch nanocrystals. However, in comparison to native starch the starch nanocrystals showed sharper peaks (Fig 2.15). Other scholars also reported similar observations (Thielemans et al., 2006, Mohammad Amini and Razavi, 2016). However, Oladebeye et al. (2013) working with lima beans and jack beans observed a change in crystalline pattern from C-type to V-type after hydrolysis of starch to starch nanocrystals.

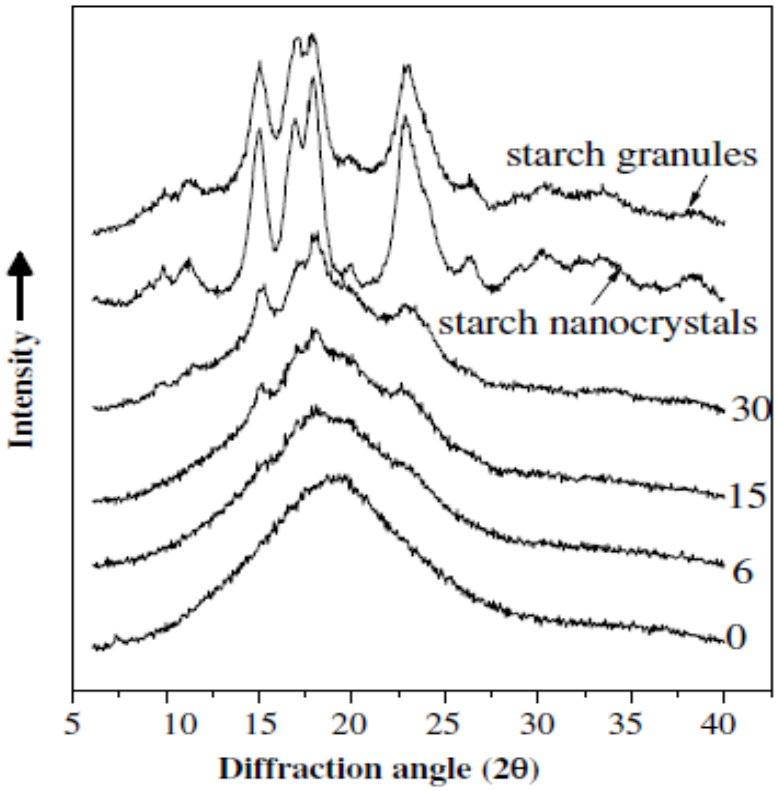

Figure 2.15: XRD spectrum of waxy maize native starch and their respective nanocrystals. Adapted from Kristo and Biliaderis (2007).

2.5.3. Thermal properties

The thermal decomposition properties of starch and starch nanocrystals can be determined using thermo-gravimetric analysis whilst the thermal transitions and enthalpy change are determined by DSC. Their thermal behaviours can be studied in both dry conditions and in excess water. The thermal properties of starch and their respective nanocrystals differ (Lecorre et al., 2012b). Native starches both in excess water and in a dry state have been found to exhibit one endothermic peak (Lecorre et al., 2012b) while starch nanocrystals have been found to exhibit two endothermic peaks both in excess water content and in the dry state (Fig 2.16) (Lecorre et al., 2012b). In excess water, the first endothermic peak has been ascribed to the first phase of crystallites melting (unpacking of the double helixes) and the second transition to the second phase of crystallites melting (unwinding of the helixes). The peaks observed in the dry state for starch nanocrystals have been reported to result from the melting of crystallites, with a direct transition from packed helixes to unwinded helixes. The presence of two peaks in a dry state has been accredited to heterogeneity in the quality of crystallites (Lecorre et al., 2012b).

In comparison to native starches several authors have reported higher transition temperatures and enthalpy change for starch nanocrystals (LeCorre et al., 2012a, Xu et al., 2014a). The findings were ascribed to increased crystallinity, compact packing and increased intermolecular bonding resulting from freeze-drying the nanocrystals, and a decrease in plasticizer (amylose) (LeCorre et al., 2012a, Xu et al., 2014a, Visakh and Yu, 2015). During acid hydrolysis of starch, the amorphous regions of starch predominantly containing amylose are selectively removed. Amylose is regarded as a plasticizer in starch hence its removal results in higher thermal transitions (LeCorre et al., 2012a). The removal of the amorphous regions also result in greater crystallinity of starch nanocrystals in comparison to their corresponding native starches thus, resulting in higher melting temperatures (LeCorre et al., 2012a). Furthermore processing of starch nanocrystals involves freeze drying the nanocrystal suspension. Freeze drying could possibly result in nanocrystals or crystallites that are tightly packed and hydrogen bonded resulting in perfect crystallites with higher melting temperatures (LeCorre et al., 2012a).

The thermal stability of starch nanocrystals has been reported to vary based on crystalline type. LeCorre et al. (2012a) working with normal corn, waxy maize, potato and wheat starches concluded that the thermal stability of B-type starch nanocrystals is greater than that of A-type starch nanocrystals (Fig 2.17). Similarly, Xu et al. (2014), also reported lower transition temperatures for nanocrystals derived from B-type starches (potato starch) in comparison to those of A-type starches (corn, barley and tapioca). The authors attributed the observations to the existence of B-type crystalline structure in potato which melt more readily unlike the more rigid crystallites in A-type starches.

The thermal decomposition properties and stability of starch nanocrystals and their respective nanocrystals can be determined using thermo-gravimetric analysis (TGA). The TGA curve shows weight loss with an increase in temperature and has 3 distinct parts. The first range of the graph represents water loss by dehydration and volatilization of volatile components within the sample. The second range represents depolymerisation of the starch and the last range represents the degradation and decomposition of the backbone of the polymer. LeCorre et al. (2012a) observed slight differences in the TGA curves of starch and starch nanocrystals (Fig 2.18). The authors noted earlier initiation of depolymerisation for starch nanocrystals in comparison to native starch (LeCorre et al., 2012a). The phenomena was attributed to the presence of residual sulphate groups on the surface of starch nanocrystals, which act as a catalyst for the reaction (LeCorre et al., 2012).

The TGA derivative which is the threshold decomposition temperature of starch nanocrystals has been reported to be lower than that of native starches. According to LeCorre et al. (2012a), the presence of sulphate groups on the surface starch nanocrystals caused the decrease in decomposition temperature. Xu et al. (2014) however postulated that the tighter packed crystalline structure and increased intermolecular bonding of the nanocrystals may be responsible for the decrease in thermal decomposition temperature. On the other hand, Namazi and Dadkhah (2010) attributed the decrease in thermal decomposition of starch after hydrolysis to the disruption on the amorphous regions

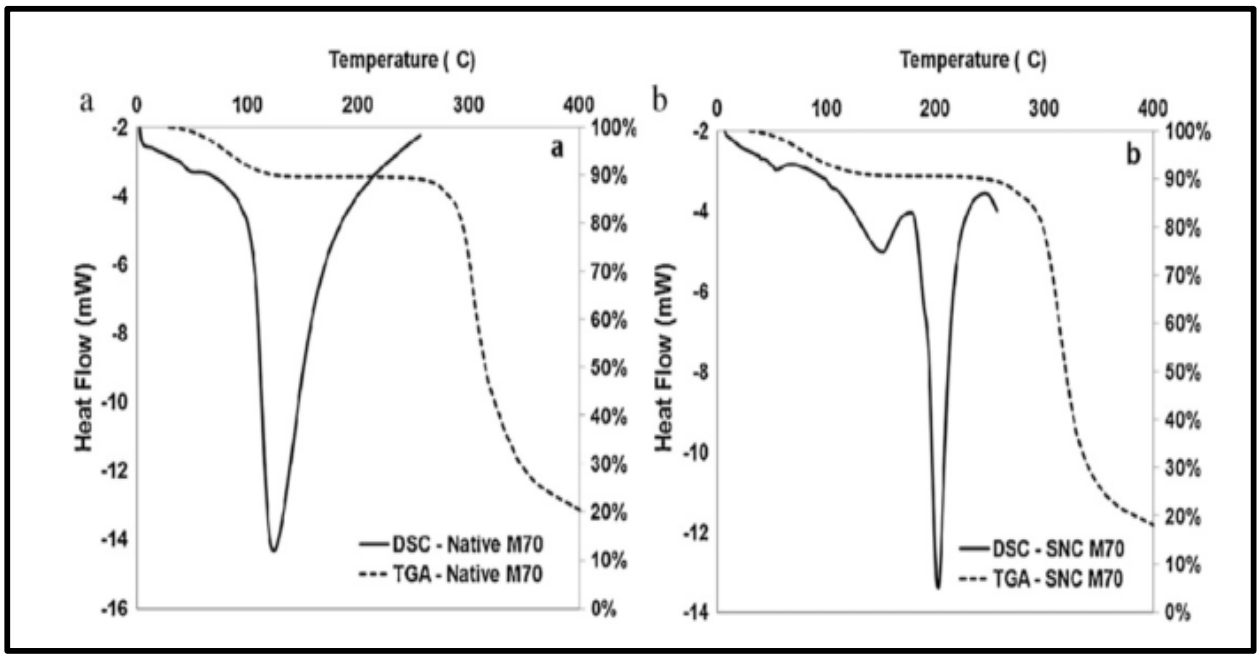

Figure 2.16: DSC and TGA curves for (a) native corn starch and (b) starch nanocrystals. Adapted from LeCorre et al. (2012)

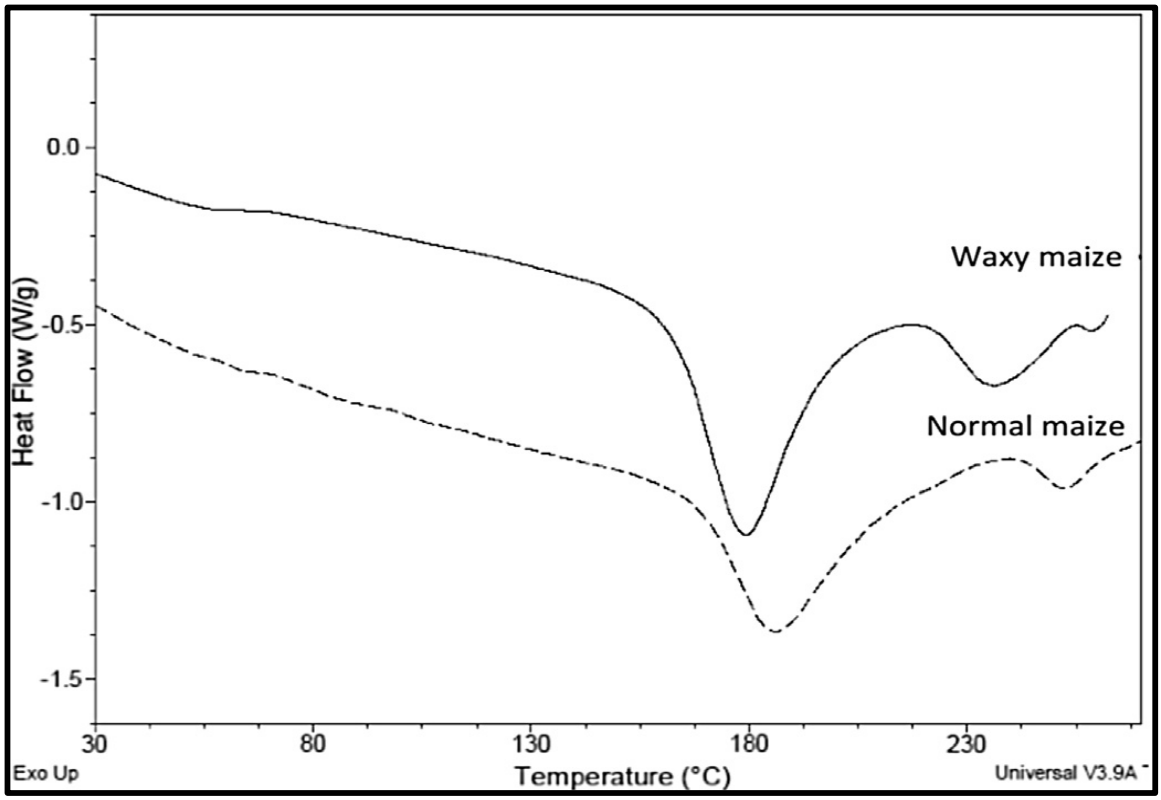

Figure 2.17: DSC thermo-graphs for normal and waxy maize starch nanocrystals. Adapted from Lecorre et al. (2012a)

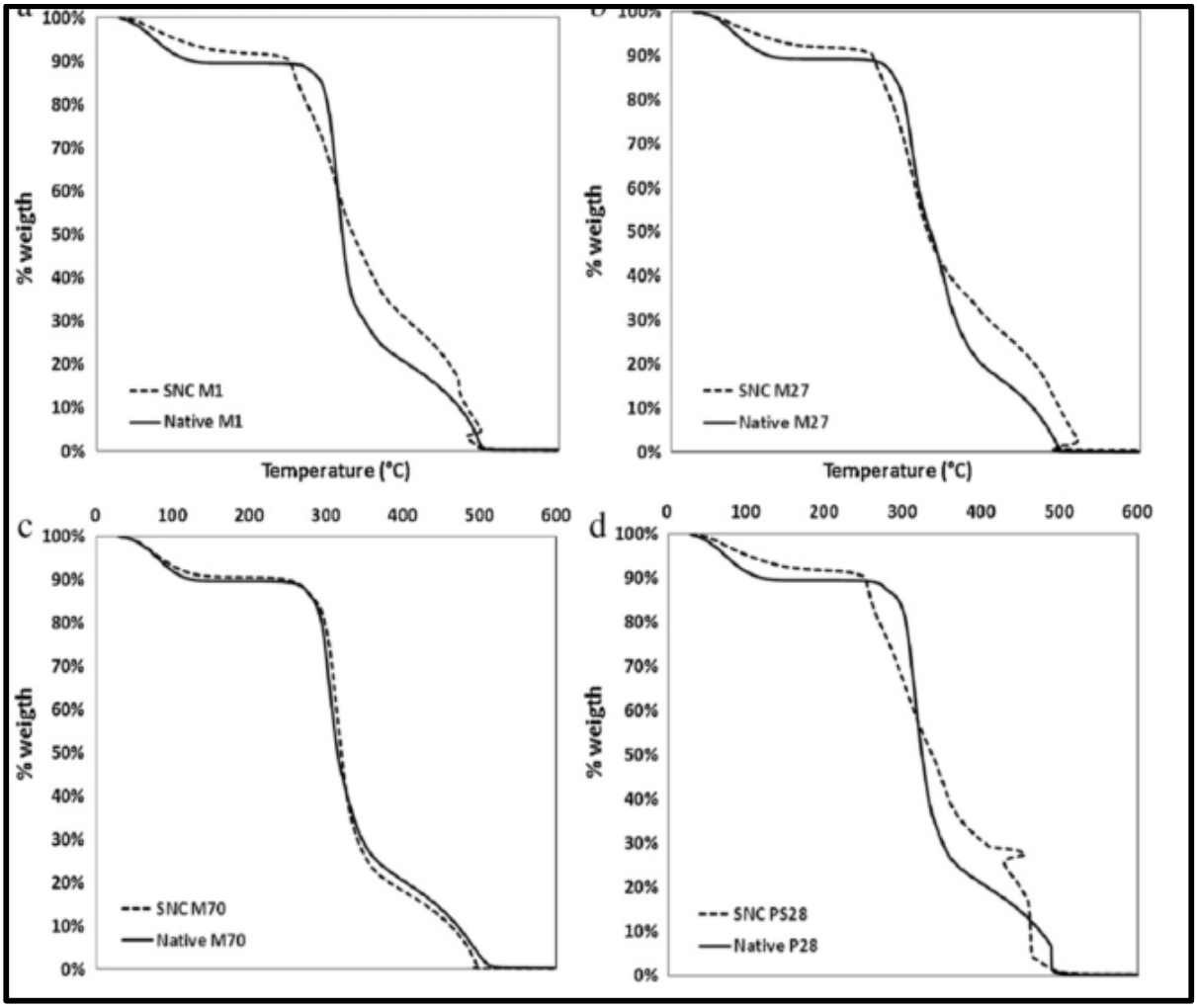

Figure 2.18: TGA curves for starch nanocrystals and their respective starch nanocrystals. M1 (waxy maize), M27 (normal maize), M70 (high amylose maize) and P28 (potato). Adapted from LeCorre et al. (2012a)

2.7. Potential applications of starch nanocrystals

Starch nanocrystals have potential applications in the food, pharmaceutical and packaging industry. Promising areas of application within the food industry are in pickering emulsions and nano-encapsulation. In the packaging industry, nanocrystals can be applied as fillers and reinforcements in composite films. This section will focus on the application of nanocrystals in pickering emulsion and in composite films.

2.7.1. Pickering emulsions

Emulsions are systems comprising of two immiscible liquids, with one being the dispersed phase and the other the continuous phase (Li et al., 2014). Emulsions are thermodynamically unstable due to the unfavourable interaction between oil and water (Akoh and Min, 2008). Water molecules tend to form strong hydrogen bonds with other water molecules, instead of oil molecules in the emulsions resulting in separation of water and oil (Akoh and Min, 2008). To ensure stability of emulsions emulsifiers are utilized. Emulsifiers are surface active compounds that stabilize emulsions through forming a protective membrane that prevents particle aggregation and consequent phase separation (Akoh and Min, 2008). The most common types of emulsifiers are lipids and amphiphilic biopolymers (Akoh and Min, 2008). However, the use of solid particles with dimensions ranging from micrometre to nanometre to stabilize emulsions has attracted a lot of research interest (Li et al., 2012, Visakh and Yu, 2015). The irreversible anchoring and intermolecular interactions at the interface form the physical basis of the unique properties of particle-stabilised emulsions (Li et al., 2012, Li et al., 2014). The size of starch nanocrystals, their platelet morphology and ease of surface modification to attain different hydrophobicities make them a good candidate for stabilizing pickering emulsions (Visakh and Yu, 2015). Due to the functional properties of starch nanocrystals, their use also provides other benefits such as short term formulation cycles for the emulsions (Visakh and Yu, 2015). In addition, starch is relatively inexpensive, abundant, biocompatible, biodegradable and non-toxic (Li et al., 2014, Visakh and Yu, 2015). Li et al. (2014) used starch nanocrystals to stabilize oil-in-water emulsions. The authors observed that the nanocrystals could adsorb at the oil-in-water interface resulting in highly stable emulsions with high stability against coalescence (Li et al., 2014).

2.7.2. Biodegradable films

Starch nanocrystals can be applied as a reinforcement to improve the mechanical, thermal and barrier properties of biodegradable films (Lin et al., 2011). Biodegradable polymers are defined as materials that have the ability to degenerate or break down naturally into biogases and biomass when exposed to a microbial environment, and moisture either under aerobic or anaerobic conditions (Avella et al., 2005, Lagaron and Lopez-Rubio, 2011). Bio-based polymers are generally categorized into three families (Fig 2.19). The first family comprises of polymers that are directly extracted from biomass such as those derived from polysaccharides like starch and proteins such as gluten and zein (Lagaron and Lopez-Rubio, 2011).

The second family comprises of polymers made from utilizing biomass-derived monomers using classical chemical synthetic routes (Lagaron and Lopez-Rubio, 2011). These include thermoplastics and thermosets such as those derived from vegetable oils and polylactates. The third group consists of polymers produced by the activity of natural or genetically modified micro-organisms such as polyhydroxyalkanoates (Rindlava et al., 1997) and polypeptides such as the elastin-like polymers (Lagaron and Lopez-Rubio, 2011).

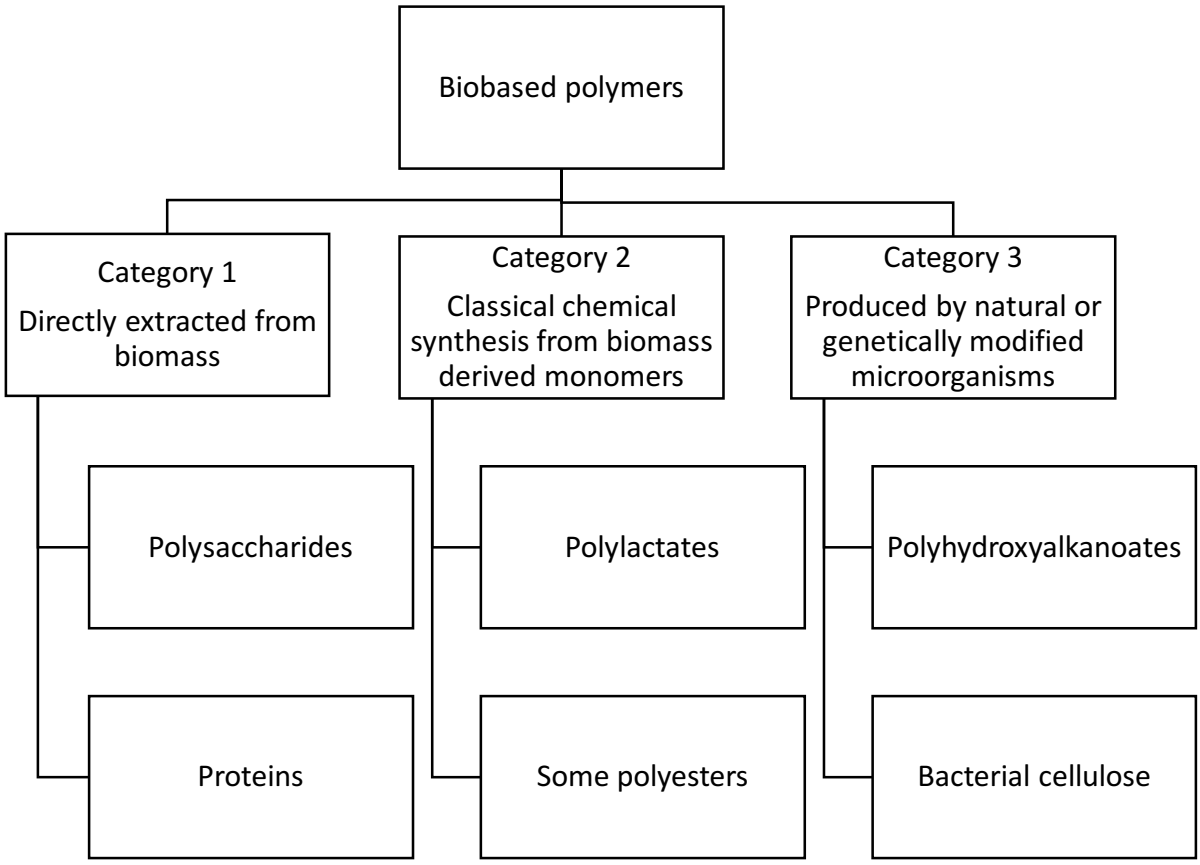

Figure 2.19: Categories of biodegradable polymers. Adapted from Lagaron and Lopez-Rubio (2011)

2.7.3. Types and properties of biodegradable films

This section will focus on the different types of biodegradable films that can be reinforced with starch nanocrystals as well as the resulting nanocomposites.

Starch films

Biodegradable or edible starch films can be produced from native starch or its major constituents amylose and amylopectin using wet or dry methods (Jiménez et al., 2012).

Native starch is not thermoplastic but under certain conditions (heat and water) it becomes a thermoplastic material (Jiménez et al., 2012).

Starch is an ideal candidate for film production because it can form a continuous matrix, it has a relatively lower permeability to oxygen compared to other non-starch films and it has a relatively low cost (Rindlava et al., 1997, Jiménez et al., 2012). Starch films are transparent, odourless, tasteless and colourless (Jiménez et al., 2012). Starch films are inherently hydrophilic in nature and have a tendency of absorbing large amounts of water in conditions of elevated relative humidity (Wilhelm et al., 2003, Mali et al., 2005). Therefore, there is a need for modification or application of fillers to starch films to improve this limitation.

Corn zein films

Zein is the main storage protein of corn and accounts for 44–79% of the endosperm protein, depending on the corn variety and separation method used (Lawton, 2002). It is an alcohol-soluble protein that is classified as a prolamin (Lawton, 2002, Park et al., 1994). Zein has exceptional film and fibre forming properties, hence, it can be utilised for the production of biodegradable films (Park et al., 1994). Zein has a high content of non-polar amino acids resulting in it being hydrophobic (Wittaya, 2012). Zein films are made through the development of hydrophobic interactions, hydrogen bonds and to a lesser extent disulphide bonds between zein chains (Wittaya, 2012).

Zein also possesses good barrier properties and good heat sealability (Ryu et al., 2002). Park et al. (1994) found zein films to reduce moisture, firmness and colour loss due to reduction of oxygen and carbon dioxide transmission. Oxygen permeability values reported for zein films are lesser in comparison to those reported for polyethylene and poly(vinyl chloride) (Lawton, 2002). Fillers and modifications (chemical and physical) can be utilized to enhance the permeability properties of zein.

Soy protein films

Soybeans contain approximately 38-44% protein which is relatively higher compared to cereal proteins (8-15%) (Wittaya, 2012). The majority (90%) of soy bean protein are globulins that can be fractionated into 2S, 7S, 11S and 15S based on their sedimentation coefficients (Wittaya, 2012). The two major storage globulins in soy beans: beta-conglycinin and glycinin (Friesen et al., 2015).

Soy protein is a good candidate for biodegradable film production due to its thermoplasticity, easy availability, low cost and bio-degradability (Zheng et al., 2009, Wittaya, 2012). Soy film formation is regarded as a two-step process that involves the disruption of the protein structure through heating of film solutions, cleavage of native disulphide bonds and exposure of the sulfhydryl groups and hydrophobic groups. The final step involves the formation of new disulphide, hydrophobic and hydrogen bonds (Wittaya, 2012). During the drying process, the unfolded proteins bond through intermolecular interactions, such as the disulphide bonds and hydrophobic interactions resulting in the formation of a strong network (Wittaya, 2012).

Soy protein films exhibit poor moisture barrier properties owing to their inherent hydrophilic nature (Wittaya, 2012). Soy protein films have relatively good tensile strength, stiffness and yield point due to the strong charge and polar interactions between side chains of soy protein molecules that restricts molecular mobility and segment rotation (Wittaya, 2012). To improve these properties there is a need for modification or application of fillers.

Wheat gluten films

Wheat gluten is a water insoluble protein derived from wheat flour. Gluten consists of a combination of polypeptide molecules, and is regarded as a globular protein (Wittaya, 2012). It comprises primarily of two groups of water insoluble proteins: gliadins, consisting of low molecular weight proteins; and glutenins containing high molecular weight proteins. Gliadins are single monomeric proteins in which disulphide bonds make up intra-chains or are absent, while glutenins form high molecular weight polymers are held together by inter-chain disulphide bonds (Belton, 1999).

The inherent cohesiveness and elasticity of gluten facilitates film formation (Wittaya, 2012). Cleavage of native disulphide bonds resulting from the heating of film-forming solutions and the formation of new disulphide bonds during film drying along with hydrogen and hydrophobic bonds, is believed to play a crucial role in the formation of wheat gluten films structure (Wittaya, 2012). Wheat gluten films possess good oxygen barrier properties, but poor water vapour barrier properties (Irissin-Mangata et al., 2001). The poor water vapour permeability of wheat gluten films is due to the inherent hydrophilic nature of the protein (Irissin-Mangata et al., 2001, Wittaya, 2012,). Gluten films have poor mechanical properties hence, have a need for plasticizer or fillers to improve flexibility (Irissin-Mangata et al., 2001).

Of the films discussed above, starch films and soy protein films have received much research attention. This is mainly due to their good film forming properties as well as their low cost and easy availability. Despite their good film forming properties, scholars generally agree that they are limited in their physicochemical properties and therefore, are not ideal packaging material. There is therefore need for effective methods of improving these properties.

2.8. Nanocomposite films

This section focuses on the application of starch nanocrystal to the above-mentioned films.

When starch nanocrystals or any other nanoscale fillers are added to a matrix such as protein or starch films the resulting material is a nanocomposite film. Composites are materials which comprise of two components: the matrix which is the continuous phase whose function is to support, protect the filler materials, transmit and distribute the applied load to them and fillers (dispersed phase), which are the stronger and stiffer components reinforcing the matrix (Arora and Padua, 2010). Polymer nanocomposites are produced by dispersing an inert, organic or inorganic nanoscale filler into a polymeric matrix (Duncan, 2011). The filler can be in the form of nanoparticles, nanotubes and nanocrystals (Duncan, 2011). These nano fillers should be homogenously dispersed in the composite for proper functionality (Dufresne et al., 2013). The dispersion of the fillers is based on the size, shape, concentration in the matrix, functional groups present on the nanofiller surface, interactions between the matrix and the filler (Dufresne et al., 2013).

When the matrix and filler are properly mixed, the resultant polymer materials have been found to show enhanced modulus, dimensional stability, barrier properties, thermal properties (melting point, degradation and glass transition temperatures), and alteration in wettability and hydrophobicity (Duncan, 2011, Sorrentino et al., 2007). The enhancement of these properties is dependent on the type and effectiveness of interactions at the interfacial region (Fig 20) (Sorrentino et al., 2007). Nanocomposites also present other benefits such as low density, transparency, good flow and surface properties (Sorrentino et al., 2007).

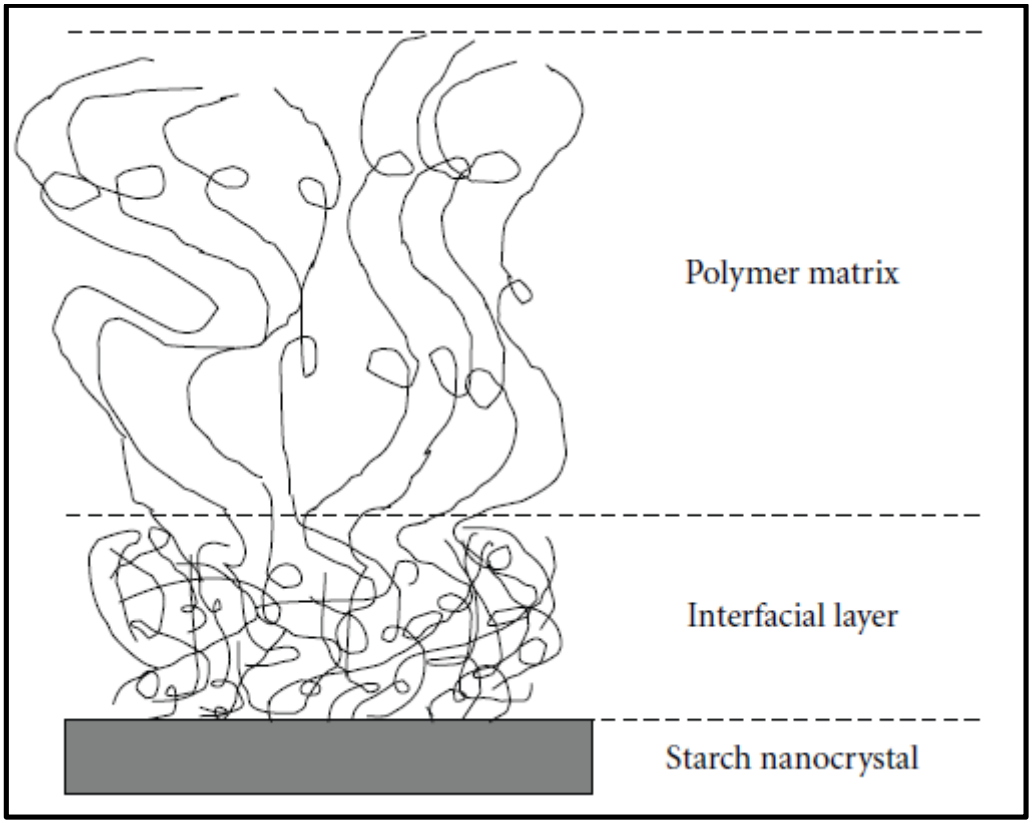

Figure 2.20: Formation of interfacial layer. Adapted from Azeredo (2009).

2.8.1 Types of fillers/Nano reinforcements

There are various types of organic and inorganic nanomaterials, other than starch nanocrystals that can be used as fillers in bio-composite films and these include cellulose, silica and chitin.

Clay and silica

Clay and silica nanoplatelets are the most researched and promising inorganic nanofillers owing to their availability, low cost, significant enhancements and relatively simple processability (Azeredo, 2009, Duncan, 2011). Depending on the strength of interfacial interactions between the matrix and the filler different morphological arrangements can be achieved by clay nanoparticles: non-intercalated nanocomposites, intercalated nanocomposites, exfoliated nanocomposites and flocculated nanocomposites (Fig 2.21) (Duncan, 2011, Azeredo, 2009). The incorporation of low contents of nanoclays (less than 10 wt%) to bio-degradable films has been found to cause a significant increase in rigidity (elastic modulus), thermal and dimensional stability. Furthermore, an improvement in gas barrier properties, UV-vis protection and conductivity was noted (Sanchez-Garcia et al., 2010, Lagaron and Lopez-Rubio, 2011).

Sadegh-Hassani and Mohammadi Nafchi (2014) observed an increase in mechanical strength and decrease in gas permeability with the addition of haloysite nanoclay to potato starch films. However, it should be noted that the homogeneous dispersion of most clays in organic polymers is difficult due to the hydrophobicity of its surface (Azeredo, 2009). This a major drawback in the utilization of clay and silica nanocrystals.

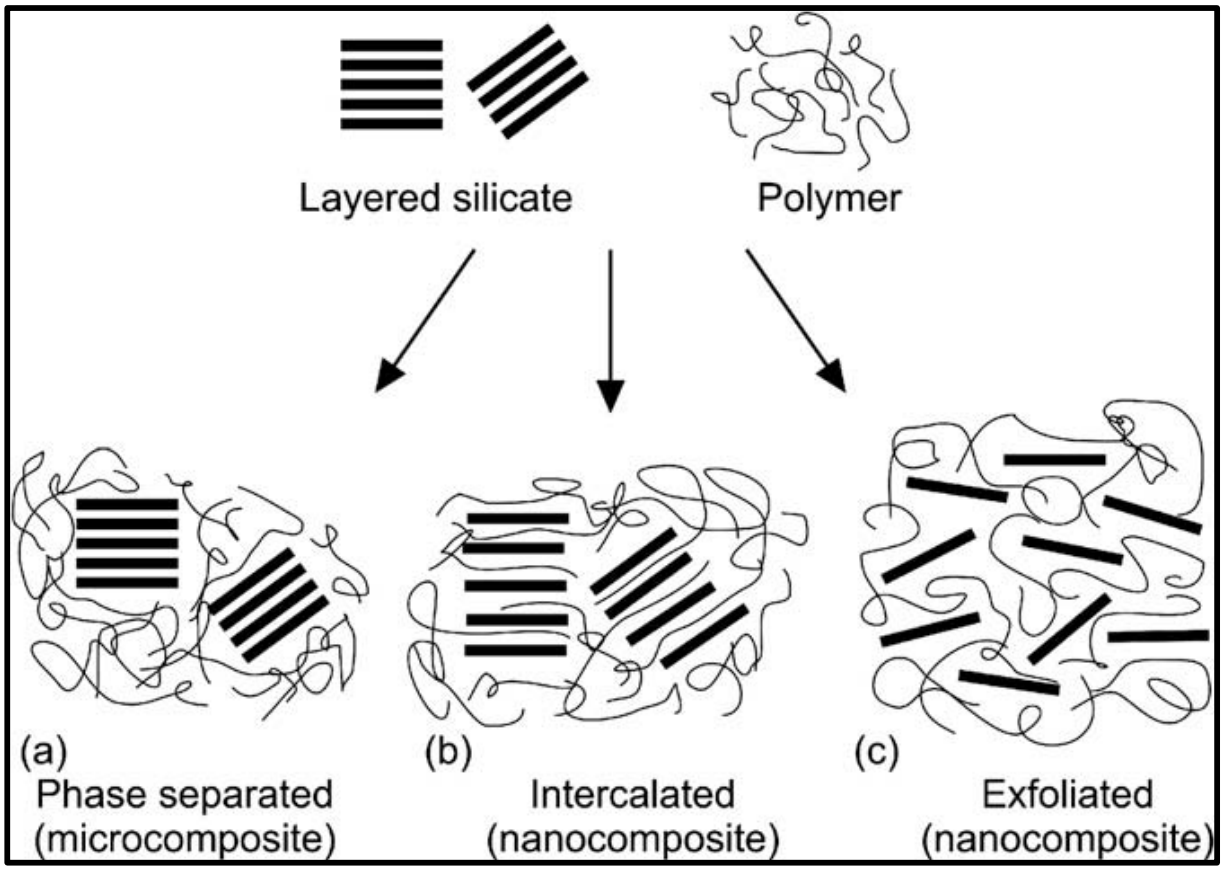

Figure 2.21 Types of composite formed from interaction between clays and polymers: (a) phase-separated microcomposite; (b) intercalated nanocomposite and (c) exfoliated nanocomposite. Adapted from Azeredo (2009)

Cellulose nanowiskers

Cellulose is a structural polysaccharide found in many plants and is a strong natural polymer with excellent reinforcing properties (Azeredo, 2009). Cellulose chains are synthesized to form nanofibres, which are bundles of molecules that are elongated and stabilised through hydrogen bonding (Fig 2.22) (Azeredo, 2009). Two types of nano-reinforcements can be obtained from cellulose and these are microfibrils (nanofibres) and nanowhiskers (Slavutsky and Bertuzzi, 2014).

Cellulose nanofibres and whiskers are an attractive source of nanomaterial due to their low cost, light weight, low energy consumption during manufacturing and high-strength nano-composites (Azeredo, 2009, Slavutsky and Bertuzzi, 2014). The microfibrils have nanosized diameters (2‑20 nm, depending on the origin), and lengths in the micrometre range (Slavutsky and Bertuzzi, 2014). Each microfibril is formed by aggregation of elementary fibrils, which are made up of crystalline and amorphous regions (Slavutsky and Bertuzzi, 2014). The crystalline parts, which can be isolated by several treatments, are the whiskers, also known as nanocrystals or nanorods (Slavutsky and Bertuzzi, 2014).

Cellulose nano-reinforcements have been reported to improve strength, modulus of polymer matrices and elongation. The addition of cellulose whiskers to starch systems has been found to enhance their thermal properties, mechanical properties, barrier properties and keeps their biodegradability properties (Azeredo, 2009). Slavutsky and Bertuzzi (2014) observed that the incorporation of cellulose nanocrystals into a starch film matrix resulted in improved water resistance and water barrier properties. These observations have been attributed to mechanical percolation effects, geometry, dimensions and consequent aspect ratios of the cellulose fibres (Azeredo, 2009).

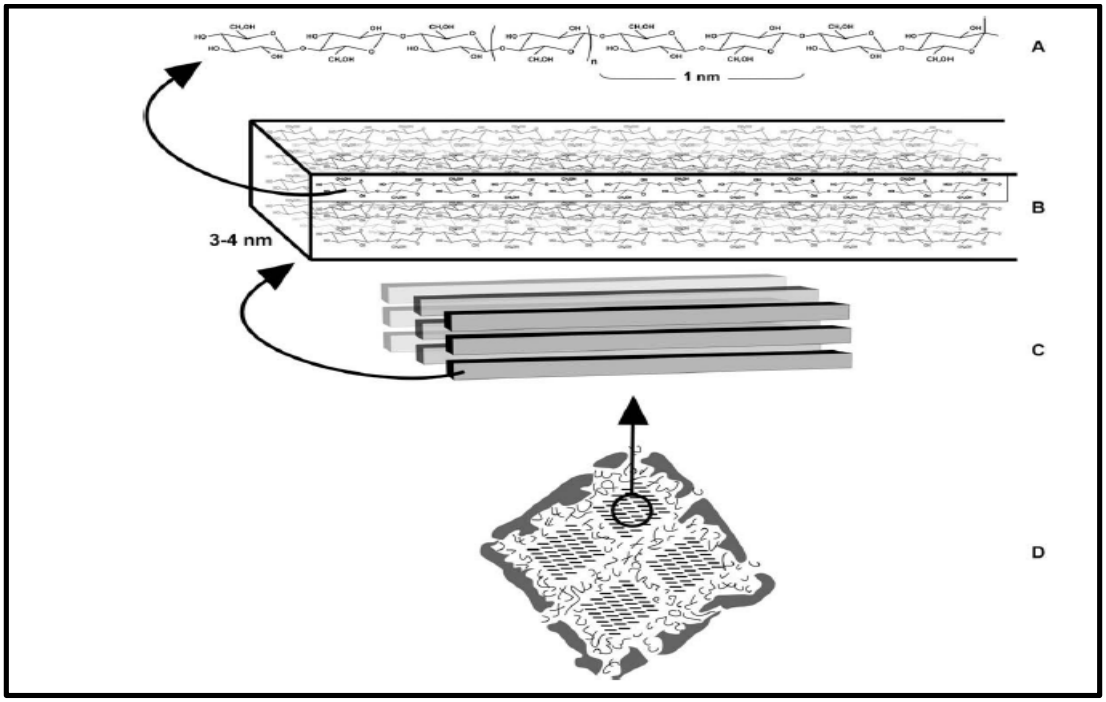

Figure 2.22: Internal structure of a cellulose microfibril: (A) a cellulose chain; (B) an elementary fibril containing bundles of cellulose chains; (C) parallel elementary fibrils; (D) four microfibrils held together by hemicellulose and lignin. Adapted from Azeredo (2009)

2.9. Effect of application of starch nanocrystals on the mechanical, thermal and permeability properties of bio-films

This section will focus on the influence of starch nanocrystals on the physico-chemical properties of biodegradable films. Starch nanocrystals have a competitive advantage over other nanofillers. Some of their advantages include their biodegradability, ease of production of the nanocrystals, their morphology, cyclic availability and low cost of starch. Starch nanocrystals can improve the thermal, mechanical and permeability properties of biodegradable films when added as fillers.

2.9.1. Permeability properties

Many food products are sensitive to oxidation and microbial growth stimulated by moisture hence, packaging material should provide good barrier properties (Sanchez-Garcia et al., 2010, Duncan, 2011, Bradley et al., 2011, Robertson, 2016). Biodegradable films generally have a low permeability in comparison to synthetic plastics. Permeability is defined as the quantification of permeate transmission, gas or vapour, through a resisting material (Siracusa, 2012). In non-defective materials the chief mechanism for transmission of water vapour or gaseous molecules is through diffusion (Siracusa, 2012). The permeability of polymers to oxygen or moisture depends upon multiple interrelated factors, and these include polarity and structural characteristics of polymeric side chains, hydrogen bonding characteristics, molecular weight, size, shape and polydispersity of the permeating molecule, degree of branching or cross-linking, processing methods and degree of crystallinity of the polymer (Duncan, 2011, Siracusa, 2012).

The major reason for adding nano-fillers in biodegradable polymeric matrices is to improve their permeability properties to gases and aromatic compounds (Sanchez-Garcia et al., 2010, Smolander and Chaudhry, 2010). The addition and dispersal of nanoscale fillers into a polymer matrix has been reported to improve the barrier properties of the polymer film in two precise ways (Duncan, 2011). Firstly, the dispersed fillers result in the creation of a tortuous pathway for diffusion of gas molecules (Fig 2.23) (Bradley et al., 2011, Dufresne et al., 2013). Gas molecules will travel around nano-fillers instead of taking a straight line path that lies perpendicular to the film surface resulting in longer mean path of diffusion (Duncan, 2011, Bradley et al., 2011). Secondly, the fillers cause changes to the polymer matrix itself at the interfacial regions thus, influencing permeability (Duncan, 2011).

If the polymer-filler interactions are favourable, polymer strands located in close proximity to nanosized filler can be partially immobilized. This results in reduced speed of diffusion of gas molecules traveling through these interfacial zones (Duncan, 2011).

García et al. (2009) observed a 40% decrease in water vapour permeability of cassava films filled with 2.5 wt.-% starch nanocrystals and the phenomena was attributed to the creation of a tortuous pathway by the starch nanocrystals, thus hindering water diffusion. Piyada et al. (2013) investigated the effect of the addition of rice starch nanocrystals between 5% and 20% concentration on the water vapour permeability of rice starch films and observed a decrease in water vapour permeability with an increase in starch nanocrystal concentration (Fig 2.24). However, Zheng et al. (2009) did not observe any significant changes in the water uptake of soy protein films with the addition of starch nanocrystals. The authors attributed the observations to the strong interfacial attraction between the starch nanocrystals (filler) and the soy protein isolate matrix (Zheng et al., 2009).

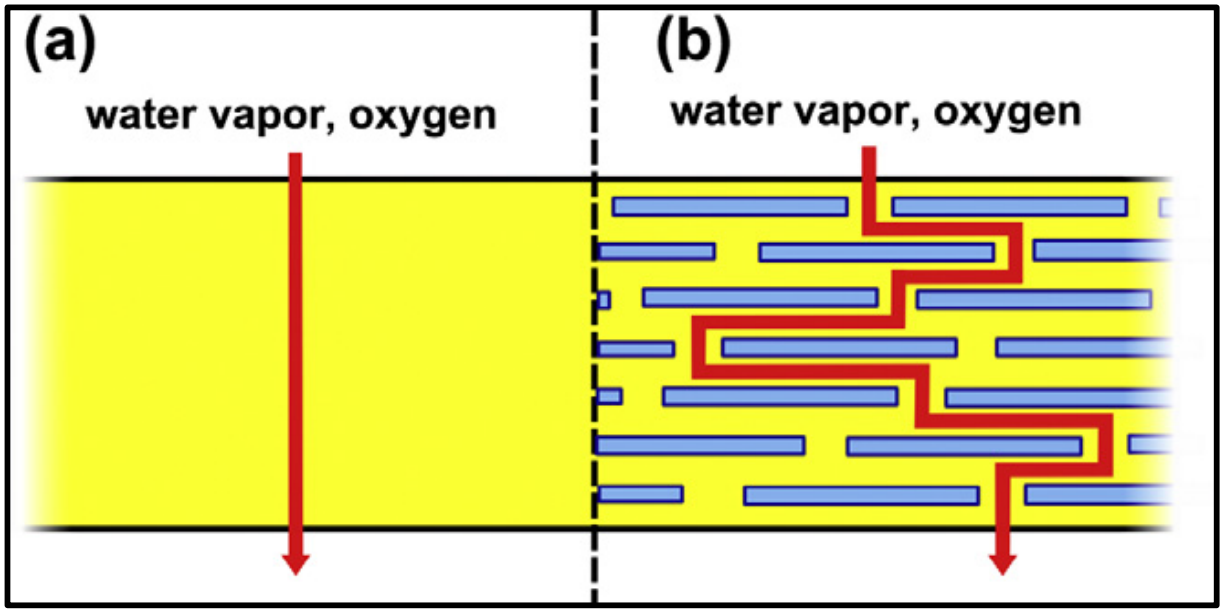

Figure 2.23: Tortuous pathway created by addition of nanocrystals. Adapted from Duncan (2011)

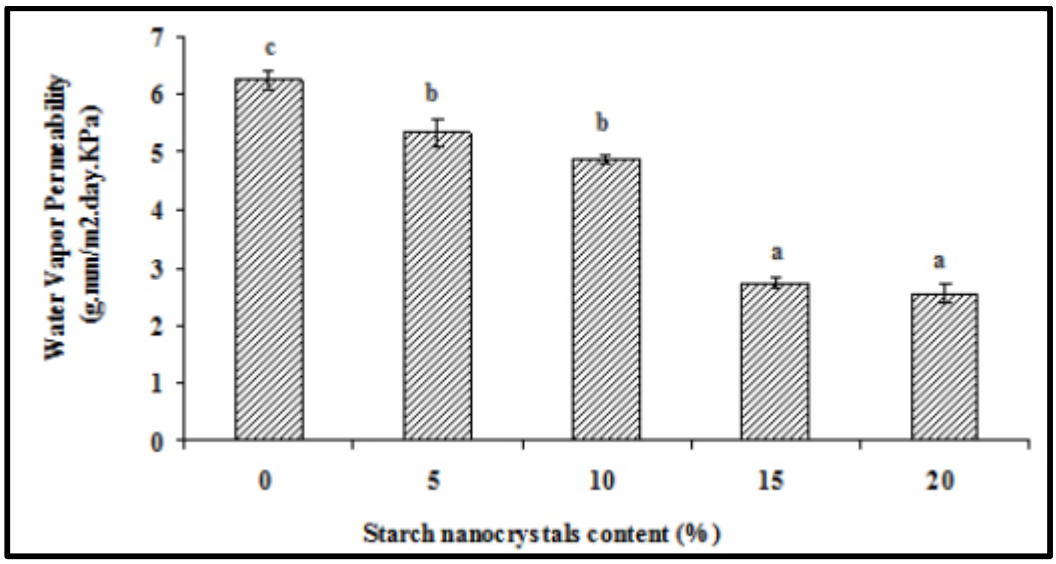

Figure 2.24: Effect of addition of starch nanocrystals on water vapour permeability. Adapted from Piyada et al. (2013).

2.9.2. Mechanical properties

The properties of nanocomposites including mechanical properties are influenced by several factors including the various structures of matrices, the network among nanofillers and polymer matrix, the interfacial interactions, the scale of dispersion, morphology, and the surface functionality of the nanocrystals (Lin et al., 2011b). A percolation mechanism, determined by three-dimensional networks formed by the interconnection of polysaccharide nanocrystals and stabilized by hydrogen bonding, is the principal contributor to reinforcement of the resultant nanocomposites as it enhances tensile strength and Young's modulus, gives a higher storage modulus, a thermally stable rubbery plateau (Lin et al., 2011b). Zheng et al. (2009) working with soy protein films noted an increase in tensile strength and young's modulus with the addition of pea starch nanocrystals up to 2% and thereafter, further increase resulted in reduction in tensile strength and young's modulus (Fig 2.25). The observation was attributed to uniform distribution of starch nanocrystals as a stress concentrated point within the soy protein film matrix. The decrease in tensile strength and Young's Modulus with an increase of starch nanocrystals beyond 2% was attributed to the tendency of nanocrystals to self-associate forming aggregates which decreased the effective active surface area of starch nanocrystal for interacting with the soy protein matrix and resulted in destruction of the ordered structure within the soy protein matrix (Zheng et al., 2009). Condés et al. (2015b) observed similar results working with amaranth protein films reinforced with maize starch nanocrystals.

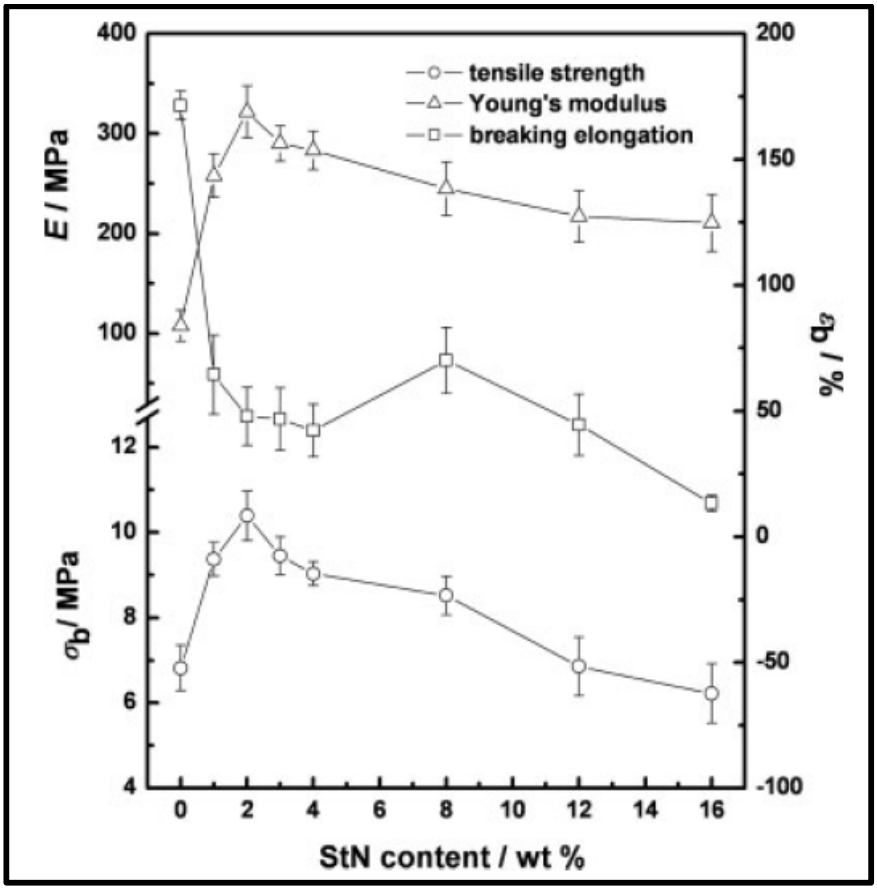

Figure 2.25: Effect of starch nanocrystal addition on the mechanical properties of soy protein films. Adapted from Zheng et al. (2009)

2.9.3. Thermal properties

The most important thermal properties of starch nanocomposites are the glass transition temperature and thermal decomposition (Dufresne et al., 2013). The glass transition temperature is critical at which the material changes behaviour from glassy (hard and brittle) to rubbery (elastic and flexible) and can be determined using DSC and DMA (Dufresne et al., 2013). The glass transition of starch-based nanocomposites shifts to a higher temperature with the addition of nanocrystals because of hindrance of polymer mobility resulting from interactions between the nanofiller and the starch matrix (Dufresne et al., 2013)

Condés et al. (2015) working with amaranth protein films observed that the glass transition temperature shifted towards higher temperatures with an increasing amount of nanocrystals (Table 2.4). The phenomena was attributed to a restriction of the mobility of protein chains due to the establishment of strong interactions through hydrogen bonding both between starch nanocrystals and also between the filler and the matrix (Condés et al., 2015). Interfacial H-bonding of that nature leads to a strong adsorption of polymer chains on the surface of

nanoparticles and formation of 'trapped entanglements' of the polymer segments, causing hindrance of mobility of polymer chains attached to the particle surface, and also those without direct contact with the filler surface (Condés et al., 2015).

Table 2.4: Glass transition temperature (Tg) for films prepared from amaranth protein isolate, and normal and waxy maize starch nanocrystals

	Starch nanocrystal content (wt %)	T_g (°C)
Control	0	-69 ± 1^a
Normal maize	6	-57 ± 2^b
	12	-57 ± 1^b
Waxy maize	6	-69 ± 1^a
	12	-55 ± 1^b

All values were average ± SD of two values. Reported average values of all parameters within a column with the same superscripts (a and b) were not significantly different ($P < 0.05$). Adapted from (Condés et al., 2015b)

2.10. Conclusion

There are limited studies on the characterization and application of starch nanocrystals in bio-composite films. Generally, the majority of the research done in this area, utilized conventional sources of starch. Therefore, this presents a research gap for nanocrystal production using alternative starch sources. Key considerations for proper selection of a good candidate source for SNC production include the high yield of starch, low amylose content and small granule size. Several alternative starch sources including amadumbe possess these qualities and hence, are potentially good candidates for SNC production.

South African grown amadumbe varieties have never been utilized for the production of starch nanocrystals. There is therefore a lack of knowledge on the physicochemical properties of nanocrystals produced from amadumbe. This knowledge is fundamental in identifying potential applications of amadumbe SNC and can thus promote its commercial utilization. Furthermore, in light of the shift by industry towards biodegradable packaging, one of the promising areas of application of amadumbe SNCs is in improving the physicochemical properties of biodegradable films.

Amadumbe SNC have never been applied as fillers in amadumbe starch, potato starch and soy protein films. Knowledge of the effect of amadumbe SNC on starch and soy protein films is important to enhance ultimate utilization.

2.10. Aim, hypothesis and objectives

2.10.1 Aim

To evaluate the physico-chemical properties of amadumbe starch nanocrystals and assess their efficacy in improving the mechanical, barrier and thermal properties when applied as fillers in protein and starch films.

2.10.2. Hypothesis

1. Acid hydrolysis of amadumbe starch will result in the production of amadumbe starch nanocrystals. Starch essentially comprises of alternating amorphous and crystalline regions (Copeland et al., 2009,BeMiller, 2009). During hydrolysis the amorphous regions are selectively removed resulting in nanocrystals, a crystalline residue with platelet morphology. Several scholars have yielded starch nanocrystals through acid hydrolysis (Angellier et al., 2004, Xu et al., 2010, LeCorre et al., 2011b).
2. The addition of amadumbe starch nanocrystals will result in improved mechanical, barrier and thermal properties of starch and protein films. The improved mechanical properties result from a synergistic effect arising from the formation of reinforcement (nanocrystals) matrix (film) interface with its own physical properties, increased by high surface/volume ratio provided by the nanocrystals. Permeability properties will improve due to creation of a tortuous pathway by the dispersed nanocrystals thereby, hindering proper diffusion of molecules. Piyada et al. (2013) working with rice starch noted an increase in the tensile strength, endothermic heat flow and a decrease in water vapour permeability with the addition of rice starch nanocrystals.

2.10.3. Objectives

1. To produce and evaluate the physico-chemical properties (morphological, thermal and crystallinity) of amadumbe starch nanocrystals using SEM-FEG, AFM,TGA, DSC, FTIR, XRD and nanosizer experiments.
2. To determine effect of adding amadumbe starch nanocrystals on the mechanical, thermal and permeability properties of starch films using a texture analyser, DSC and permeability tests respectively.
3. To determine effect of adding amadumbe starch nanocrystals on the mechanical, thermal and permeability properties of protein films using a texture analyser, DSC and permeability tests respectively.

CHAPTER 3

3.0. Characterization of amadumbe starch nanocrystals

Abstract

Amadumbe (*Colocasia esculenta*), commonly known as taro is a tropical tuber that produces starch-rich underground corms. In this study, the physicochemical properties of starch nanocrystals (SNC) prepared by acid hydrolysis of amadumbe starches were investigated. Two varieties of amadumbe corms were used for starch extraction. Amadumbe starches produced a substantially high yield (25%) of SNC's. These nanocrystals appeared as aggregated and individual particles, and possessed square-like platelet morphology with the size of 50-100 nm. FTIR revealed high peak intensities corresponding to O-H stretch, C-H stretch and H_2O bending vibrations for SNCs compared to their native starch counterparts. Both the native starch and SNC exhibited the A–type crystalline pattern. However, amadumbe SNCs showed a higher degree of crystallinity and slightly reduced melting temperatures than their native starches. Amadumbe SNCs presented similar thermal decomposition properties as their native starches. Amadumbe starch nanocrystals may have potential application in bio-composite films due to their square-like platelet morphology.

Key words: Amadumbe; Starch; Starch nanocrystals

3.1. Introduction

Starch is a major storage polysaccharide found in plant tissue. It is bio-synthesized as semi-crystalline granules consisting of concentric alternating amorphous and crystalline lamellae (BeMiller, 2009, Copeland et al., 2009, LeCorre et al., 2012a). The crystalline regions of starch granules can be isolated by preferential hydrolysis of the amorphous regions to produce starch nanocrystals (Lin et al., 2011a). These nanocrystals are discrete crystalline platelets that have at least one dimension of the order of 100 nm or less (Cushen et al., 2012, Kim et al., 2015). Starch nanocrystals have received much attention from both academia and the industry owing to their biodegradability, ease of production, low cost, and cyclic availability. Furthermore, in comparison to nanocrystals derived from other sources such as cellulose and chitin that are rod shaped (Condés et al., 2015), starch nanocrystals present a platelet morphology (Lin et al., 2011, Condés et al., 2015). The platelet geometry is more ideal in bio-composite applications as it allows for greater enhancement of barrier properties (González et al., 2015). Nanocrystals have a broad range of applications within the food and

beverage industry. Promising areas of application are in the form of bioplastic packaging (Condés et al., 2015) and pickering emulsions (Tan et al., 2012).

Many factors may influence the production yield and morphology of starch nanocrystals and consequently their application in the food industry. Based on previous research, the production yield of starch nanocrystals is predominantly influenced by hydrolysis conditions and amylose content whilst morphology is influenced by the botanical origin of the starch, amylose content and crystalline pattern (Jayakody and Hoover, 2002, Lin et al., 2011). Acid hydrolysis is the most commonly used method for nanocrystal production. High amylose content has been reported to hinder acid hydrolysis and consequently, reduce nanocrystal yield (Lin et al., 2011, Kim et al., 2015). Starch sources with low amylose should therefore be preferable in starch nanocrystal production. LeCorre et al. (2011b) compared the size of nanocrystals obtained from 1%, 27% and 70% amylose maize and found an increase in size with increasing amylose content of maize starches. According to these authors, amylose appeared to jam the pathways for hydrolysis thereby making it slower and harder, hence, resulting in bigger particles and a lower yield.

Starch can exhibit three crystalline patterns namely A, B and C based on the packing arrangement of amylose double helices and the degree of hydration (Hoover, 2001, Tester et al., 2004, Qiang, 2005). It has been demonstrated in previous studies that acid hydrolysis of starch does not change the crystalline pattern of the resulting nanocrystals (González and Igarzabal, 2015). However, acid hydrolysis of starch can cause an increase in the XRD reflection peak intensity. The removal of amylose during hydrolysis therefore enhances the crystallinity of starch without changing its native pattern. The morphology of starch nanocrystals nevertheless differs with regard to the crystalline pattern. In general, A-type starches have been found to produce square-like nanocrystals, whereas those produced from B-type starches were round-like particles (LeCorre et al., 2010). Furthermore, LeCorre et al. (2011b) reported parallel square-like nanocrystals for waxy maize (A type) and wheat starch (A type) whilst those obtained from high amylose maize (B-type) were round in shape.

Starch nanocrystals can be derived from various sources of starch including cereals, legumes and tubers. At present, the most common source of starch for nanocrystal production is corn. The major drawback in starch nanocrystal production is the low yield of nanocrystals, which could be influenced by the hydrolysis conditions and botanical origin of starch.

Low amylose content and small sized starch granules have been shown to ease the hydrolysis process (Vasanthan and Bhatty, 1996, Jayakody and Hoover, 2002, LeCorre et al., 2010), which in turn enhances the yield of starch nanocrystals. Starch sources with small granules and a low amylose content can therefore be explored for improved starch nanocrystal yield. Amadumbe (*Colocassia esculenta*), also known as taro is an underutilized tuber crop that produces underground corms. It is mostly grown in the tropical parts of the world. In Southern Africa, amadumbe is grown in many countries including South Africa (Aboubakar et al., 2009). Amadumbe corms may contain 70-80% starch (Aboubakar et al., 2008). The starch granules have been reported to be small in size and with a relatively low amylose content (12-20%) (Naidoo et al., 2015). The high starch content, low amylose and small starch granules thus make amadumbe a potentially good candidate for nanocrystal production. Taro starch nanoparticles (referred to as amadumbe starch nanocrystals in this study) have been previously produced, characterised and applied in corn starch films (Dai et al., 2015). Amadumbe starch nanoparticles were obtained by hydrolysis with pullulanase and recrystallization of gelatinised starch. This study suggest that amadumbe starch is indeed a promising alternative starch source and worthy of further exploration. To the best of our knowledge, there have not been any reports on production and characterisation of amadumbe starch nanocrystals. Therefore, in this study, amadumbe starch nanocrystals were produced from two commonly cultivated amadumbe varieties in Southern Africa and their physio-chemical properties (e.g. morphological, thermal and crystallinity) evaluated.

3.2. Materials and methods

3.2.1. Materials

Full matured amadumbe corms were purchased from farmers in the Jozini area of KwaZulu Natal Province, South Africa. Two varieties, namely white and purple varieties were used.

3.2.2. Starch extraction

Amadumbe starch was extracted following the method described by Naidoo et al. (2015) with minor modifications. Amadumbe corms were washed, peeled, cut into thin slices and oven dried at 50°C for 48 h. The dried amadumbe chips were milled using a Warring blender to obtain amadumbe flour. Amadumbe flour was then dispersed in distilled water and stirred for 6 h and the mixture thereafter sieved. The resulting filtrate was allowed to settle. Distilled water was then added to the filtrate and the suspension was centrifuged repeatedly at 14000 x g until the starch was clean and free of any non-starch material.

The starch pellet was oven dried at 50°C for 24 h, ground into powder, packed, sieved and stored at room temperature. The starch yield was calculated as the ratio of the starch obtained to the amount of flour used.

3.2.3. Apparent amylose content

The apparent amylose content of amadumbe starch was determined using an iodine binding method as described by Williams et al., (1970). Amadumbe starch (20 mg) was weighed in a beaker. To the starch, 10 ml of 0.5 N KOH was added. The solution was then dispersed using a magnetic stirrer, transferred to a 100 ml flask and diluted to the mark. A 10 ml aliquot of the starch solution was then transferred into a 50 ml volumetric flask and 5 ml of 0.1 N HCL was added. Iodine reagent B (0.5 ml) was then added and the solution diluted to the mark. The absorbance of the resulting solution was measured at 625 nm using a spectrophotometer.

3.2.4. Preparation of Starch Nanocrystals (SNC)

The optimized method for nanocrystal production by Angellier et al. (2004) was adopted. Amadumbe starch (20 g) was mixed with 140 ml of diluted sulphuric acid (3.16 M). The resulting suspension was transferred to a shaking incubator set at 100 rpm at 40°C for 5 days. After 5 days the final suspensions were washed by successive centrifugation with distilled water until reaching neutrality and re-dispersed using a homogenizer to break aggregates. The samples were then freeze-dried.

3.2.5. Microscopy

The morphology of native amadumbe starch was determined using an environmental scanning electron microscope (ESEM) on a Quanta 200 FEI device at a high voltage of 10 kV. Atomic force microscopy (AFM) measurements to determine the size of starch nanocrystals were performed on a Multimodal AFM (DI, Veeco, Instrumentation Group) with both tapping and conductive mode (C-AFM). The Multi130 tips were used for tapping and MESP for C-AFM. A drop a SNC suspension was deposited on a mica substrate (split with adhesive tape) and dried for 20 min at 40°C and viewed.

SEM-FEG was used to determine the morphology of starch nanocrystals. A suspension of 0.002% starch nanocrystals was prepared and 2.5 µL of suspension deposited onto a carbon grid. A thin layer of approximately 1 nm of Au-Pd conductive coating was deposited on top of the samples and they were viewed.

3.2.6. Dynamic Light Scattering Analysis

Particle size measurements of amadumbe starch nanocrystals were performed using a Zeta-sizer (Zetasizer NanoZS, Malvern, France). A 0.02% (w.t) suspension of amadumbe starch nanocrystals was prepared and homogenized with an ultrasonic bath. A given volume of starch nanocrystal suspension was injected in the Zeta-sizer cell and size measurements were recorded after reaching stable values.

3.2.7. Thermo gravimetric analysis

Thermogravimetric analysis (STA 6000, Perkin Elmer Instruments model, USA) of native amadumbe starch and amadumbe starch nanocrystals was carried out to assess the thermal stability of samples under nitrogen flow of 20 mL/min. The samples were heated from 30°C to 900°C with a heating rate of 10°C/min.

3.2.8. Differential scanning calorimetry

Differential scanning calorimetry measurements for both amadumbe native starch and starch nanocrystals were performed using DSC Q100 (TA Instruments, New Castle) filled with a manual liquid nitrogen cooling system. Freeze-dried SNC powder and dry native starch were conditioned at 50% relative humidity and placed in a hermetically sealed pan. The samples were heated from 40°C to 240°C with a heating rate of 10°C/min.

3.2.9. X-ray diffraction analysis

Wide-angle X-ray diffraction analysis was performed on powders obtained from both native starch and freeze-dried starch nanocrystals. The samples were placed in a 2.5 mm deep cell, and measurements were performed with a PANanalytical, X'Pert PRO MPD diffractometer equipped with an X'celerator detector. The operating conditions for the refractometer were: Cu Kα radiation, 2θ between 4 and 44°, step size 0.067°, and counting time 90 s.

3.2.10. FTIR

Fourier Transform Infrared (ATR FTIR) spectra of native amadumbe starch and starch nanocrystals were recorded on a Nicolet FTIR machine using the attenuate total reflectance (ATR) accessory. The resolution was 4 cm^{-1} and a total of 32 scans performed.

3.2.11. Statistical analysis

Duplicate samples were prepared and analyses performed in triplicate or duplicate where necessary. Data were analysed using analysis of variance (ANOVA) and means were compared using the Fisher Least Significant Difference (LSD) test ($p < 0.05$).

3.3. Results and Discussion

3.3.1. Starch yield, granule morphology and amylose content

Amadumbe starch yields were approximately 34% and 37% for white and purple varieties, respectively. Comparable starch yields have been reported for taro in literature (Jane et al., 1992, Nand et al., 2008). Native amadumbe starch granules appeared irregular and polygonal in shape, suggesting that these were compound starches (Fig 3.1 a & e). However, few spherical granules were observed for the white variety (Fig 1e). This is in agreement with previous works on amadumbe (Naidoo et al., 2015, Aboubakar et al., 2009, Agama-Acevedo et al., 2011). In general, amadumbe starch granules were very small in size ranging from 1 to 6 μm (Table 3.1). However, in comparison to the purple variety, the starch granules obtained from white amadumbe variety appeared larger, almost double the size of the purple variety granules. Similarly, small sized granules have been previously reported in literature for amadumbe (Agama-Acevedo et al., 2011, Aboubakar et al., 2009). The amylose content (approx. 7.5%) of starches was very low and similar for the two varieties of amadumbe. Naidoo et al. (2015) reported a comparable level of amylose content for starches obtained from cultivated amadumbe varieties in South Africa. However, higher amylose contents (14-31%) have been reported for some amadumbe varieties obtained elsewhere (Aboubakar et al., 2008).

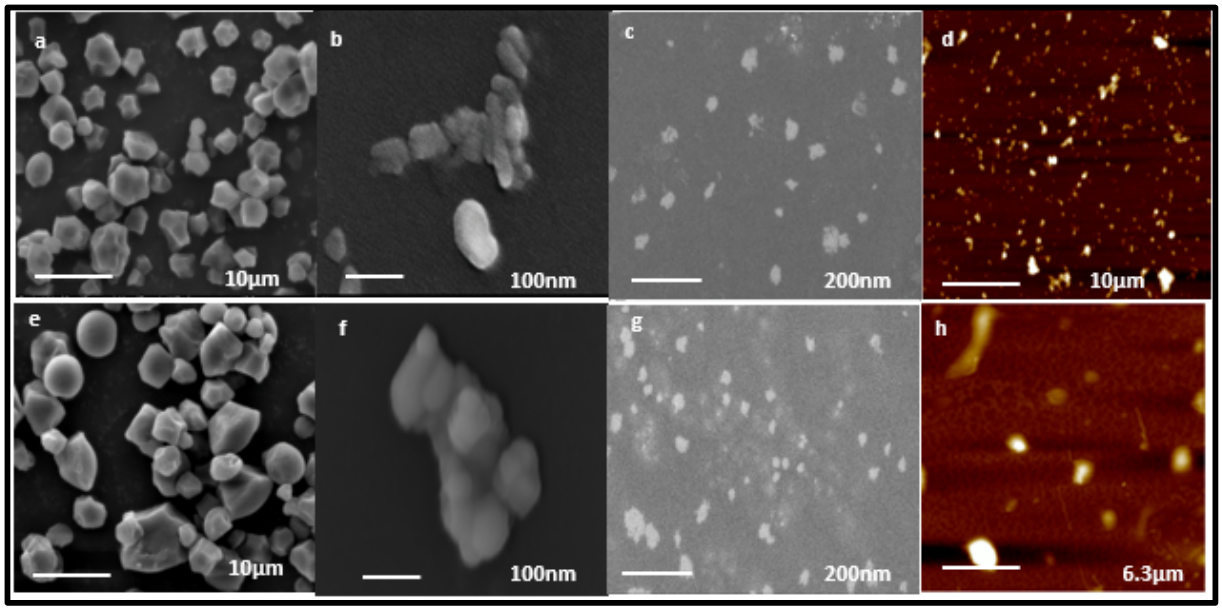

Fig. 3.1: Microscopy images for native amadumbe starch and starch nanocrystals [a) purple variety native starch by SEM, b) and c) purple variety nanocrystals by SEM-FEG d) purple variety nanocrystals by AFM e) white variety native starch by SEM, f) and g) white variety nanocrystals by SEM-FEG h) white variety nanocrystals by AFM].

Table 3.1: Main features of native starch and corresponding nanocrystals

Amadumbe variety	Amylose content (%)	Starch nanocrystal yield (%)	Granular size (µm)	SNC diameter (nm)	Nanosizer average size (nm)	PDI
White	7.0 ± 0.30	25.0 ± 0.20	3.7^{a} ± 0.8	50-100	220.6^{b}±0.01	0.2630
Purple	8.0 ± 0.12	25.0 ± 0.10	2.0^{b} ± 0.4	50-100	263.3^{a} ±0.02	0.1650

Mean ± SD (n = 3) is reported; means with different superscript letters in columns are significantly different ($p < 0.05$), PDI: polydispersity index

3.3.2. Starch nanocrystal yield (SNC)

Amadumbe starch was used to prepare starch nanocrystals by acid hydrolysis. The yield of starch nanocrystals was high (approx. 25%) and similar for both varieties (Table 3.1). The SNC yields of amadumbe starches were relatively high in comparison with previous reports (15% and less) on maize starch nanocrystals (Angellier et al., 2004). The low yields of starch nanocrystals have been the major hindrance to extensive use of starch nanocrystals in various industries.

Various factors could influence the starch hydrolysis and consequently, the yield of starch nanocrystals. Differences in granule size, granule porosity and amylose content have been found to influence the extent and yield of hydrolysis (Jayakody and Hoover, 2002, Vasanthan and Bhatty, 1996, LeCorre et al., 2010). Jayakody and Hoover (2002) found waxy maize to be more susceptible to hydrolysis than normal maize and amylomaize starches, thus confirming the influence of amylose on starch hydrolysis. Furthermore, pores on granules surface were reported to increase the accessibility of acid to the interior of the granule (Jayakody and Hoover, 2002). Surface pores were not observed on amadumbe starch granules hence porosity could not have contributed to the yield. However, the small granule size and low amylose content could have enhanced the starch nanocrystal yield. According to Vasanthan and Bhatty (1996) smaller sized starch granules from barley genotypes were more susceptible to hydrolysis compared to the larger ones, which resulted in a better yield.

3.3.3. Microscopy of SNCs

Amadumbe starch nanocrystals were viewed using SEM-FEG and AFM (Fig 3.1). AFM confirmed the presence of both individual and aggregated starch nanocrystals (Table 3.1). The size of individual nanocrystals ranged from 50-100 nm. However, the majority of nanocrystals appeared as aggregates with sizes ranging from 180 to 280 nm. Starch nanocrystal aggregation has previously been reported for nanocrystals derived from various sources (LeCorre et al., 2011a, Oladebeye et al., 2013). Aggregation of starch nanocrystals has been attributed to hydrogen bond formation resulting from the interaction of hydroxyl groups on the surface of starch nanocrystals (Xu et al., 2010).

Amadumbe starch nanocrystals viewed under SEM-FEG appeared as square like platelets. Nanocrystals have generally been observed as either round or square like platelets depending on their crystalline type. Round platelets have been observed for B-type starches such as potato whilst square-like platelets were reported for A-type corn starches (LeCorre et al., 2011b). Square-like platelet shaped nanocrystals were therefore expected for amadumbe starch since it displayed the A-type crystallinity pattern as discussed further in the subsequent section.

3.3.4. Particle size of SNCs

The average particle size and polydispersity index (PDI) of amadumbe starch nanocrystals were determined using a light scattering method. The nanocrystals were generally observed as aggregates and the average size of particles and PDI in suspension are displayed in Table

3.1. The average size of particles (260-220 nm) was significantly different for the two amadumbe varieties. A relatively larger average size of particles was observed for the purple variety compared to the white variety. In comparison to literature, remarkably larger aggregate sizes (823 nm and 1287 nm) were reported for normal and waxy maize, respectively (Condés et al. 2015). Smaller aggregate sizes of the amadumbe starch nanocrystals could be attributed to exposure of the samples to sonication prior to analysis. Sonication could have disintegrated the aggregates thus reducing their size.

3.3.5. X-ray Diffraction

Fig 3.3 shows the X-ray diffraction pattern of amadumbe starch nanocrystals and their corresponding native starches. The major and distinct X–ray diffraction peaks for the native starches appeared at $2\theta = 15°$, a doublet peak at 17-18.1° and the third one at 23.07° which is typical of A-type starches (Hoover, 2001, Tester et al., 2004, Qiang, 2005). There was no change in crystallinity pattern after hydrolysis. However, starch nanocrystals showed increased reflection peak intensity compared to their native starch counterparts. This was expected due to selective hydrolysis of the amorphous regions of starch by acid, thus resulting in a more distinct crystalline region. Similar observations were previously reported for starch nanocrystals derived from normal corn starch (González and Igarzabal, 2015). These authors attributed the enhancement in peak reflections of the corn SNC to a higher amylopectin proportion in nanocrystals. The higher amylopectin proportion in nanocrystals results from the selective hydrolysis of the amorphous regions. The amorphous areas of starch are less dense and more susceptible to chemical and enzymatic modification. The degree of crystallinity of starch nanocrystals also increased by 29% and 21% after hydrolysis for purple and white varieties, respectively. This was in agreement with previous reports (Qin et al., 2016). It is however important to note that the degree of crystallinity for both varieties was less than 50%, thus indicating a certain amount of amorphous material could be present in the produced nanocrystals.

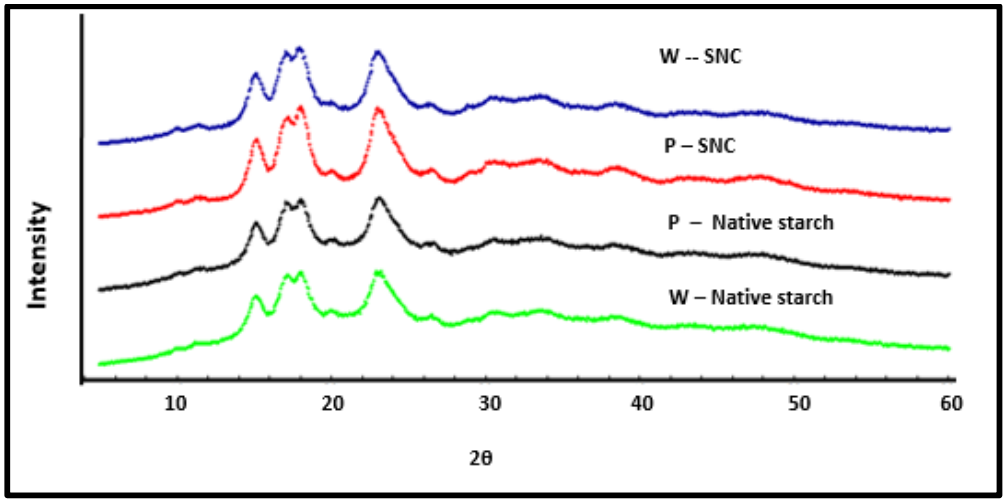

Fig. 3.3: X-ray diffraction pattern for amadumbe starch and nanocrystals. (W) White variety (P) Purple variety

3.3.6. Thermal properties of native starch and starch nanocrystals

Typical DSC curves of amadumbe starch and starch nanocrystals are shown in Fig 4. The endothermic transition temperatures of amadumbe starch and nanocrystals measured in dry state are shown in Table 3.2. A single endothermic peak was observed for both native amadumbe starch and starch nanocrystals. This observation is consistent with previous reports by LeCorre et al. (2012a). The single endothermic peak is attributed to melting of crystallites with a direct transition from packed helixes to unwinded helixes. Starch from the purple variety showed a relatively high peak temperature in comparison to the white variety, which could be attributed to the differences in amylose contents. Previous studies have suggested that amylose acts as plasticizer or diluent, which affects the melting temperature (LeCorre et al., 2012a).

The transition temperatures of native starches were lower than the theoretical melting point (160 and 210°C) of perfect crystallites in the absence of water (Colonna and Buleon, 2010) . These observations could possibly be attributed to the presence of residual moisture in amadumbe starch samples. Water acts as a plasticiser, which decreases the melting temperature of starch.

Furthermore, amadumbe starch nanocrystals showed lower peak melting temperatures in comparison with their native starch counterparts. The melting properties of starch may be influenced by many factors including the presence of plasticizer (e.g. water, amylose), molecular weight, degree of branching/crosslinking and crystallinity (Slade and Levine,

1988). The starch network is stabilised by strong hydrogen bonds, giving rise to high melting temperature in dry state. However, during SNC production the crystallinity of starch increases due to the selective removal of the amorphous regions. The remaining crystalline portion of starch consists of amylopectin, a highly branched molecule with α–(1→6) glycosidic linkages (BeMiller, 2009). Previous studies confirmed the depressing effect of molecule branching on Tg and consequently, the melting temperature (BeMiller, 2009). According to these authors, the presence of α-(1→6) linkages increases the total free volume and chain mobility, thus resulting in low energy input to initiate phase transition and ultimately resulting in a lower melting temperature. It is important to note that other scholars observed a higher melting temperature for starch nanocrystals in comparison to native starch (Thielemans et al., 2006, Xu et al., 2014b, LeCorre et al., 2012a). Based on their findings and adopting a polymeric approach, these authors attributed the increase in melting temperature of SNC to increased crystallinity and a decrease in plasticizer (amylose). Furthermore, the authors also attributed the increase in melting temperature to tighter packing and increased intermolecular bonding in nanocrystals resulting from freeze-drying.

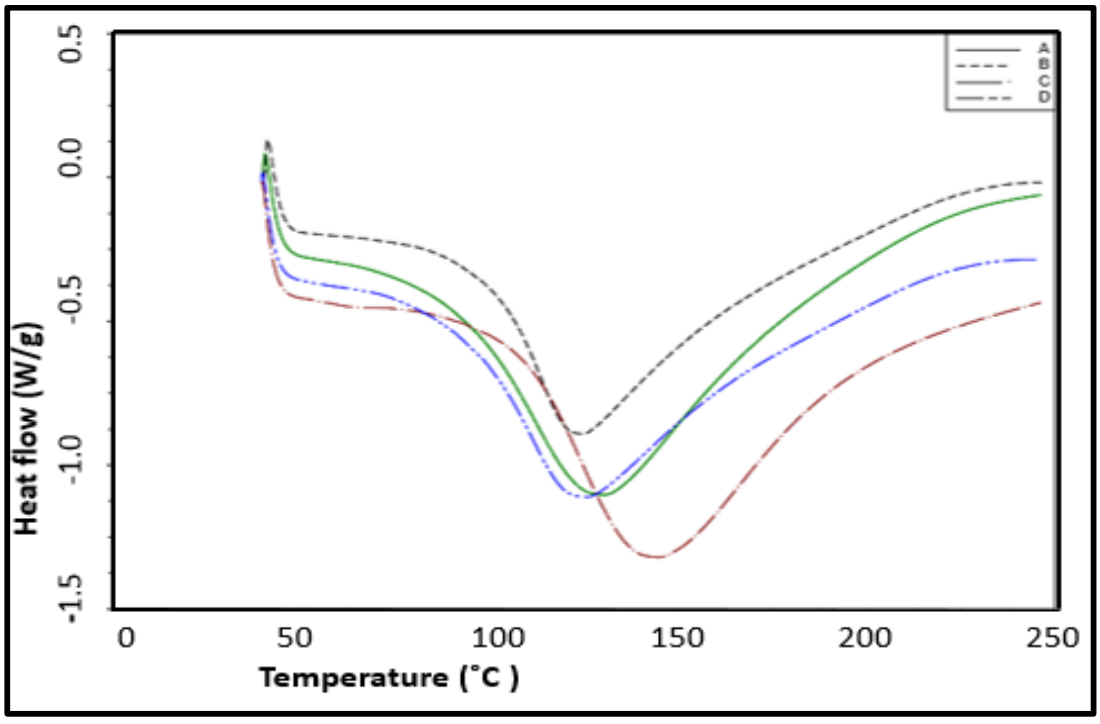

Fig 3.4: DSC curves for amadumbe starch and starch nanocrystals. A-Native starch white variety B-SNC purple variety C-native starch purple variety D SNC white variety

Table 3.2: Thermal properties of amadumbe and respective nanocrystals

Amadumbe	T_p (°C)	T_d (°C)	ΔH (J/g)	Water Content (%)
White	131 ±0.1	312.2 ±0.2	386 ±0.2	9.3±0.1
WSNC	126 ±0.1	304.9±0.1	319 ±0.2	8.3±0.3
Purple	144 ±0.2	311.3±0.2	350 ±0.1	12.0±1.4
Purple SNC	125 ±0.1	307.0±0.1	285 ±0.4	8.2± 0.1

Mean of triplicates ± SD [White-white variety starch; White SNC- white variety starch nanocrystals; Purple – purple variety starch Purple SNC- purple variety starch nanocrystals] T_p -peak melting temperature T_d - thermal decomposition temperature ΔH-melting enthalpy

The thermal stability of both native amadumbe starch and starch nanocrystals was determined using thermo-gravimetric analysis. The TGA curve showed weight loss with increase in temperature (Fig 3.5). The first range of the graph represents water loss by dehydration and volatilization of volatile components within the sample. The second range represents depolymerisation of the starch and the last range represent the degradation and decomposition of the backbone of the polymer (Namazi and Dadkhah, 2010). The TGA curves of starch and nanocrystals were similar. However, the depolymerisation initiated earlier in starch nanocrystals. This can be attributed to the presence of sulphate groups on the surface of the starch nanocrystals which catalyse depolymerisation reaction (LeCorre et al., 2012a). The T_d for starch nanocrystals decreased in comparison to that of their native starches. According to Xu et al (2014), the decomposition of starch is caused by inter or intra-molecular dehydration reactions of the starch molecule where water is the main decomposition product. In view of this, these authors hypothesised the tight packing of crystalline structure and increased inter-molecular interactions as main factors that could influence the thermal decomposition of starch. The lower decomposition temperatures observed in amadumbe starch nanocrystals could be attributed to the tight packing of crystallites resulting from hydrolysis and freeze-drying of the nanocrystals. It is noteworthy that a five day period was used for acid hydrolysis and to some extent, may have affected the crystalline structure of amylopectin and the nature of interaction between these molecules.

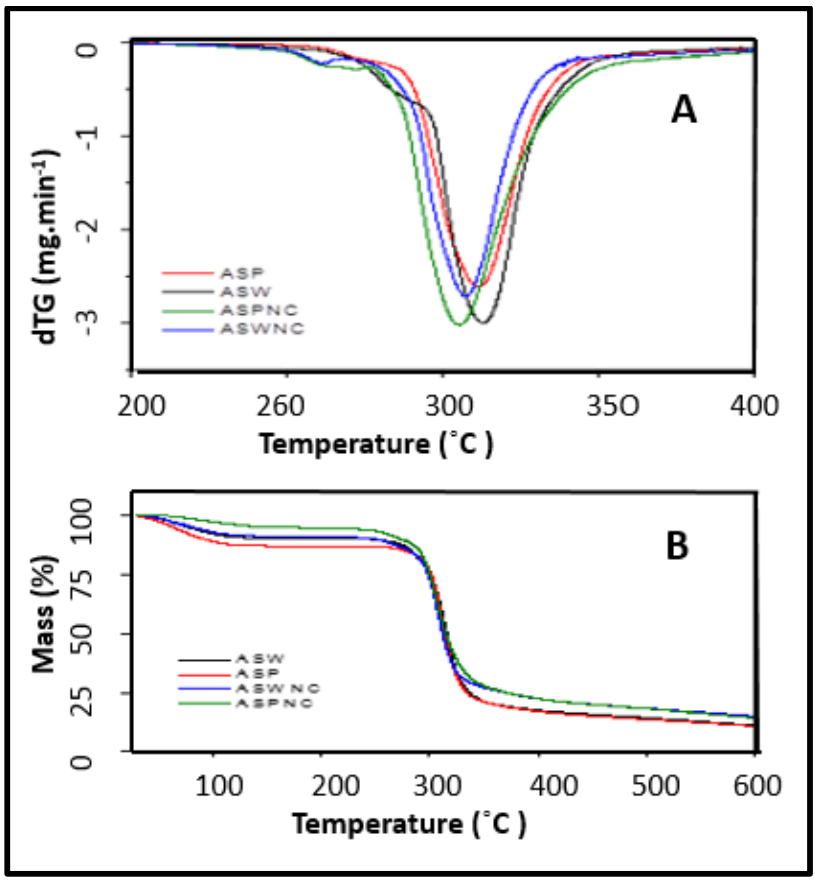

Fig 3.5: dTG (A) and TGA curves for amadumbe starch and starch nanocrystals [ASW-White variety starch, ASWNC-White variety starch nanocrystals, ASP-Purple variety starch and ASPNC-Purple variety starch nanocrystals].

3.3.7. FTIR

Amadumbe starch and its nanocrystals displayed characteristic FTIR spectra for starch (Fig 3.6). The major bands displayed were, a broad band in the region of 3000-3600 cm^{-1}, a sharp peak in the region 2800-3000 cm^{-1} and a third peak at 1644 cm^{-1}. These peaks correspond to O-H stretching-H stretching and water bending vibrations respectively (Kizil et al., 2002). The transmittance intensity of these bands was relatively higher in starch nanocrystals than their native counterparts. Similar results were reported for potato starch nanocrystals (Jivan et al., 2013). The peak at around 2928 cm^{-1} in the C-H region has been found to vary with the ratio of amylose to amylopectin (Kizil et al., 2002, Oyeyinka et al., 2015). Reduction in the amount of amylose results in increased peak intensity in the C-H region. The higher peak intensity of amadumbe starch nanocrystals in the C-H region thus confirms selective hydrolysis of the amorphous regions which predominantly contains amylose.

The increase in broadness of the OH stretch and intensity of water bending vibrations can be ascribed to changes in the inter and intra molecular hydrogen bonding of starch molecules resulting from the hydrolysis treatment (Visakh and Yu, 2015). The band at 1644 cm^{-1} is a result of water adsorbed in the amorphous regions of starch and has been reported to vary based on crystallinity (Kizil et al., 2002).

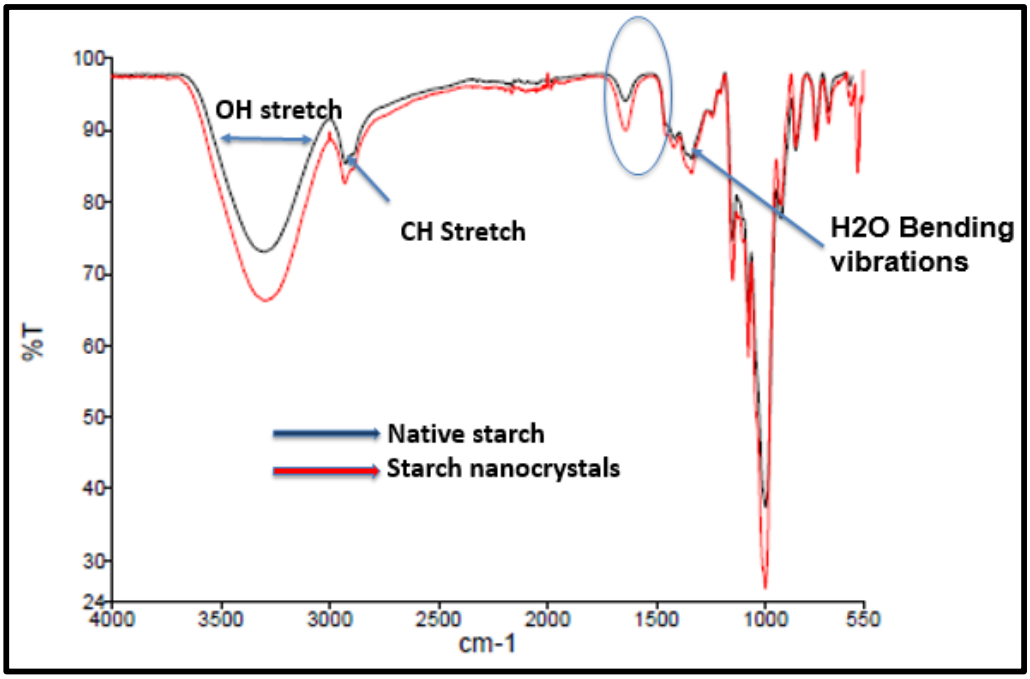

Fig 3.6**:** FTIR spectra of amadumbe native starch and respective nanocrystals.

3.3.4. Conclusions

Amadumbe starches produced substantially high yields (25%) of starch nanocrystals. These observations could be attributed to the small granule size and low amylose content of amadumbe starch that positively influences starch hydrolysis. The starch nanocrystals appeared as individual as well as aggregated particles. The majority of the nanocrystals however appeared as aggregates. Individual nanocrystals appeared as square-like platelets. Native amadumbe starch exhibited an A–type X-ray diffraction pattern. There was no change in the crystallinity pattern after hydrolysis of starch, however, the peak intensity was higher for nanocrystals. Based on their morphology, amadumbe starch nanocrystals could potentially be used as nano-reinforcements in bio-composite films as previous studies reported square-like nanocrystals to be preferred for nanocomposite production. The significantly higher yield of amadumbe starch nanocrystals relative to previous studies thus gives amadumbe a competitive advantage over other sources of starch nanocrystals.

CHAPTER FOUR

4.0. Effect of the inclusion of amadumbe SNC in starch bio-composite film matrices

Abstract

The influence of amadumbe starch nanocrystals (SNCs) at varying concentrations (2.5, 5 and 10%) on the physicochemical properties of bio-composite films prepared using two starch matrices, amadumbe and potato starches were investigated. Amadumbe SNCs exhibited square-like platelet morphology, typical of SNC derived from A-type starches. In general, the inclusion of SNCs significantly decreased water vapour permeability (WVP) of composite films whilst thermal stability and opacity were increased. Amadumbe starch films showed substantially high tensile strength (TS) compared to potato starch in the presence of SNCs. At 2.5% SNCs, TS of composite amadumbe film (8 MPa) was about four times that of composite potato films. However, SNCs ≥ 5% generally decreased TS of both potato and amadumbe films. Amadumbe SNCs can potentially be used as fillers to improve the properties of biodegradable starch films. Amadumbe starch has better film forming properties compared to potato starch.

Key words: nanocrystals, starch, amadumbe, potato, bio-composite films

4.1. Introduction

Food packaging materials play a crucial role in ensuring the production of safe and quality food. Currently, petrochemical based synthetic polymers are the dominant packaging material due to their versatility, low cost of production, lightness, excellent barrier properties and relatively easy processing (Avella et al., 2005, Duncan, 2011, Lagaron and Lopez-Rubio, 2011, González and Igarzabal, 2015). However, their long term sustainability is being questioned due to environmental pollution and the imminent depletion of petrochemical resources (Azeredo, 2009, García et al., 2011, Lagaron and Lopez-Rubio, 2011, Jiménez et al., 2012). These concerns have led to the growing research interest in sustainable biodegradable polymers. Biodegradable polymers can be derived from renewable raw materials such as proteins and polysaccharides (Lagaron and Lopez-Rubio, 2011, González and Igarzabal, 2015). They degrade rapidly in the environment, leading to complete mineralization or bio-assimilation of the plastic polymers (Avella et al., 2005, Lagaron and Lopez-Rubio, 2011).

Starch is particularly regarded as an ideal raw material for the production of biodegradable polymers due to its ability to form a continuous matrix, its low permeability to oxygen in comparison to non-starch films, its cyclic availability and low cost (Rindlava et al., 1997, Jiménez et al., 2012). In addition, starch films have been found to be transparent, odourless, and colourless, properties that are characteristic of good packaging materials (Jiménez et al., 2012). However, starch based films are inherently hydrophilic in nature and have the tendency to absorb large amounts of water in conditions of elevated relative humidity (Wilhelm et al., 2003, Mali et al., 2005). They also exhibit poor permeability and mechanical and thermal properties in comparison to synthetic polymers (Duncan, 2011, González and Igarzabal, 2015, Dai et al., 2015). Furthermore, retrogradation and crystallization of the mobile starch chains result in undesirable variations of the films' thermo-mechanical properties (Visakh and Yu, 2015). These disadvantages have limited the widespread application of starch films in food packaging.

Starch films with improved mechanical, thermal and permeability properties can be obtained through the addition of nanosized fillers (Azeredo, 2009, Duncan, 2011). These nanosized fillers can be inorganic (e.g. silica) or organic (e.g. starch) (Azeredo, 2009, Duncan, 2011). However, to maintain the biodegradability of the films and for safety reasons, organic fillers have been widely embraced. Starch nanocrystals are organic fillers that have received much attention due to their biodegradability, ease of production, cyclic availability and low cost of starch (Reddy et al., 2013, Piyada et al., 2013). They are produced through the isolation of the crystalline regions of starch granules by acid hydrolysis (Le Corre et al., 2010, Lin et al., 2011b). Starch comprises of alternating crystalline and amorphous regions (Buléon et al., 1998, BeMiller, 2009, Williams, 2009). When exposed to acid at sub gelatinization temperatures, the acid molecules preferentially attack the amorphous regions of the starch granules resulting in nanosized crystalline residue i.e. nanocrystals (Lin et al., 2011b, Le Corre et al., 2010). The addition of starch nanocrystals to starch matrices was reported to improve the mechanical, thermal and permeability properties of the resulting composite films through the formation of a filler-matrix interface (Duncan, 2011, González and Igarzabal, 2015). According to some authors, the inclusion of nanocrystals, also creates a tortuous pathway for diffusion of gas molecules which reduces the film permeability (Bradley et al., 2011, Duncan, 2011, Dufresne et al., 2013).

The source of starch may be important in the production of nanocrystals intended for bioplastic applications. This is because the yield, structural characteristics and functionality

of starch nanocrystals are influenced by several factors including botanical origin, amylose content and crystalline pattern (Jayakody and Hoover, 2002, Lin et al., 2011a, Visakh and Yu, 2015). For instance, high amylose content has been reported to hinder hydrolysis by jamming the pathways for hydrolysis and consequently, reducing the yield of nanocrystals (Lin et al., 2011a, Kim et al., 2015). Low amylose starch should therefore be the preferred choice for nanocrystal production. Besides the consideration for starch amylose content, the starch granules size and crystalline type are equally important. Small sized starch granules were reported easy to hydrolyse by acid, which also leads to better yields of SNCs compared to large granules (Vasanthan and Bhatty, 1996, Jayakody and Hoover, 2002, LeCorre et al., 2010). A-type starches, on the other hand, produce starch nanocrystals with a square-like platelet morphology (LeCorre et al., 2011b) that are more desired as nano-reinforcements in bioplastic applications compared to round-like nanocrystals obtained from B type starches (Kim et al., 2015).

Amadumbe (*Colocasia esculenta*), is an underutilized tropical tuber crop that produces underground corms. Amadumbe corms may contain 70-80% starch (Aboubakar et al., 2008) thus making it a good source of starch. Amadumbe starch granules have low amylose contents (Naidoo et al., 2015), are small in size (Hoover, 2001) and display the A-type crystalline pattern (Hoover, 2001). All these characteristics of amadumbe starch makes it a potentially good candidate for the production of starch nanocrystals intended for bio-composite film applications. There is currently limited research on starch nanocrystals, particularly those derived from non-conventional sources of starch such as amadumbe. The aim of this work was therefore to determine the effect of incorporating amadumbe starch nanocrystals on the physicochemical and mechanical properties of the resulting nanocomposites films.

4.2. Materials and methods

4.2.1 Materials

Amadumbe corms were purchased from farmers in Jozini area, of KwaZulu-Natal Province, South Africa. Commercial potato starch was purchased from Sigma-Aldrich. Laboratory grade glycerol (99.5% purity) and sulphuric acid (95-99% purity) were purchased from Merck Pty Ltd.

4.2.2. Starch extraction

Amadumbe starch was extracted following the method described by Naidoo et al. (2015) with minor modifications. Amadumbe corms were washed, peeled, sliced and oven dried at 50°C for 48 h. The dried amadumbe chips were milled into flour. Amadumbe flour was then dispersed in distilled water and stirred for 6 h and the mixture thereafter sieved. The resulting filtrate was allowed to settle. Distilled water was then added to the filtrate and the suspension was centrifuged repeatedly at 14000 g until the starch was clean and free of any non-starch material. The starch pellet was oven dried at 50°C for 24 h, ground into powder, packed, sieved and stored at room temperature. The starch yield was calculated as the ratio of the starch obtained to the amount of flour used.

4.2.3. Apparent amylose content

The apparent amylose content of amadumbe starch and potato starch was determined using the iodine binding method (Williams et al. (1970b).

4.2.4. Preparation of starch nanocrystals (SNC)

Amadumbe starch nanocrystals were produced using the optimized method by Angellier et al. (2004). Amadumbe starch (20 g) was mixed with 140 ml of diluted sulphuric acid (3.16 M). The resulting suspension was transferred to a shaking incubator set at 100 rpm at 40°C for 5 days. After 5 days, the final suspensions were washed by successive centrifugation with distilled water until reaching neutrality and re-dispersed using a homogenizer to break aggregates. The samples were then freeze-dried.

4.2.5. Microscopy of native amadumbe starch and nanocrystals

The morphology of native amadumbe starch was analysed using an environmental scanning electron microscope (ESEM) on a Quanta 200 FEI device at a high voltage of 10 kV. A field emission gun scanning electron microscopy (FEG-SEM) was used to determine the morphology of starch nanocrystals. A suspension of 0.002% starch nanocrystals was prepared and 2.5 µL of suspension deposited onto a carbon grid. A thin layer of Au-Pd conductive coating was deposited on the samples and they were viewed.

4.2.6. Preparation of films

Two starch matrices, amadumbe and potato were used in film preparation. Amadumbe and potato are both tubers but they have different amylose contents hence they were selected as matrices to determine the influence of amylose on film properties. The starch films were

prepared using a method described by Piyada et al. (2013) with several modifications. A 3% (w/v) dispersion of starch and distilled water was prepared. The dispersions were stirred and heated concurrently at 95°C for 30 min to allow gelatinization of the starch. The plasticizer glycerol at a concentration of 30% (w/w) of starch was added and the mixture stirred. The starch dispersions were allowed to cool to 40°C and thereafter starch nanocrystals were added at concentrations 0, 2.5, 5 and 10%. The dispersions were homogenized for 5 min using a rotor-stator homogenizer (Ultraturax). The dispersions were then poured evenly on petri dishes and allowed to dry in an oven at 45°C for 24 h. Once dry, the films were cooled off and peeled of the petri dishes.

4.2.7. Microscopy of starch films

The surfaces of unfilled and composite films were observed using a scanning electron microscope (EVO 15 HD) with an accelerating potential of 4 kV. Films were equilibrated at 53% RH in desiccators for 48 h. Equilibrated films were fixed on copper stubs, gold coated and observed using an accelerating voltage of 2 and 5 kV.

4.2.8. Opacity

Opacity measurements of the starch films were determined using a UV-visible spectrophotometer (Jenway 7305, UK). Rectangular specimens of the starch films were cut and placed in cuvettes. Measurements were taken at 500 nm absorbance using air as the reference. The opacity of the films (1/mm) was calculated by dividing the absorbance at 500 nm by the film thickness (mm) (Cao et al., 2007)

4.2.9. Moisture content of starch films

The moisture content of starch films was determined using AACC methods 44-15. Strips of the starch films were dried at 105^{o}C for 24 h and weight loss determined.

4.2.10. Water Solubility

The solubility of starch films in water was determined using the method described by Condés et al. (2015b) with modifications. Starch films were cut into disks (30 mm diameter, weighed and fully immersed in distilled water for 24 h). The samples were then dried at 105^{o}C for 24 h to determine final dry matter in the samples.

4.2.11. Water vapour permeability (WVP)

Water vapour permeability of the starch films was determined using a modified ASTM method E96- 97, employed by Taylor et al. (2005). Starch films were cut into circles of 30

mm diameter and their average thickness was determined. The screw tops of centrifuge tubes (50 ml) were drilled to produce a circular opening to be covered by the film samples. Distilled water (40 ml) was dispensed into centrifuge tubes, which were then covered with films and secured by screw tops. The tubes mounted with films were placed in a fume cupboard at 25°C and relative humidity of 40%, with the fan switched on. Weight loss measurements were recorded daily for 14 days.

4.2.12. Mechanical properties

The tensile properties of amadumbe and potato starch films were determined using a universal testing machine (EZ-SX, Shimadzu Japan). Amadumbe starch films were conditioned at 75% RH using NaCL prior to analysis. The films were cut into 6 × 1.5 cm rectangular strips. The initial distance of separation and velocity were adjusted to 40 mm and 1 mm/s respectively.

4.2.13. DSC

The thermal properties of starch films were measured using Differential Scanning Calorimeter (SDT Q600, USA). Approximately 3 mg of starch, films were cut and placed into pans and thereafter hermetically sealed. The samples were heated from 25 to 250°C with an interval heating rate of 10°C/min.

4.2.14. Dynamic mechanical analysis (DMA)

Dynamic mechanical measurements were performed on the virgin and composite films using a DMA Q800 V21.1 Build 51. The dimensions of the film samples were 16 × 6 × 0.1 mm^3. The analysis was carried out at the temperature range 20 to 120°C and a heating rate of 2°C/min. The analysis was used to determine the glass transition temperatures of the films.

4.2.15. X-ray diffraction analysis

Wide-angle X-ray diffraction analysis was performed on native starch, SNCs as well as potato and amadumbe films. The samples were placed in a 2.5 mm deep cell, and measurements were performed with a PANanalytical, X'Pert PRO MPD diffractometer equipped with an X'celerator detector. The operating conditions for the refractometer were: Cu Kα radiation, 2θ between 4 and 44°, step size 0.067°, and counting time 90 s.

4.2.16. Statistical analysis

All experiments were carried out in triplicate. Data were analysed using analysis of variance (ANOVA) and means were compared using Fischer's Least Significant Difference Test

($p<0.05$). The size of nanocrystals was determined by measuring the diameter of at least 50 particles from SEM-FEG images.

4.3. Results and discussion

4.3.1. Microscopic appearance of films

Micrographs of unfilled potato and amadumbe starch films showed smooth surfaces (Fig 4.1). However, with increasing concentration of SNCs in the starch matrices, the surfaces of the films became uneven and rough. These changes observed on film surfaces could be attributed to the presence of aggregated SNCs and possibly, the interactions between nanocrystals and amylose in the starch as reported by Li et al. (2015).

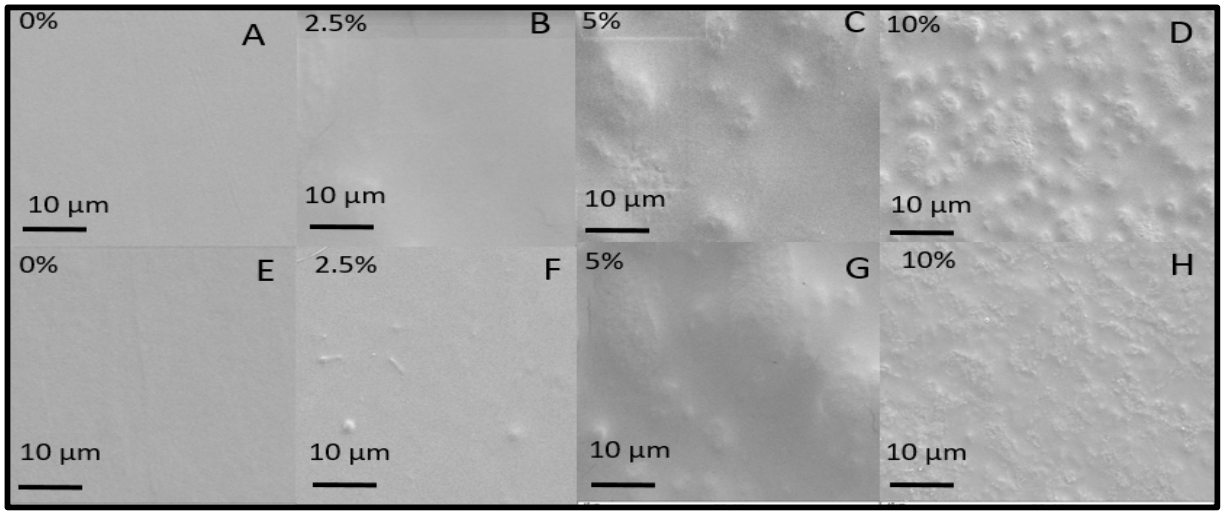

Fig 4.1: Surface SEM images of amadumbe and potato starch films at varying concentration of SNCs. A-amadumbe films (0%) B-amadumbe films (2.5%) C-amadumbe films (5%) D-amadumbe films (10%) E-potato films (0%) F-potato films (0%) G-potato films (0%) H-potato films (0%)

4.3.2. Opacity

Opacity is an important parameter in food packaging as many food products are affected by light. Amadumbe starch films were more opaque compared to potato starch films (Table 4.1). Potato starch contains high molecular weight amylose and phosphate groups that are esterified to amylopectin (Singh et al., 2004). These have been reported to contribute towards high transparency thereby lowering the opacity of the corresponding films (Singh et al., 2004). The inclusion of SNCs progressively increased the opacity of both amadumbe and potato starch films. This could be attributed to embedment of starch nanocrystals in the

interspaces of the films, thus preventing light transmittance. In essence, the presence of starch nanocrystals resulted in light scattering and the magnitude of the scattering is dependent on particle size. Generally, 40 - 50 nm is regarded as the upper limit of nanoparticle diameter to avoid intensity loss of transmitted light via Rayleigh scattering (Bel Haaj et al., 2016). Despite the size of starch nanocrystals being within the threshold level in this study, nanocrystals have the tendency of self-interacting through hydrogen bonding to form aggregates (Lin et al., 2012, Le Corre et al., 2010). The increase in opacity of starch films reinforced with SNCs could therefore be attributed to nanocrystal aggregation into a percolated network during film production. Similar observations were reported by several authors (Dai et al., 2015b, Bel Haaj et al., 2016, Shi et al., 2013). It is important to note highly opaque films are preferred for packaging foods that are susceptible to light-induced lipid oxidation or colour loss (Sun et al., 2014).

Table 4.1: Moisture, opacity, solubility, tensile strength and WVP of pure and composite amadumbe and potato starch films.

Film	SNC Content (%)	Moisture (%)	Opacity (1/mm)	Solubility (%)	WVP (10^{-5}gPa^{-1}h^{-1}m^{-1})	Tensile Strength (Mpa)
Amadumbe	0	13.4 ± 2.25^{a}	3.5 ± 0.07$^{b\ c}$	34.4 ± 0.28^{a}	1.8 ± 0.01^{a}	2.09 ± 0.01^{b}
	2.5	13.3 ± 0.86^{a}	4.9 ± 0.39^{a}	35.0 ± 0.85^{a}	1.6 ± 0.01^{b}	8.11 ± 1.67^{a}
	5	10.5 ± 0.25^{b}	3.0 ± 0.38^{c}	34.7 ± 0.65^{a}	1.5 ± 0.01^{b}	5.91 ± 1.17^{a}
	10	9.3 ± 0.21^{b}	3.8 ± 0.53^{b}	35.4 ± 0.96^{a}	1.5 ± 0.01^{b}	6.70 ± 1.19^{a}
Potato	0	15.6 ± 0.52^{b}	2.2 ± 0.10^{b}	29.4 ± 0.01^{a}	2.3 ± 0.01^{a}	2.40 ± 0.05^{c}
	2.5	16.7 ± 1.44^{a}	3.3 ± 0.08^{a}	30.4 ± 0.37^{a}	2.1 ± 0.01^{b}	3.89 ± 0.04^{a}
	5	16.0 ± 0.86^{b}	3.2 ± 0.07^{a}	30.8 ± 0.01^{a}	2.0 ± 0.01^{b}	3.37 ± 0.09^{b}
	10	14.8 ± 1.15^{b}	3.2 ± 0.01^{a}	30.0 ± 0.01 ^{a}	1.8 ± 0.01^{c}	2.08 ± 0.07^{d}

Mean ± SD is reported. Means with different superscript columns are significantly different.

4.3.3. Moisture content and water solubility

Water solubility is a crucial parameter in defining the applications of biopolymer composite films. Certain applications may require low water solubility to maintain product integrity whilst other applications such as in encapsulation, may require significantly higher solubility (Slavutsky and Bertuzzi, 2014). Generally, both the pure films and the nanocomposites exhibited relatively low water solubility.

Varying the concentration of SNCs in starch matrices did not have any major effect on film solubility. Similar findings were reported for amaranth films reinforced with SNCs (Condés et al. 2015). However, some authors observed a decrease in solubility of films with the addition of SNCs (González et al. 2015). These results were attributed to strong hydrogen bonds formed between the hydroxyl group of nanocrystals and starch chains (Slavutsky and Bertuzzi, 2014, González and Igarzabal, 2015).

4.3.4. Water Vapour Permeability

Water vapour permeability of any food packaging material should be as low as possible to minimize moisture transfer from the surroundings to the food. WVP of both amadumbe and potato starch films decreased significantly with increasing concentration of SNCs from 2.5 - 10% (Table 4.2). The highest percentage reduction was observed at 10% nanocrystal concentration. A 22 and 17% reduction in WVP were observed for potato and amadumbe starch films respectively, in comparison to pure starch films. Previous studies similarly observed a reduction in WVP of films, but only at low concentrations, 2.5% SNC (García et al., 2009) and 5% SNCs (Li et al. (2015). These observations were attributed to good dispersion of SNCs at low concentrations. The presence of SNC appeared to have reduced the affinity of the starch films for water, which could be ascribed to the formation of a strong reinforcement-matrix interface between the starch nanocrystals and the starch matrices. Both SNCs and starch films have similar polarity, which could have possibly led to strong SNC-matrix interactions on the interface and minimal matrix-water interactions. In addition, an earlier report suggested that the presence of dispersed starch nanocrystals creates a tortuous pathway for the movement of water molecules, which causes a decrease in WVP (Dai et al., 2015). In essence, the longer the diffusive pathway of the penetrant (in this case the water molecules), the lower the permeability (Dai et al., 2015). Piyada et al. (2013) reported a decrease in WVP of rice starch films with the addition of 5-20% starch nanocrystals. The authors attributed the reduction in WVP to the formation of a compact network structure, making the pathway of the permeate complex, and thus reducing its diffusion through the composite system (Piyada et al., 2013). Furthermore, when comparing the two starch matrices, films prepared with potato starch generally had high WVP compared to those prepared with amadumbe starch. The presence of a phosphate group esterified to amylopectin chains in potato starch could be a contributing factor.

4.3.5. Tensile strength

Tensile strength (TS) is an important parameter for packaging material for food. High TS enables packaging materials to tolerate the typical stress encountered by packaging materials during food handling and transportation (Sadegh-Hassani and Mohammadi Nafchi, 2014). In the absence of SNCs, potato starch films showed slightly higher tensile strength than did amadumbe films (Table 4.1). This could be attributed to differences in amylose contents between the two starches. Starches with higher amylose contents reportedly produce films with higher TS (Tharanathan, 2003, Piyada et al., 2013).This is because the linear structure of amylose chains enhances its ability to form hydrogen bonds in the starch matrix compared to branched amylopectin chains (Piyada et al., 2013, Tharanathan, 2003).

The addition of SNCs generally increased TS of the resulting composite films, with the exception of potato starch where a slight reduction was observed at 10% SNCs. The general increase in tensile strength with the addition of SNCs could be ascribed to the strong filler-matrix interfacial interactions on the reinforcement matrix interface. It is important to note that, even though TS values of composite starch films remained higher than their respective pure films, there was a reduction in TS values with increasing SNC concentrations above 2.5%. This is because low concentrations of SNCs allow uniform distribution of starch nanocrystals as a stress concentrated point in the starch matrix, which results in TS increase (Zheng et al., 2009). The interfacial bonding on the reinforcement matrix causes the effective transfer of stress through a shear mechanism from the matrix to the nanocrystals that can effectively carry the load and enhance the composite's strength (Dai et al., 2015). The decrease in TS observed for both composite potato and amadumbe starch films at SNCs > 2.5% is possibly due to self-aggregation of starch nanocrystals. Aggregation of SNCs reduces their active surface area for interacting with the matrix, which in turns weakens their adhesion on the composite matrix interface. Several scholars reported a similar trend of increase in TS at low nanocrystals levels followed by a decrease at higher nanocrystal levels (Zheng et al., 2009, Dai et al., 2015). When comparing the two starch matrices, composite amadumbe starch films had better TS compared to composite potato starch films at any given SNCs concentration. In fact, at 2.5% SNCs, TS of composite amadumbe starch film (8 MPa) was about four times higher than that of composite potato starch films. The reinforcing effect of amadumbe SNCs in amadumbe starch matrices could result from their ability to form rigid three-dimensional networks (Kristo and Biliaderis, 2007, Rajisha et al., 2014, Condés et al.,

2015b). This further suggests a better interaction between amadumbe SNCs and its native starch.

4.3.6. X-ray Diffraction

X-ray Diffraction analysis was performed on starch, SNC and starch films. Native amadumbe starch exhibited the A-type crystalline pattern with peaks at 2θ = 15°, a doublet peak at 17-18° and a third one at 23° (Fig 4.2). The A-type crystalline pattern was preserved after starch hydrolysis to form nanocrystals. However, sharper reflective peaks were observed for SNCs in comparison to native starch. This could be ascribed to more distinct crystalline regions in nanocrystals resulting from the selective acid hydrolysis of the amorphous regions of starch. The XRD spectra of unfilled amadumbe and potato films was characterised by an obvious broad bump centred around 2θ = 17.7°. The broad peak indicates the presence of amorphous material (Kristo and Biliaderis, 2007). With the addition of SNC the A-type crystalline pattern peaks eventually appeared. The peak intensity increased with an increase of starch nanocrystal concentration from 2.5 to 10%. This was expected as starch nanocrystals are crystalline in nature and their addition to the films would inherently increase the crystallinity of the films. Similar results have been reported elsewhere (Kristo and Biliaderis, 2007, (Piyada et al., 2013).

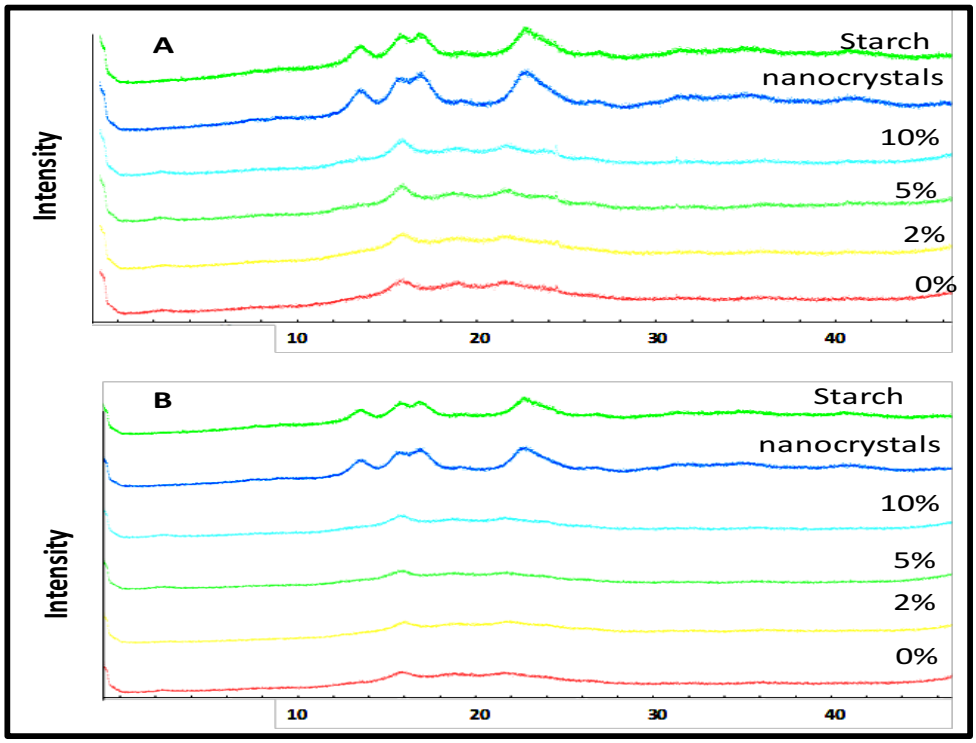

Fig 4.2: X-ray diffraction pattern of native starch, starch nanocrystals and starch composite films at varying concentration of SNCs [A - Amadumbe and B - potato]

4.3.7. Thermal properties of amadumbe and potato starch films

The thermal properties of starch nanocomposites are a critical factor in determining their processing conditions and their end use. The melting peak temperatures of starch films significantly increased with the addition of SNCs (Table 4.2). The improvement on thermal stability of the composite films is an indication of strong interactions between the starch nanocrystals and the films. The melting point of semi-crystalline polymers has a direct correlation with the thickness of the crystalline lamellae (Visakh and Yu, 2015). With the addition of starch nanocrystals (crystalline in nature) to the starch polymers, the crystallinity increases which could result in a higher melting temperature. Other scholars similarly reported an increase in melting temperature of films with the addition of starch nanocrystals (Piyada et al., 2013, Li et al., 2015, Dai et al., 2015b). The enthalpy change of the films decreased with increasing concentration of SNC to the starch films. This could possibly be caused by the starch nanocrystals hindering lateral arrangements of starch chains and crystallization of starch films (Li et al., 2015).

The glass transition temperature of the starch films as determined by DMA increased successively with the addition of amadumbe starch nanocrystals at concentrations 2.5, 5 and 10% (Table 4.2). The presence of starch nanocrystals restricted the molecular mobility of amylopectin chains. The restriction in molecular mobility could be ascribed to strong interactions through the formation of hydrogen bonds between the amorphous polymer matrix and the starch nanocrystals. Viguié et al. (2007) observed a similar trend for waxy maize films reinforced with varying concentrations of starch nanocrystals. These authors attributed the findings to the direct contact between amylopectin-rich domains of the starch matrix and the nanocrystals (Viguié et al., 2007). Kristo and Biliaderis (2007) working with starch pullulan films also reported an increase in the glass transition temperature with the addition of starch nanocrystals. According to these authors, the observed increase in Tg was attributed to strong absorption of polymer chains to nanocrystal surfaces and creation of trapped entanglements of matrix polymer chains (Kristo and Biliaderis 2007) .

Table 4.2: Thermal properties of amadumbe and potato starch films

Film type	Onset Temp (°C)	Peak Temp (°C)	Final Temp (°C)	ΔH (J/g)	T_g (°C)
Amadumbe 0% SNC	53.81 ± 2.46^{b}	78.19±1.46 ^{c}	84.3^{c}±1.78	14.32 ± 0.92^{a}	64
Amadumbe 2.5% SNC	63.43 ± 6.54^{b}	88.59 ±5.23^{b}	93.49 ±4.37^{b}	16.69 ±0.29^{a}	72
Amadumbe 5% SNC	49.7 ±1.20^{a}	107.31±1.35^{a}	107.93 ±1.26^{a}	2.39 ±1.84^{b}	94
Amadumbe 10% SNC	105.14 ±1.58^{a}	105.52 ±1.18^{a}	105.87 ±0.98^{a}	0.91 ±0.88^{b}	94
Potato 0% SNC	53.11± 2.42^{b}	66.03±1.14^{b}	74.62 ±0.50^{c}	24.92 ± 3.34^{a}	60
Potato 2.5%SNC	63.70 ± 0.90^{b}	72.49 ±1.28^{b}	80.14 ±1.28^{b}	20.68 ± 0.12^{b}	70
Potato 5% SNC	62.67 ± 7.70^{b}	73.07 ±6.74^{b}	81.56 ±3.70^{b}	15.63 ±0.07^{b}	86
Potato 10% SNC	90.64 ±8.90 ^{a}	96.24 ±4.32^{a}	99.80 ±1.65^{a}	15.27± 0.84^{c}	92

Mean ±SD is reported. Mean values with different superscript letters in columns are significantly different

4.4 Conclusion

Composite amadumbe starch films exhibit better water vapour permeability and tensile strength compared to those of potato starch. The inclusion of nanocrystals at low concentration (up to 2.5%) to starch matrices reinforces the physicochemical properties e.g. opacity, WVP, and TS of the resulting composite films. Although, both starch matrices seem to be compatible with amadumbe SNC, findings from this study seem to suggest a better interaction between amadumbe SNCs and its native starch matrix. Composite amadumbe starch films seem to have better tensile strength compared to composite potato starch films counterpart at any given SNC concentration. Amadumbe SNC can therefore potentially be used as a filler to improve the properties of biodegradable starch films

CHAPTER 5

5.0. Effect of the inclusion of amadumbe starch nanocrystals in soy protein matrices

Amadumbe, commonly known as taro is a good source of starch for nanocrystal production. In this study, the physico-chemical properties of soy protein films containing 0, 2.5, 5 and 10% amadumbe starch nanocrystals (SNCs) were determined. The incorporation of SNCs in the soy protein matrix decreased solubility and water vapour permeability (WVP) of composite films whilst tensile strength and melting temperatures increased. At 5% SNCs, the tensile strength of composite films (5MPa) was over 2-fold that of unfilled soy protein film, indicating a good dispersion of SNCs and strong attractions between the SNCs and soy protein matrix. Amadumbe starch nanocrystals can potentially be used to improve the film forming properties of soy proteins.

Keywords: nanocrystals, amadumbe, nanocomposite, soy protein

5.1. Introduction

Soya bean protein has been extensively utilized as a food ingredient (Wittaya, 2012). In non-food applications, soy protein and its derivatives have been used in drug delivery, filtration systems and tissue regeneration (Kang et al., 2016). In recent years, soy protein has been promoted as a good candidate for biodegradable film production due to its thermoplasticity, easy availability and low cost (Zheng et al., 2009, Denavi et al., 2009, Wittaya, 2012). Soy protein films also exhibit good barrier properties to oxygen and aromatic compounds under intermediate moisture environments (González and Igarzabal, 2015). However, due to the inherent hydrophilic nature of soy protein, its films exhibits poor water vapour permeability properties (Wittaya, 2012, Echeverría et al., 2014). In addition, soy protein films have been reported to be brittle and display poor mechanical properties (Cho and Rhee, 2002, Wittaya, 2012).

Several techniques including blending, incorporation of hydrophobic compounds and cross-linking have been utilized to improve the performance of soy protein isolate based films (Denavi et al., 2009, Song et al., 2011, Kang et al., 2016). However, the application of nanomaterials as fillers in soya protein films could open new possibilities of improving the limitations of soya protein films. The addition of nano-fillers to films results in the formation of a reinforcement-matrix interface that show improved physicochemical properties (Duncan, 2011). Furthermore, filler-filler interactions often lead to the formation of a particle percolating network resulting in good reinforcement effect (Kristo and Biliaderis, 2007).

The dispersed fillers also result in the creation of a tortuous pathway for diffusion of gas molecules thus improving permeability (Bradley et al., 2011, Dufresne et al., 2013).

Starch nanocrystals are organic nano-fillers that have gained much attention in recent years due to their versatile functional properties, biodegradability, ease of production and low cost of starch (Dufresne, 2010, González and Igarzabal, 2015). Starch nanocrystals are crystalline platelets that are produced through acid hydrolysis of starch. The hydrolysis yield of starch nanocrystals is influenced by amylose content, starch granule size and the crystalline pattern of the starch source (Jayakody and Hoover, 2002, Lin et al., 2011a). Previous studies have shown that amylose hinders hydrolysis through jamming pathways for hydrolysis, thus reducing nanocrystal yield (Lin et al., 2011a, Kim et al., 2015). In light of these findings, starch sources with low amylose are more ideal for nanocrystal production. Small sized starch granules have also been reported to be easily hydrolysed, thus enhancing the yield of starch nanocrystals (Vasanthan and Bhatty, 1996, Jayakody and Hoover, 2002, LeCorre et al., 2010). Amadumbe (*Colocassia Esculenta*) is a tropical tuber that contains relatively high amounts of starch. The starch granules are small and have a low amylose content, thus making it a promising resource for nanocrystal production. Therefore, in this study, amadumbe starch nanocrystals were produced and applied as a reinforcement in soy protein films and the physico-chemical properties of the resulting nanocomposite films were evaluated.

5.2. Material and methods

5.2.1. Materials

Amadumbe corms were purchased from farmers in Jozini area, of KwaZulu-Natal Province, South Africa. Soy protein isolate was purchased from Sigma-Aldrich. Laboratory grade glycerol (99.5% purity) and sulphuric acid (95-99% purity) were purchased from Merck Pty Ltd.

5.2.2. Starch extraction

Amadumbe starch was extracted following the method described by Naidoo et al. (2015) with modifications. Amadumbe corms were washed, peeled, cut into thin slices and oven dried at 50°C for 48 h. The dried amadumbe chips were milled using a Warring blender to obtain amadumbe flour. Amadumbe flour was then dispersed in distilled water and stirred for 6 h and the mixture thereafter sieved. The resulting filtrate was allowed to settle. Distilled water

was then added to the filtrate and the suspension was centrifuged repeatedly at 14000 x g until the starch was clean and free of any non-starch material. The starch pellet was oven dried at 50°C for 24 h, ground into powder, packed, sieved and stored at room temperature. The starch yield was calculated as the ratio of the starch obtained to the amount of flour used.

5.2.3. Starch nanocrystals (SNC) production

Amadumbe starch nanocrystals were produced using the optimized method by Angellier et al. (2004). Amadumbe starch (20 g) was mixed with 140 mL of dilute sulphuric acid (3.16 M). The resulting suspension was transferred to a shaking incubator set at 100 rpm at 40°C for 5 days. After 5 days the final suspensions were washed by successive centrifugation with distilled water until reaching neutrality and re-dispersed using a homogenizer to break aggregates. The samples were then freeze-dried.

5.2.4. Preparation of protein films

Soy protein films were prepared using the method described by (Condés et al., 2015b) with minor modifications. Soy protein films were prepared by making a 5% (w/v) dispersion of soy protein isolate and distilled water. The dispersions were stirred and heated simultaneously at 95°C for 30 min. Glycerol at a concentration of 20% (w/w) of starch was added as a plasticizer and the mixture stirred. The mixture was cooled to 40°C and starch nanocrystals were added at concentrations 0, 2.5, 5 and 10%.The pH of the dispersions was adjusted to 10.5 with 2 mol/L NaOH, and they were stirred. Thereafter, the dispersions were homogenized for 5 min using a rotor-stator homogenizer (Ultraturax). A 20 ml aliquot of the dispersion was then poured evenly on individual petri dishes and allowed to dry in an oven at 30°C for 24 h. The films were cooled off and peeled of the petri dish.

5.2.5. Film thickness

The average thickness of soy protein films was measured using a manual micrometre screw gauge. The thickness on several locations of the soy protein films was measured and the average determined.

5.2.6. Moisture content of starch films

Moisture content of pure and composite films was determined using AACC methods 44-15. Pieces of protein films were dried at 105^{o}C for 24 h and weight loss determined.

5.2.7. Water Solubility

The water solubility of pure and composite soy protein films was determined using the method described by Condés et al. (2015) with minor modifications. The films were cut into disks (30mm diameter), weighed and completely immersed in distilled water for 24 h. Thereafter the samples were dried at 105^{o}C for 24 h to determine final dry matter.

5.2.8. Opacity

The opacity measurements of pure and composite soy protein films were determined using a UV-visible spectrophotometer (Jenway 7305, UK). The films were cut into thin rectangular strips and placed in the cuvettes. Measurements were taken at 500 nm absorbance using air as the reference. The opacity of the films (1 mm) was calculated by dividing the absorbance at 500 nm by the film thickness (mm).

5.2.9. SEM

The surface images of pure and composite soy protein films were taken using a scanning electron microscope (EVO 15 HD) with an accelerating potential of 4 kV. The films were mounted on copper stubs, gold coated and observed using an accelerating voltage of 2 and 5 kV.

5.2.10. Mechanical properties

The tensile properties of pure and composite films were determined using a universal testing machine (EZ-SX, Shimadzu Japan). Prior to analysis, soy protein films were conditioned at 75% RH using NaCl. Thereafter ,the films were cut into 6 cmx 2 cm rectangular strips. The initial distance of separation and velocity were adjusted to 40 mm and 1 mm/s respectively.

5.2.11. DSC

The thermal properties of pure and composite soy protein films were measured using Differential Scanning Calorimeter (SDT Q600, USA). Approximately 3 mg of starch films were cut and placed into pans and thereafter hermetically sealed. The samples were heated from 25 to 250°C with an interval heating rate of 10°C/min.

5.2.12. Water vapour permeability (WVP)

The water vapour permeability of soy films was determined using a modified ASTM method E96- 97, (American Society for Testing & Materials, 1997) employed by Taylor et al. (2005). Soy films were cut into circles of 30 mm diameter. The thickness of the soy films was measured. The screw tops of centrifuge tubes (50 ml) were drilled to produce a circular

opening to be covered by the films. Distilled water (40 ml) was dispensed into the tubes. The films were then mounted on the tubes and were tightly secured by the drilled screw tops. The tubes mounted with films were then placed in a fume cupboard at 25°C and relative humidity of 40%, with the fan switched on. Weight loss measurements were recorded daily for 14 days.

5.2.13. Statistical analysis

Experiments were done in triplicate. The data was analysed using analysis of variance (ANOVA) and means were compared using Fischer's Least Significant Difference Test ($p<0.05$).

5.3. Results and discussion

5.3.1. Macroscopic and microscopic film appearance

Soy protein nanocomposite films were yellowish in colour with smooth and translucent surfaces, similar to unfilled protein films (Fig 5.1). Similar visual appearance has previously been reported for soy protein films in literature (González and Igarzabal, 2015). Microscopic observations of the surface of soy protein films showed a progressive increase in surface roughness with increasing concentration of starch nanocrystals in the matrix (Fig 5.2). Li et al. (2015) also noted a progressive increase in surface roughness of pea starch films with the inclusion of starch nanocrystals. The surface roughness could be ascribed to self-assembly of starch nanocrystals and possibly, the interactions between the nanocrystals and amylose in the starch (Li et al., 2015). González and Igarzabal (2015) also reported an increase in solid structures with an increase in the quantity of corn starch nanocrystals in soy protein films. These authors concluded that the solid particles were either a small percentage of individual starch nanocrystals that were larger than the average size or aggregated starch nanocrystals resulting from poor dispersion of the SNC.

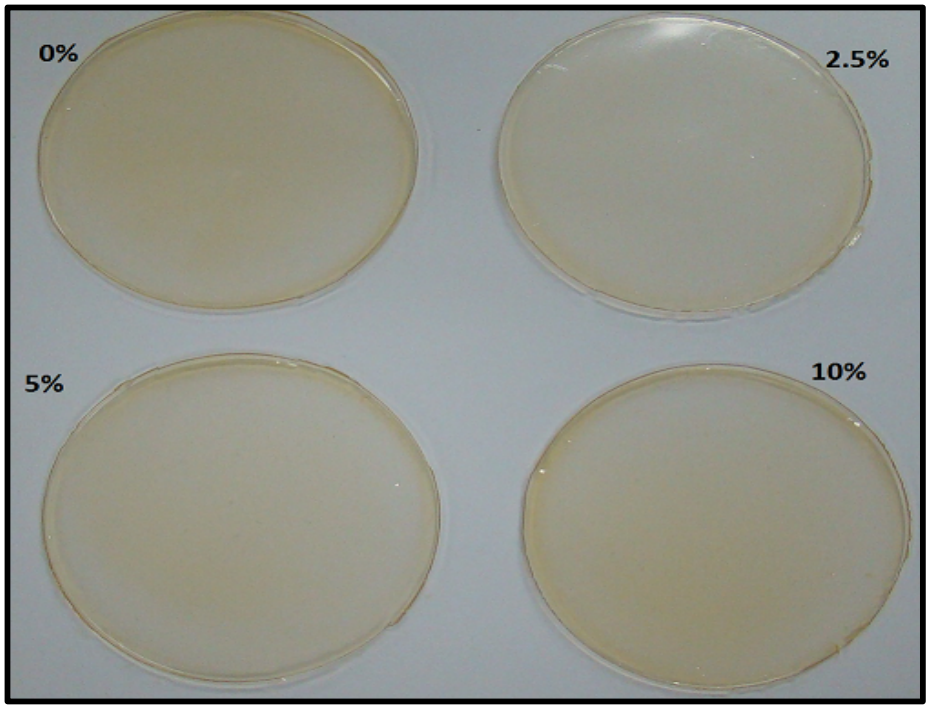

Fig 5.1 : Macroscopic images of soy protein films

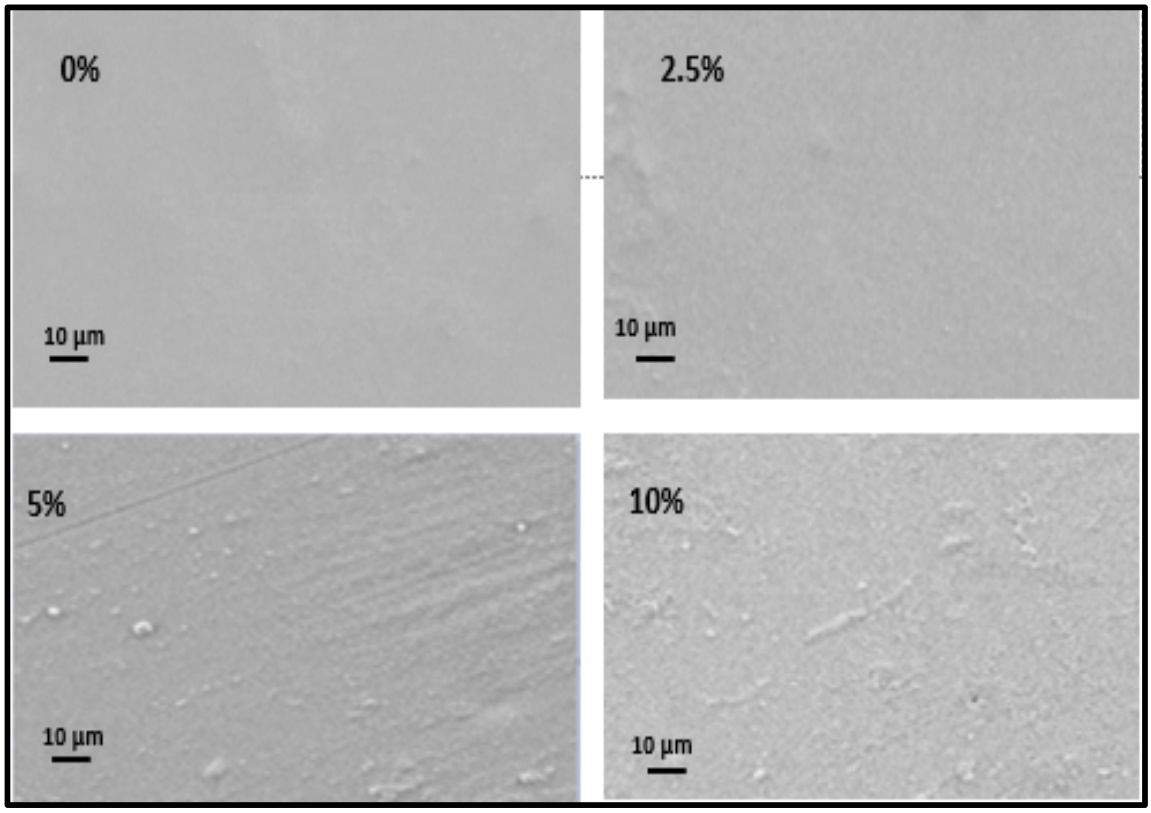

Fig 5.2: Surface SEM images of soy protein films

5.3.2. Opacity of starch nanocrystals

The opacity of soy protein films did not vary significantly with the inclusion of starch nanocrystals in the protein matrix (Table 5.1). This could be attributed to several factors, including good dispersion of the SNCs within the matrix, small SNCs size and the degree of exfoliation of the nanocrystals. Petersson and Oksman (2006) proposed that UV and visible light transmittance of nanocomposite films is largely influenced by the degree of exfoliation of the nano-reinforcement. These authors stated that a fully exfoliated nano-reinforcement does not cause a significant change in the light transmittance of the film. Furthermore, Bel Haaj et al. (2016) suggested that particle size influences the magnitude of light scattering, with particle size of 40-50 nm being the upper limit for avoiding loss of transmitted light via Rayleigh scattering. It can therefore be proposed that amadumbe SNCs were fully exfoliated and properly dispersed as individual nanocrystals within the matrix, thus resulting in a similar opacity of the unfilled and the composite films. Condés et al. (2015) also did not find any significant difference in the opacity of pure amaranth protein films and composite amaranth protein films, containing varying concentrations of corn starch nanocrystals. González and Igarzabal (2015) however, noted an increase in opacity of soy films with the addition of starch nanocrystals. The findings of González and Igarzabal (2015) were consistent with those reported for starch films (Dai et al., 2015, Bel Haaj et al., 2016). These results were attributed to the similarity in starch nanocrystals sizes to that of the interspaces in films, thus resulting in obstruction in light transmittance and consequently higher opacity. Starch nanocrystal aggregation resulting from ineffective dispersion was also reported to contribute to an increase in light scattering, and inherently increasing opacity (Dai et al., 2015b, Bel Haaj et al., 2016).

Table 5.1: Properties of soy protein films

SNC Concentration (%)	Opacity (1/mm)	Solubility (%)	WVP (10^{-5} g Pa $^{-1}$h $^{-1}$ m $^{-1}$)	Tensile strength (Mpa)
0	$1.03^{a} \pm 0.04$	$51.39^{a} \pm 0.36$	$2.0^{ab} \pm 0.1$	$2.05^{b} \pm 0.04$
2.5	$0.96^{a} \pm 0.07$	$46.65^{bc} \pm 0.10$	$1.8^{b} \pm 0.1$	$3.34^{b} \pm 0.86$
5	$1.02^{a} \pm 0.07$	$46.57^{c} \pm 0.24$	$1.7^{c} \pm 0.1$	$5.0^{a} \pm 0.50$
10	$1.10^{a} \pm 0.02$	$47.03^{b} \pm 0.1$	$2.1^{a} \pm 0.1$	$2.85^{b} \pm 0.60$

5.3.3. Solubility of films

The percentage water solubility of pure and composite soy protein films reinforced with 2.5%, 5% and 10% amadumbe starch nanocrystals is shown in Table 5.1. Generally, all the films showed a relatively high water solubility. The addition of amadumbe starch nanocrystals to soy protein films resulted in a significant decrease in their solubility. The highest decrease in film water solubility was noted at 5% SNC concentration. The addition of starch nanocrystals to the polymer matrix probably reduces the affinity of the films for water through hindering water penetration, swelling and disruption of intermolecular forces holding the polymer chains together. In addition, SNC interactions through hydrogen bonding often leads to the formation of a rigid 3-dimensional network structure that inhibits swelling and consequently reducing solubility (Kristo and Biliaderis, 2007). Furthermore, the decrease in solubility could also be attributed to strong interactions at the soy matrix and the SNC interface that leads a reduction in water absorbance. González and Igarzabal (2015) also reported a reduction in solubility of protein films with the addition of corn starch nanocrystals. However Condés et al. (2015) working with amaranth protein films reported no significant differences in the solubility of films with the addition of starch nanocrystals at concentrations below 12%. The authors attributed the findings to the breaking of interactions, particularly hydrogen bonds under the conditions of the film solubility test.

5.3.4. Water vapour permeability

The water vapour permeability of pure and nanocomposite soy protein films reinforced with amadumbe starch nanocrystals is shown in table 5.1. At low concentrations (2.5% and 5%), the addition of SNCs to soy protein films resulted in a successive reduction in water vapour permeability. However, upon the addition of 10% SNCs, the water vapour permeability of the films increased beyond that of the control (unfilled soy protein films). Permeability of polymers is dependent on several factors including their crystallinity, degree of cross-linking and polymer chain segmental motion of the polymer matrix (Siracusa, 2012). Gas molecules cannot permeate through crystallites due to the insolubility of the crystallites (Duncan, 2011, Siracusa, 2012). Furthermore, the presence of crystallites results in a decrease in available surface area of polymer for gas penetration and creation of a tortuous pathway for gases to move between the crystallites. It can therefore be hypothesised that the presence of amadumbe starch nanocrystals that are crystalline in nature had a similar effect on the polymer matrix resulting in a decrease in permeability. At 10% SNC concentration, the trend however changes as an increase in WVP is observed.

This is probably due to starch nanocrystal aggregation resulting from poor dispersion of the SNC in the matrix. At high concentrations, starch nanocrystals have a tendency to self-interact through the formation of hydrogen bonds, thus forming aggregates. The formation of these aggregates reduces the active surface area for the nanocrystals to form strong interactions with the polymer matrix. González and Igarzabal (2015) observed a decrease in permeability with the addition of maize starch nanocrystals to soy protein films even at a nanocrystal concentration as high as 40%.

5.3.5. Tensile strength

A general increase in tensile strength was observed with the incorporation of SNCs to soy protein films (Table 5.1). In comparison to unfilled soy protein films, the highest increase in tensile strength (5.0 Mpa), was a two-fold increase noted at 5% SNCs. The increase in tensile strength of soy protein films with the addition of SNCs could be ascribed to effective dispersion of SNCs and the strong filler-matrix interfacial interactions at their interface. Several scholars also reported an increase in tensile strength with the addition of starch nanocrystals (Kristo and Biliaderis, 2007, González and Igarzabal, 2015, Condés et al., 2015). The authors attributed the behaviour to the reinforcing effect of starch nanocrystals resulting from their ability to form rigid three-dimensional networks (Kristo and Biliaderis, 2007, Rajisha et al., 2014, Condés et al., 2015). However, (Zheng et al., 2009) working with soy protein films reinforced with pea starch nanocrystals, observed the maximum increase in tensile strength at 2% starch nanocrystal. The authors also reported that further increase in the nanocrystal concentration resulted in decreasing tensile strength (Zheng et al., 2009). The authors hypothesised that low levels of starch nanocrystals resulted in uniform distribution of starch nanocrystals as a stress concentrated point in the starch matrix, thus increasing tensile strength (Zheng et al., 2009). The decrease in tensile strength at higher nanocrystal concentrations was ascribed to the tendency of starch nanocrystals to self-interact causing aggregations resultantly reducing their active surface area for interacting with the matrix, thus weakening the attractions at the reinforcement matrix interface (Zheng et al., 2009).

5.3.6. X-ray Diffraction

The x-ray diffractograms of amadumbe starch powder, freeze dried amadumbe starch nanocrystals, unfilled as well as the composite protein films with 2.5, 5 and 10% starch nanocrystal are shown in Fig 5.3. Both amadumbe native starch and their starch nanocrystals exhibited an A-type crystalline pattern with typical peaks at $2\theta = 15°$, a doublet peak at 17-

18° and at 23°. Starch nanocrystals however showed sharper crystalline peaks in comparison to native starch. This is possibly due to selective removal of the amorphous regions of the starch by acid hydrolysis resulting in a higher proportion of crystalline amylopectin. The XRD spectra of protein films exhibited the amorphous nature of the films. The addition of starch nanocrystals resulted in the appearance of peaks characteristic of crystalline phases. The crystalline peaks became more distinct with the addition of higher concentration of starch nanocrystals. This was due to an increase of crystalline materials in the films. González and Igarzabal (2015) also reported the appearance of XRD crystalline phases with the addition of starch nanocrystals to protein films.

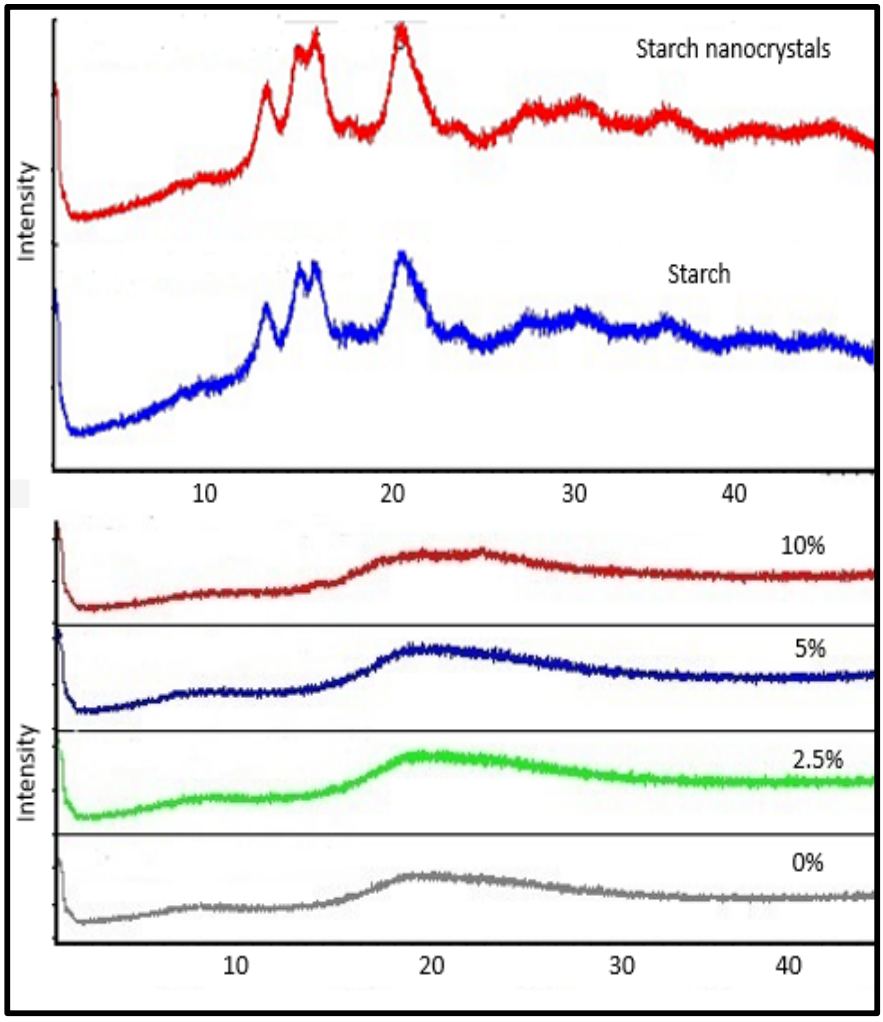

Fig 5.3: X-ray diffraction pattern of native starch, starch nanocrystals and soy protein composite films

5.3.7. Thermal properties

The melting temperatures of soy protein composite films containing 2.5 and 5% SNCs were similar to those of unfilled soy protein films (Table 5.2). However, further increase of SNCs concentration to 10% resulted in a significant increase of the melting temperature. These results suggest that at 10% SNC concentration, there was a significant amount of SNC to form strong interactions with the matrix. Melting temperatures have been reported to increase with an increase in crystallinity (LeCorre et al., 2012a). Therefore, it can be hypothesized that at 10% SNC concentration, there was a significant increase in crystallinity to effect an increase in the melting temperature. Piyada et al. (2013) and Dai et al. (2015) observed an increase in melting temperature with an increase in starch nanocrystal concentration. The authors ascribed the results to strong crystal structures and strong interfacial attractions. The enthalpy of the pure films and the composite soy protein films were similar.

Table 5.2: Thermal properties of pure and composite soy protein films

SNC Concentration (%)	Onset (T_O) (°C)	Peak (T_p) (°C)	Final (°C)	Enthalpy (J/g)
0	92.43 ± 3.02^{b}	95.41 ± 2.92^{b}	96.93 ± 2.11^{b}	12.14 ± 1.95^{a}
2.5	88.57 ± 0.07^{bc}	92.51 ± 0.04^{b}	94.86 ± 0.04^{b}	14.14 ± 0.20^{a}
5	87.58 ± 0.52^{c}	91.34 ± 0.18^{b}	90.43 ± 4.53^{b}	13.95 ± 0.82^{a}
10	105.79 ± 0.05^{a}	106.94 ± 0.01^{a}	107.9 ± 0.08^{a}	14.54 ± 2.74^{a}

5.4. Conclusion

The incorporation of amadumbe starch nanocrystals to soy protein films seem to improve WVP, mechanical and thermal properties of the resulting nanocomposite without affecting the optical properties of the films. The inclusion of starch nanocrystals at concentration 5% or less resulted in the optimum improvement of the WVP and tensile strength. Solubility and thermal properties however seemed to be positively affected by higher concentrations of SNCs (10%). Amadumbe starch nanocrystals are therefore a potentially good filler for improving the properties of soy protein films.

CHAPTER 6

6.0. General discussion

In this study, amadumbe starch nanocrystals were produced, characterized and thereafter, applied in protein and starch films. The first part of this section discusses the production and characterization of amadumbe starch nanocrystals derived from starch extracted from two amadumbe varieties. The second part focuses on the effect of the addition of amadumbe starch nanocrystals on the physicochemical and functional properties of soy protein, potato and amadumbe starch films.

6.1. Characterization of amadumbe starch nanocrystals

The white and purple varieties of amadumbe yielded approximately 34% and 37% starch respectively. By SEM, native amadumbe starch granules appeared irregular and polygonal in shape. However, for the white variety a number of spherical granules were also observed. The starch granules were very small, with their size ranging from 1 to 6 μm. However, by contrast, starch granules obtained from the white variety seemed almost double the size of those derived from the purple variety. The two varieties were characterised by a low amylose content (approx. 7.5%). Using acid hydrolysis amadumbe starch yielded approximately 25% starch nanocrystals. The yield was similar for both varieties. It is noteworthy that the SNC yield was relatively high in comparison to previous yields reported for both cereals and tubers (15% and less) (Angellier et al., 2004, Xu et al., 2014). Two factors that could have possibly been responsible for the differences in the yield are the starch amylose content and granule size. Previous studies confirmed that high amylose reduces the hydrolysis yield through jamming hydrolysis pathways (Jayakody and Hoover, 2002). Other studies also showed that smaller sized starch granules are more susceptible to acid hydrolysis in comparison to the larger ones (Vasanthan and Bhatty, 1996). The low amylose content and small granule size of amadumbe starch possibly played a role in facilitating the ease of hydrolysis, and consequently, the yield of the SNC.

After hydrolysis, the presence of starch nanocrystals was confirmed by the use of AFM and SEM-FEG. Both microscopic techniques confirmed the presence of individual nanocrystals as well as aggregated nanocrystals. The size of the individual nanocrystals ranged from 50-100 nm whilst that of the aggregates ranged from 180 to 280 nm. Starch aggregation is a common phenomenon that has been previously reported for nanocrystals (LeCorre et al., 2011b, Oladebeye et al., 2013). Similar to all polysaccharide based materials, starch

nanocrystals inherently possess a large number of hydroxyl groups on their surfaces that interact via hydrogen bonding resulting in aggregation (Xu et al., 2010, García et al., 2011). The starch nanocrystals exhibited a square-like platelet morphology. Both the native starch and SNC displayed the A-type crystalline pattern. However, the distinct difference was in the reflection peak intensity as the SNC showed sharper peaks. This was anticipated due to the selective removal of the amorphous regions during the hydrolysis process which results in a higher proportion of the crystalline regions. Previous studies have linked the crystalline pattern of the starch source to the shape of the resulting nanocrystals (LeCorre et al., 2011b). Nanocrystals from A–type starches reportedly produce square-like platelets whilst B-type starches produce round shaped platelets (LeCorre et al., 2011b). The finding of this research was consistent with this postulate as amadumbe an A-type starch produced square-like platelets.

The thermal analysis of native starch and SNC was carried out in dry state. Both native starch and SNC showed a single endothermic peak which represents the melting of crystallites with a direct transition from packed helixes to unwinded helixes. However, amadumbe starch nanocrystals showed a lower peak melting temperature in comparison to the native starches. Crystallinity is one factor that may influence the melting temperature of starch (Slade and Levine, 1988). During the production of starch nanocrystals, the crystallinity increases due to selective removal of the amorphous region. The crystalline regions of starch predominantly contain amylopectin which is a highly branched molecule with α-(1→6) glycosidic linkages (BeMiller, 2009, Le Corre et al., 2010) . The presence of α-(1→6) linkages increases the total free volume and chain mobility, thus resulting in low energy input to initiate phase transition, and consequently lowering the melting temperature (BeMiller, 2009). Other scholars however, reported higher melting temperatures for starch nanocrystals in comparison to the native starches (Thielemans et al., 2006, LeCorre et al., 2012a, Xu et al., 2014). The authors adopted a polymeric approach to explain melting, thus attributing an increase in crystallinity and a decrease in plasticizer, the cause of an increased melting temperature of the SNC. The thermal stability of native amadumbe starch and SNC as determined by TGA were similar. The only difference observed on the TGA curves was that depolymerisation initiated earlier in starch nanocrystals. Two factors that could have played a role in early initiation of depolymerisation are the presence of sulphate groups on the surface of the starch nanocrystals which catalyse depolymerisation reaction and the tight packing of crystallites (LeCorre et al., 2012a).

6.2 The effect of amadumbe SNCs on the physico-chemical properties of starch and protein films

Amadumbe SNC were incorporated into soy protein, potato and amadumbe starch film matrices at concentrations 0, 2.5, 5 and 10%. The general visual appearance of the films was not affected by the addition of SNC at any concentration. Soy protein, potato and amadumbe films were generally smooth and translucent. Soy protein films however, exhibited a yellowish colour owing to flavonoid compounds present in soy. To better understand the surface morphology of the films, microscopic analysis was carried out. With the addition of SNC, there was a transition from a smooth surface morphology exhibited by the unfilled films to rough and uneven surfaces with each successive addition of SNCs. These changes observed on film surfaces could be ascribed to the presence of aggregated SNCs and possibly, the interactions between nanocrystals and amylose in the starch as reported by Li et al. (2015).

With the inclusion of amadumbe SNC in amadumbe and potato starch films, a progressive increase in opacity was observed. It can be hypothesised that the nanocrystals resulted in an increase in the magnitude of light scattering. Previous reports stated that the magnitude of the scattering is dependent on particle size. The particle size range 40 - 50 nm is considered as the upper limit of nanoparticle diameter to circumvent intensity loss of transmitted light via Rayleigh scattering (Bel Haaj et al., 2016). Although, the size of some of the starch nanocrystals produced in this study were within the threshold level, nanocrystals have the tendency of aggregating into larger particles (Le Corre et al., 2010, Lin et al., 2012). The increase in opacity of starch films reinforced with amadumbe SNCs could therefore be attributed to SNC aggregation into a percolated network that embeds in the interspaces of the films, thus causing light scattering. The opacity of soy protein films however, seemed unaffected by the incorporation of amadumbe SNC as there was no significant difference between the opacity of unfilled and composite films. This could be ascribed to a number of factors including good dispersion of the SNCs within the matrix, small SNCs size and complete exfoliation of the nanocrystals. Petersson and Oksman (2006) proposed that fully exfoliated nano-reinforcements do not cause any significant change in light transmittance of the films and consequently opacity.

The WVP of amadumbe and potato starch films decreased significantly with increasing concentration of SNCs from 2.5-10%. However, for soy protein films, reduction in permeability was only observed at low nanocrystal concentrations (2.5 and 5%). A further

increase in SNC content to 10% resulted in an increase in WVP. Permeability properties of polymers are influenced by several factors including their crystallinity, degree of cross-linking and polymer chain segmental motion of the polymer matrix (Siracusa, 2012). Amadumbe SNC are crystallites hence, water molecules could not diffuse through them thus reducing the WVP. In addition, their presence possibly resulted in the creation of a tortuous pathway for gases to move between the crystallites. Furthermore, amadumbe SNC and the matrices had a similar polarity which could have possibly led to strong SNC-matrix interactions on the interface and nominal matrix-water interactions. All these factors could have played a role in reducing the WVP. An increase in WVP observed in soy protein films at 10% SNC concentration can be ascribed to starch nanocrystal aggregation. Starch nanocrystals possess a large number of hydroxyl groups on their surface, thus at high concentrations, they tend to self-interact via hydrogen bonding. Comparing the three starch matrices, potato starch films generally had high WVP than amadumbe starch films and soy protein films. Potato starch has hydrophilic phosphate groups esterified to amylopectin chains which could have contributed to the higher WVP.

In comparison to the pure films, composite films showed a higher tensile strength possibly due to the formation of strong filler-matrix interfacial interactions that provide high cohesion to the film, thus increasing the tensile strength. The peak increase in tensile strength was observed at 2.5% SNC concentration for the starch matrices whilst at 5% for soy protein. The findings were in line with previous studies that reported that low SNC concentrations promote uniform distribution of starch nanocrystals as a stress concentrated point in the starch matrix, which results in a TS increase (Zheng et al., 2009). Of the three matrices, composite amadumbe starch films seemed to have superior tensile properties. This possibly suggests a better interaction of amadumbe SNC and its native starch.

The melting peak temperatures of starch films significantly increased with the addition of amadumbe SNCs. However, for soy protein films a significant increase in the peak melting temperature was only observed at 10% SNC. According to Visakh & Yu, 2015, the melting point of semi-crystalline polymers has a direct correlation with the thickness of the crystalline lamellae (Visakh and Yu, 2015). The incorporation of SNC into polymers, increases the crystallinity which could result in higher melting temperatures.

A model was proposed to explain how amadumbe starch nanocrystals improve the physico-chemical properties of soy protein, potato and amadumbe starch films. Starch nanocrystals

are polar molecules with a high density of hydroxyl groups on their surfaces. The hydroxyl groups are very reactive, providing the possibility of strong associations via hydrogen bonding. When effectively dispersed within the polymer matrix, strong interactions via hydrogen bonding are formed at the reinforcement–matrix interface, thus improving the physico-chemical properties

6.3. Conclusion and recommendations

Amadumbe represents a good alternative source of starch for application in various industries. Due to its low amylose content and small granule size, amadumbe starch produced a substantially high yield of SNC thus making it a potentially promising and competitive source of starch nanocrystals. Amadumbe starch produced square-like nanocrystals that have been reckoned more ideal for application in nanocomposite films. In general, the inclusion of nanocrystals to starch and protein matrices reinforces their physicochemical properties. The degree of improvement in the physicochemical properties of the films varied with the type of matrix, as well as the concentration of the nanocrystals. It generally appeared that the enhancement of the physicochemical properties of starch matrices occurred at a lower SNC concentration in comparison to that of soy protein films. Despite all the three matrices being compatible with amadumbe SNC, the findings of this study seem to suggest a better interaction between amadumbe SNCs and its native starch matrix. Amadumbe SNC can indeed, potentially be used as a filler to improve the properties of biodegradable starch and protein films.

The findings of this research provide fundamental knowledge on the physicochemical properties of amadumbe starch nanocrystals, however, there is need for further research. Despite a relatively high yield of starch nanocrystals reported in this research in comparison to previous reports, the yield could be further enhanced. An optimized acid hydrolysis technique was utilized, but new methodologies like reactive extrusion, ultrasonication and high-pressure homogenization could be explored to improve yield whilst also shortening production time. Further research can also be undertaken on ways of reducing starch aggregation as it was evident during starch nanocrystal production and composite production. Further probing could also be done on the effect of parameters such as time, rate, and method of mixing on the physicochemical properties of the resulting composite films.

6.4. References

Aboubakar, Njintang, N. Y., Scher, J. & Mbofung, C. M. F. 2009. Texture, microstructure and physicochemical characteristics of taro (Colocasia esculenta) as influenced by cooking conditions. *Journal of Food Engineering,* 91**,** 373-379.

Aboubakar, N., Scher, J. & Mbofung, C. 2008. Physicochemical, thermal properties and microstructure of six varieties of taro (Colocasia esculenta L. Schott) flours and starches. *Journal of Food Engineering,* 86**,** 294-305.

Agama-acevedo, E., Garcia-Suarez, F. J., Gutierrez-Meraz, F., Sanchez-Rivera, M. M., San-Martin, E. & Bello-Pérez, L. A. 2011. Isolation and partial characterization of Mexican taro (*Colocasia esculenta L.*) starch. *Starch-Stärke,* 63**,** 139-146.

Akoh, C. C. & Min, D. B. 2008. *Food lipids: chemistry, nutrition, and biotechnology*, CRC press.

Angellier, H., Choisnard, L., Molina-Boisseau, S., Ozil, P. & Dufresne, A. 2004. Optimization of the Preparation of Aqueous Suspensions of Waxy Maize Starch Nanocrystals Using a Response Surface Methodology. *Biomacromolecules,* 5**,** 1545-1551.

Avella, M., De vlieger, J. J., Errico, M. E., Fischer, S., Vacca, P. & Volpe, M. G. 2005. Biodegradable starch/clay nanocomposite films for food packaging applications. *Food Chemistry,* 93**,** 467-474.

Azeredo, H. M. C. D. 2009. Nanocomposites for food packaging applications. *Food Research International,* 42**,** 1240-1253.

Bel-haaj, S., Thielemans, W., Magnin, A. & Boufi, S. 2016. Starch nanocrystals and starch nanoparticles from waxy maize as nanoreinforcement: A comparative study. *Carbohydrate Polymers,* 143**,** 310-317.

Belton, P. S. 1999. Mini Review: On the Elasticity of Wheat Gluten. *Journal of Cereal Science,* 29**,** 103-107.

Bemiller, J., Whistler, R. 2009. *Starch Chemistry And Technology,* Boston, Academic Press.

Bradley, E. L., Castle, L. & Chaudhry, Q. 2011. Applications of nanomaterials in food packaging with a consideration of opportunities for developing countries. *Trends in Food Science & Technology,* 22**,** 604-610.

Buléon, A., Colonna, P., Planchot, V. & Ball, S. 1998. Starch granules: structure and biosynthesis. *International Journal of Biological Macromolecules,* 23**,** 85-112.

Cao, N., Fu, Y. & He, J. 2007. Preparation and physical properties of soy protein isolate and gelatin composite films. *Food Hydrocolloids,* 21**,** 1153-1162.

Cho, S. Y. & Rhee, C. 2002. Sorption Characteristics of Soy Protein Films and their Relation to Mechanical Properties. *LWT - Food Science and Technology,* 35**,** 151-157.

Colonna, P. & Buleon, A. 2010. Thermal transitions of starches. *Starches, characterization, properties and applications***,** 59-102.

Condés, M. C., Anon , M., Mauri , A. & Dufresne, A. 2015. Amaranth protein films reinforced with maize starch nanocrystals. *Food Hydrocolloids,* 47**,** 146-157.

Copeland, L., Blazek, J., Salman, H. & Tang, M. C. 2009. Form and functionality of starch. *Food Hydrocolloids,* 23**,** 1527-1534.

Cui, S. 2005. *Food Carbohydrates:Chemistry,Physical Properties, And Application,* Boca Baton, Taylor and Francis Group.

Cushen, M., Kerry, J., Morris, M., Cruz-romero, M. & Cummins, E. 2012. Nanotechnologies in the food industry – Recent developments, risks and regulation. *Trends in Food Science & Technology,* 24**,** 30-46.

Dai, L., Dai, L., Qiu, C., Xiong, L. & Sun, Q. J. 2015. Characterisation of corn starch-based films reinforced with taro starch nanoparticles. *Food chemistry,* 174**,** 82-88.

Denavi, G., Tapia-blácido, D. R., Añón, M. C., Sobral, P. J. A., Mauri, A. N. & Menegalli, F. C. 2009. Effects of drying conditions on some physical properties of soy protein films. *Journal of Food Engineering,* 90**,** 341-349.

Dufresne, A. 2008. Polysaccharide nano crystal reinforced nanocomposites. *Canadian Journal of Chemistry,* 86**,** 484-494.

Dufresne, A. 2010. Processing of polymer nanocomposites reinforced with polysaccharide nanocrystals. *Molecules,* 15**,** 4111-4128.

Dufresne, A., Thomas, S., Pothan, L. A., Grossman, R. F. & Nwabunma, D. 2013. *Biopolymer Nanocomposites : Processing, Properties, and Applications,* Hoboken, Wiley.

Duncan, T. V. 2011. Applications of nanotechnology in food packaging and food safety: Barrier materials, antimicrobials and sensors. *Journal of Colloid and Interface Science,* 363**,** 1-24.

Echeverría, I., Eisenberg, P. & Mauri, A. N. 2014. Nanocomposites films based on soy proteins and montmorillonite processed by casting. *Journal of Membrane Science,* 449**,** 15-26.

Eliasson, A. C. 2004. *Starch in food ,structure,function and applications*.

Falade, K. O. & Okafor, C. A. 2013. Physicochemical properties of five cocoyam (Colocasia esculenta and Xanthosoma sagittifolium) starches. *Food Hydrocolloids,* 30**,** 173-181.

Friesen , K., Chang , C. & Nickerson , M. 2015. Incorporation of phenolic compounds, rutin and epicatechin, into soy protein isolate films : Mechanical, barrier and cross-linking properties. *Food Chemistry,* 172**,** 18-23.

García, N. L., Ribba, L., Dufresne, A., Aranguren, M. & Goyanes, S. 2011. Effect of glycerol on the morphology of nanocomposites made from thermoplastic starch and starch nanocrystals. *Carbohydrate Polymers,* 84**,** 203-210.

García, N. L., Ribba, L., Dufresne, A., Aranguren, M. I. & Goyanes, S. 2009. Physico-Mechanical Properties of Biodegradable Starch Nanocomposites. *Macromolecular Materials and Engineering,* 294**,** 169-177.

González, A. & Igarzabal, C. 2015. Nanocrystal-reinforced soy protein films and their application as active packaging. *Food Hydrocolloids,* 43**,** 777-784.

González, K., Retegi, A., González, A., Eceiza, A. & Gabilondo, N. 2015. Starch and cellulose nanocrystals together into thermoplastic starch bionanocomposites. *Carbohydrate Polymers,* 117**,** 83-90.

Hoover, R. 2001. Composition, molecular structure, and physicochemical properties of tuber and root starches: a review. *Carbohydrate polymers,* 45**,** 253-267.

Irissin-mangata, J., Bauduin, G., Boutevin, B. & Gontard, N. 2001. New plasticizers for wheat gluten films. *European Polymer Journal,* 37**,** 1533-1541.

Jane, J., Shen, L., Chen, J., Lim, S., Kasemsuwan, T. & Nip, W. 1992. Physical and Chemical Studies of Taro Starches and Flours1 2. *Cereal Chemistry,* 69**,** 528-535.

Jayakody, L. & Hoover, R. 2002. The effect of lintnerization on cereal starch granules. *Food Research International,* 35**,** 665-680

Jayakody, L., Hoover, R., Liu, Q. & Donner, E. 2007. Studies on tuber starches. II. Molecular structure, composition and physicochemical properties of yam (Dioscorea sp.) starches grown in Sri Lanka. *Carbohydrate Polymers*, 69.148-163.

Jiménez, A., Fabra, M. J., Talens, P. & Chiralt, A. 2012. Edible and biodegradable starch films: a review. *Food and Bioprocess Technology,* 5**,** 2058-2076.

Jivan, M. J., Madadlou, A. & Yarmand, M. 2013. An attempt to cast light into starch nanocrystals preparation and cross-linking. *Food Chemistry,* 141**,** 1661-1666.

Kang, H., Wang, Z., Zhang, W., LI, J. & Zhang, S. 2016. Physico-chemical properties improvement of soy protein isolate films through caffeic acid incorporation and tri-functional aziridine hybridization. *Food Hydrocolloids,* 61**,** 923-932.

Kim, H.-Y., Park, S. S. & Lim, S.-T. 2015. Preparation, Characterization and Utilization of Starch Nanoparticles. *Colloids and Surfaces B: Biointerfaces*.

Kizil, R., Irudayaraj, J. & Seetharaman, K. 2002. Characterization of irradiated starches by using FT-Raman and FTIR spectroscopy. *Journal of agricultural and food chemistry,* 50**,** 3912-3918.

Kristo, E. & Biliaderis, C. G. 2007. Physical properties of starch nanocrystal-reinforced pullulan films. *Carbohydrate Polymers,* 68**,** 146-158.

Lagaron, J. M. & Lopez-rubio, A. 2011. Nanotechnology for bioplastics: opportunities, challenges and strategies. *Trends in Food Science & Technology,* 22**,** 611-617.

Lawton, J. W. 2002. Zein: A history of processing and use. *Cereal Chemistry,* 79**,** 1-18.

Lebot, V. 2009. *Tropical root and tuber crops: cassava, sweet potato, yams and aroids*, Cabi.

Lecorre, D., Bras, J. & Dufresne, A. 2010. Starch Nanoparticles: A Review. *Biomacromolecules,* 11**,** 1139-1153.

Lecorre, D., Bras, J. & Dufresne, A. 2011a. Ceramic membrane filtration for isolating starch nanocrystals. *Carbohydrate Polymers,* 86**,** 1565-1572.

Lecorre, D., Bras, J. & Dufresne, A. 2011b. Influence of botanic origin and amylose content on the morphology of starch nanocrystals. *Journal of Nanoparticle Research,* 13**,** 7193-7208.

Lecorre, D. B., Vahanian, E., Dufresne, A. & Bras, J. 2011c. Enzymatic pretreatment for preparing starch nanocrystals. *Biomacromolecules,* 13**,** 132-137.

Lecorre, D., Bras, J. & Dufresne, A. 2012. Influence of native starch's properties on starch nanocrystals thermal properties. *Carbohydrate Polymers,* 87**,** 658-666.

Li, C., Li, Y., Sun, P. & Yang, C. 2014. Starch nanocrystals as particle stabilisers of oil-in-water emulsions. *Journal of the Science of Food and Agriculture,* 94**,** 1802-1807.

Li, C., Sun, P. & Yang, C. 2012. Emulsion stabilized by starch nanocrystals. *Starch-Stärke,* 64**,** 497-502.

Li, X., Qiu, C., Ji, N., Sun, C., Xiong, L. & Sun, Q. 2015. Mechanical, barrier and morphological properties of starch nanocrystals-reinforced pea starch films. *Carbohydrate Polymers,* 121**,** 155-162.

Lin, N., Huang, J., Chang, P. R., Anderson, D. P. & Yu, J. 2011. Preparation, modification, and application of starch nanocrystals in nanomaterials: A review. *Journal of Nanomaterials,* 2011*,* 11*,* 1–11..

Lin, N., Huang, J. & Dufresne, A. 2012. Preparation, properties and applications of polysaccharide nanocrystals in advanced functional nanomaterials: a review. *Nanoscale,* 4**,** 3274-3294.

Mali, S., Sakanaka, L. S., Yamashita, F. & Grossmann, M. V. E. 2005. Water sorption and mechanical properties of cassava starch films and their relation to plasticizing effect. *Carbohydrate Polymers,* 60**,** 283-289.

Mare, R. 2009. *Taro (Colocasia esculenta l. schott) yield and quality response to planting date and organic fertilisation.* University of KwaZulu-Natal Pietermaritzburg.

Mcewan, R., Madivha, R., Djarova, T., Oyedeji, O. & Opoku, A. 2010. Alpha-amylase inhibitor of amadumbe (Colocasia esculenta): Isolation, purification and selectivity toward-amylases from various sources. *African Journal of Biochemistry Research,* 4**,** 220-224.

Mcwilliams , M. 2001. *Foods Experimental Perspectives*, Prentice Hall.

Mohammad amini, A. & Razavi, S. M. A. 2016. A fast and efficient approach to prepare starch nanocrystals from normal corn starch. *Food Hydrocolloids,* 57**,** 132-138.

Naidoo, K., Amonsou, E. & Oyeyinka, S. 2015. In vitro digestibility and some physicochemical properties of starch from wild and cultivated amadumbe corms. *Carbohydrate Polymers,* 125**,** 9-15.

Namazi, H. & Dadkhah, A. 2010. Convenient method for preparation of hydrophobically modified starch nanocrystals with using fatty acids. *Carbohydrate Polymers,* 79**,** 731-737.

Nand, A. V., Charan, R. P., Rohindra, D. & Khurma, J. R. 2008. Isolation and properties of starch from some local cultivars of cassava and taro in Fiji. *The South Pacific Journal of Natural Science,* 26**,** 45-48.

Oladebeye, A. O., Oshodi, A. A., Amoo, I. A. & Karim, A. A. 2013. Morphology, X-ray Diffraction and Solubility of Underutilized Legume Starch Nanocrystals. *International Journal of Science and Research,* 2**,** 497-503.

Onwueme, I. C. & Charles, W. B. 1994. *Tropical root and tuber crops: production, perspectives and future prospects*, Food & Agriculture Org.

Oyeyinka, S. A., Singh, S., Adebola, P. O., Gerrano, A. S. & Amonsou, E. O. 2015. Physicochemical properties of starches with variable amylose contents extracted from bambara groundnut genotypes. *Carbohydrate Polymers,* 133**,** 171-178.

Park, H., Chinnan, M. & Shewfelt, R. 1994. Edible corn-zein film coatings to extend storage life of tomatoes. *Journal of food processing and preservation,* 18**,** 317-331.

Pérez, E., Schultz, F. S. & De delahaye, E. P. 2005. Characterization of some properties of starches isolated from Xanthosoma sagittifolium (tannia) and Colocassia esculenta (taro). *Carbohydrate Polymers,* 60**,** 139-145.

Petersson, L. & Oksman, K., 2006. Biopolymer based nanocomposites: comparing layered silicates and microcrystalline cellulose as nanoreinforcement. *Composites Science and Technology*, *66*, 2187-2196.

Piyada , K., Waranyou, S. & Thawien, W. 2013. Mechanical,thermal and structural properties of rice starch films reinforced with rice starch nanocrystals. *International Food Research Journal,* 20**,** 439-449.

Qiang, L. 2005. Understanding Starches and Their Role in Foods. *Food Carbohydrates.* CRC Press.

Qin, Y., Liu, C., Jiang, S., Xiong, L. & Sun, Q. 2016. Characterization of starch nanoparticles prepared by nanoprecipitation: Influence of amylose content and starch type. *Industrial Crops and Products,* 87**,** 182-190.

Rajisha, K. R., Maria, H. J., Pothan, L. A., Ahmad, Z. & Thomas, S. 2014. Preparation and characterization of potato starch nanocrystal reinforced natural rubber nanocomposites. *International Journal of Biological Macromolecules,* 67**,** 147-153.

Reddy, M. M., Vivekanandhan, S., Misra, M., Bhatia, S. K. & Mohanty, A. K. 2013. Biobased plastics and bionanocomposites: Current status and future opportunities. *Progress in Polymer Science,* 38**,** 1653-1689.

Rindlava, Å., Hulleman, S. H. D. & Gatenholma, P. 1997. Formation of starch films with varying crystallinity. *Carbohydrate Polymers,* 34**,** 25-30.

Robertson, G. L. 2016. *Food packaging: principles and practice*, CRC press.

Ryu, S. Y., Rhim, J. W., Roh, H. J. & Kim, S. S. 2002. Preparation and Physical Properties of Zein-Coated High-Amylose Corn Starch Film. *LWT - Food Science and Technology,* 35**,** 680-686.

Sadegh-hassani, F. & Mohammadi nafchi, A. 2014. Preparation and characterization of bionanocomposite films based on potato starch/halloysite nanoclay. *International Journal of Biological Macromolecules,* 67**,** 458-462.

Sanchez-garcia, M. D., Lopez-rubio, A. & Lagaron, J. M. 2010. Natural micro and nanobiocomposites with enhanced barrier properties and novel functionalities for food biopackaging applications. *Trends in Food Science & Technology,* 21**,** 528-536.

Shi, A.-M., Wang, L. J., Li, D. & Adhikari, B. 2013. Characterization of starch films containing starch nanoparticles: Part 1: Physical and mechanical properties. *Carbohydrate Polymers,* 96**,** 593-601.

Singh, N., Chawla, D. & Singh, J. 2004. Influence of acetic anhydride on physicochemical, morphological and thermal properties of corn and potato starch. *Food Chemistry,* 86**,** 601-608.

Singh, N., Singh, J., Kaur, L., Singh sodhi, N. & Singh gill, B. 2003. Morphological, thermal and rheological properties of starches from different botanical sources. *Food Chemistry,* 81**,** 219-231.

Siracusa, V. 2012. Food packaging permeability behaviour: a report. *International Journal of Polymer Science,* 2012.

Slade, L. & Levine, H. 1988. Non-equilibrium melting of native granular starch: Part I. Temperature location of the glass transition associated with gelatinization of A-type cereal starches. *Carbohydrate Polymers,* 8**,** 183-208.

Slavutsky, A. M. & Bertuzzi, M. A. 2014. Water barrier properties of starch films reinforced with cellulose nanocrystals obtained from sugarcane bagasse. *Carbohydrate Polymers,* 110**,** 53-61.

Smolander, M. & Chaudhry, Q. 2010. Nanotechnologies in food packaging. *Nanotechnologies in food,* 14**,** 86-101.

Song, F., Tang, D. L., Wang, X. L. & Wang, Y. Z. 2011. Biodegradable soy protein isolate-based materials: a review. *Biomacromolecules,* 12**,** 3369-3380.

Sorrentino, A., Gorrasi, G. & Vittoria, V. 2007. Potential perspectives of bio-nanocomposites for food packaging applications. *Trends in Food Science & Technology,* 18**,** 84-95.

Sun, Q., Xi, T., Li, Y. & Xiong, L. 2014. Characterization of Corn Starch Films Reinforced with CaCO(3) Nanoparticles. *PLoS ONE,* 9**,** e106727.

Tan, Y., Xu, K., Liu, C., Li, Y., Lu, C. & Wang, P. 2012. Fabrication of starch-based nanospheres to stabilize pickering emulsion. *Carbohydrate Polymers,* 88**,** 1358-1363.

Taylor J., Taylor J., Dutton M. & De Kock S. (2005). Identification of kafirin film casting solvents. *Food Chemistry,* 90, 401-408.

Tester, R. F., Karkalas, J. & Qi, X. 2004. Starch—composition, fine structure and architecture. *Journal of Cereal Science,* 39**,** 151-165.

Tharanathan, R. N. 2003. Biodegradable films and composite coatings: past, present and future. *Trends in Food Science & Technology,* 14**,** 71-78.

Thielemans, W., Belgacem, M. N. & Dufresne, A. 2006. Starch nanocrystals with large chain surface modifications. *Langmuir,* 22**,** 4804-4810.

Vasanthan, T. & Bhatty, R. 1996. Physicochemical properties of small-and large-granule starches of waxy, regular, and high-amylose barleys. *Cereal Chemistry,* 73**,** 199-207.

Viguié, J., Molina-Boisseau, S. & Dufresne, A. 2007. Processing and characterization of waxy maize starch films plasticized by sorbitol and reinforced with starch nanocrystals. *Macromolecular bioscience,* 7**,** 1206-1216.

Visakh, P. & Yu, L. 2015. *Starch-based Blends, Composites and Nanocomposites*, Royal Society of Chemistry.

Wilhelm, H. M., SierakowskI, M. R., Souza, G. P. & Wypych, F. 2003. Starch films reinforced with mineral clay. *Carbohydrate Polymers,* 52**,** 101-110.

Williams, P., Kuzina, F. & Hlynka, I. 1970. Rapid colorimetric procedure for estimating the amylose content of starches and flours. *Cereal chemistry,* 47**,** 411-420..

Williams, P. A., Phillips, G.O. 2009. *Handbook of hydrocolloids,* Cambridge, Woodhead Publishers.

Wittaya, T. 2012. *Protein-Based Edible Films:Characteristics and Improvement of Properties*.

Xu, Y., Ding, W., Liu, J., Li, Y., Kennedy, J. F., Gu, Q. & Shao, S. 2010. Preparation and characterization of organic-soluble acetylated starch nanocrystals. *Carbohydrate Polymers,* 80**,** 1078-1084.

Xu, Y., Sismour, E. N., Grizzard, C., Thomas, M., Pestov, D., Huba, Z., Wang, T. & Bhardwaj, H. L. 2014a. Morphological, Structural, and Thermal Properties of Starch Nanocrystals Affected by Different Botanic Origins. *Cereal Chemistry Journal,* 91**,** 383-388.

Zheng, H., AI, F., Chang, P. R., Huang, J. & Dufresne, A. 2009. Structure and properties of starch nanocrystal-reinforced soy protein plastics. *Polymer Composites,* 30**,** 474-480.